

Physicochemical and Ignition Properties of Dust from Loblolly Pine Wood

by

Gurdeep Singh Hehar

A dissertation submitted to the Graduate Faculty of
Auburn University
in partial fulfillment of the
requirements for the Degree of
Master of Science

Auburn, Alabama
August 3, 2013

Keywords: bioenergy, loblolly pine, dust, ignition, explosion

Copyright 2013 by Gurdeep Singh Hehar

Approved by

Oladiran O. Fasina, Chair, Professor of Biosystems Engineering
Sushil Adhikari, Associate Professor of Biosystems Engineering
John P. Fulton, Associate Professor of Biosystems Engineering

Abstract

Energy derived from biomass has attracted considerable attention because of increasing energy demand, high crude oil prices and environment and climate concerns. Biomass must be harvested and processed before conversion to a desirable form of energy. However, dust particles can be generated during biomass processing with humans working in dusty environments potentially causing health problems such as skin and eye allergies, respiratory issues and lung cancer. Additionally, the risk of fire and explosion also exists with biomass dust due to its combustible nature. Loblolly pine tree in southern forestland of the United States serves as a potential biomass feedstock for the bioenergy industry. Therefore, this research was conducted to study the ignition risk associated with dust generation during the grinding process of loblolly pine chips. The specific objectives were to: 1) determine the effect of moisture content (5%, 15% and 25% on w.b.) and screen size (1.20, 3.18 and 6.35 mm) of a hammer mill on energy required to grind loblolly pine chips and the amount of dust generated during grinding, 2) quantify the physical and chemical properties of ground material and associated dust, and 3) quantify the physicochemical and ignition properties of fractionated pine dust (<90, 90-180, 180-420 μm). Results suggested that the grinding energy, amount of dust generated and the physicochemical properties of ground material and dust were significantly affected by wood chip moisture content and hammer-mill screen size. Grinding energy increased from 39.65 to 360.00 kJ/kg when moisture content and screen size increased from 4.7% and 6.35 mm to 23.6% and 1.20 mm, respectively. The amount of dust generated decreased with increase in moisture content and

decrease in screen size. About 21.5 % of the dust was observed in ground material when wood chips at 4.7% moisture content was ground through a 1.20 mm hammer mill screen.

Further, the fine fraction (<90 μm) of dust had the higher bulk density (208.33 kg/m^3), and ash content (1.70% d.b.) compared to the medium (90-180 μm) and coarse (180-420 μm) fractions. Other physicochemical properties such as particle density, volatile matter and energy content were not significantly different ($p>0.05$). Fine dust fraction had lower hot surface ignition temperature than the other dust fractions. Temperature of volatilization, temperature of maximum mass loss rate and temperature of oxidation were not significantly affected by particle size. The exothermic reaction started at a significantly ($p<0.05$) lower temperature for fine dust fractions compared to other fractions. The maximum temperature during exothermic reaction was almost the same for all three fractions. According to the plot of activation energy versus oxidation temperature, three fractions (<90, 90-180, 180-420 μm) were at high to medium risk of ignition. The hot surface temperature and temperature of rapid exothermic reaction indicated that the risk of ignition increased with decrease in particle size.

Acknowledgements

Firstly, I would like to thank my parents, S. Chamkaur Singh and Smt. Gurmail Kaur for their love, support and guidance throughout my life. Also I would like to thank my fiancé Saran for her personal support and great patience at all times. I would also like to recognize my parents in law, S. Jasbir Singh and Smt. Amarjit Kaur for their love and encouragement in the due course. I would like to thank my uncle Balwant Singh for his guidance during my studies up to this point.

This thesis would not have been possible without the help, support and patience of my advisor Dr. Oladiran Fasina. I would like to thank him for teaching me the valuable lessons of academic and professional life. I would like to appreciate my committee members Dr. Sushil Adhikari and Dr. John Fulton for sharing their knowledge and experience in this project.

I am grateful to Anshu Shrestha for her support during lab experiments. I would like to thank Dr. Jatinder Singh Aulakh for his guidance in thesis writing. I also want to thank Shyam, Vaishnavi, Ravi, and Qun for their friendship and emotional support during these two years.

Finally thanks to my friends, Gurjot, Harpreet, Daljit, Raman, Jaskaran, Sumit and Harpreet Grewal for being there when I needed them the most.

Table of Contents

Abstract	ii
Acknowledgements.....	iv
List of Figures	x
List of Tables	xiii
Chapter 1 Introduction	1
Chapter 2 Review of Literature.....	4
2.1 Energy Overview	4
2.1.1 Petroleum Products	5
2.1.2 Coal and Natural Gas	6
2.1.3 Renewable Energy	7
2.2 Fossil Fuels	7
2.3 Bioenergy	9
2.3.1 Thermochemical Conversion	11
2.3.2 Biochemical conversion.....	14
2.4 Biomass Logistics and Pre-processing.....	19
2.5 Health Problems from Dust.....	21

2.6 Combustible Dusts	22
2.7 Ignition of Dusts	23
2.7.2 Factors affecting Ignition	25
2.8 Dust Explosion.....	27
2.8.1 Factors effecting Dust Explosion Characteristics	29
Summary	33
Chapter 3 Physicochemical Properties of Ground Material and Dust	34
3.1 Abstract	34
3.2 Introduction.....	35
3.3 Materials and Methods.....	39
3.3.1 Wood Chips	39
3.3.2 Conditioning of Wood Chips	39
3.3.3 Grinding of Wood Chips.....	39
3.3.4 Moisture Content	40
3.3.5 Bulk Density	40
3.3.6 Particle Density.....	40
3.3.7 Particle Size Distribution	41
3.3.8 Ash Content	42
3.3.9 Volatile Matter	42
3.3.10 Energy Content	43
3.3.11 Data Analysis	43

3.4 Results and Discussion.....	44
3.4.1 Dust Generation during Grinding	44
3.4.2 Energy Requirement for Grinding	45
3.4.3 Moisture Content	46
3.4.4 Particle Size Distribution	47
3.4.5 Bulk Density	49
3.4.6 Particle density.....	51
3.4.7 Ash Content	52
3.4.8 Volatile Matter	53
3.4.9 Energy Content	54
3.5 Conclusion	56
Chapter 4 Physicochemical and Ignition Properties of Dust	57
4.1 Abstract.....	57
4.2 Introduction.....	58
4.3 Materials and Methods.....	61
4.3.1 Sample Preparation and Physicochemical Properties Determination	61
4.3.2 Particle Size Distribution	62
4.3.3 Moisture Content	63
4.3.4 Bulk Density	63
4.3.5 Particle Density.....	64
4.3.6 Energy Content	64

4.3.7 Ash Content	64
4.3.8 Volatile Matter	65
4.3.9 Hot Surface Ignition Temperature	65
4.3.10 Volatilization Properties	67
4.3.11 Exothermic Reaction Parameters	68
4.2.12 Data Analysis	68
4.4 Results and Discussion.....	68
4.4.1 Particle Size Distribution and Moisture Content	68
4.4.2 Bulk and Particle Density	70
4.4.3 Ash Content	70
4.4.4 Volatile Matter	71
4.4.5 Energy Content	71
4.4.6 Hot Surface Ignition Temperature	72
4.4.7 Volatilization Properties	74
4.4.8 Exothermic Parameters (DSC).....	79
4.5 Conclusion	82
Chapter 5 Summary and Future Recommendation	84
5.1 Summary	84
5.2 Future Recommendation	85
References.....	87

Appendix A -Amount of Dust Generated, Energy Required for Grinding and Physicochemical Properties Data.....	96
Appendix B Results of Objective 1 and Objective 2	108
Appendix C Physical, Chemical and Ignition Properties Data of Dust Samples.....	113
Appendix D SAS Code and ANOVA Results	116

List of Figures

Figure 2.1. Rise in world energy consumption and human population (data EIA, 2013).....	4
Figure 2.2. Energy Sources in the United States in 2011 (EIA, 2013).	5
Figure 2.3. Electricity generation in the United States in 2011 (EIA, 2013).....	6
Figure 2.4. Renewable energy production in the United States, India and China (EIA, 2013).	9
Figure 2.5. Flow chart showing conversion of biomass into bioenergy (Akpınar et al., 2008).	11
Figure 2.6. Schematic diagram of biomass power plant (Biomass, 2013).....	12
Figure 2.7. Schematic diagram of aerobic digestion (Biogas Technology, 2013).	15
Figure 2.8. Schematic diagram of ethanol production (Mussatto, et a., 2010).	16
Figure 2.9. Pretreatment of lignocellulose crops for ethanol production (Kumar et al., 2009).	17
Figure 2.10. Chemical process to produce biodiesel from vegetable oil (Moser, 2011).	18
Figure 2.11. Flowchart representing a Biomass logistics system.	19
Figure 2.12. Dust generation during the handling of biomass (Wypch et al., 2005).	20
Figure 2.13. Components of fire triangle (fuel, oxygen and heat) (Gillman and Le May, 2007). .	23
Figure 2.14. Effect of volatile content of material (coal and biomass) on ignition temperature (Grotkjær et al., 2003).	27
Figure 2.15. Dust explosion from ignited dust layer (Combustible Dusts, 2013).....	27
Figure 2.16. (a) A 1mm dust layer of biological material (bulk density is 500kg/m ³) (b) Dust forms a concentration of 100g/m ³ when dispersed in a room of 5 m ³ (Amyotte and Eckhoff, 2010).	28

Figure 3.1. Dust explosion pentagon and its components (fuel, mixing, ignition source, oxidant, and confinement) (Abbasi and Abbasi, 2007).....	37
Figure 3.2. Effect of moisture content and screen size on the quantity (%) of dust produced (vertical bars represent standard deviation at each level of moisture content and screen size).....	45
Figure 3.3. Effect of wood chips moisture content and screen size on the energy required (kJ/kg) for grinding.....	46
Figure 3.4. Moisture content (% w.b.) of ground material and dust at different wood chips moisture content levels and hammer mill screen sizes (vertical bars represents standard deviation at each level of moisture content and screen size).	47
Figure 3.5. Particle size distribution of ground material as affected by moisture contents of wood chips and hammer mill screen size.....	48
Figure 3.6. Geometric particle size of dust and ground material at different wood chips' moisture levels and hammer mill screens.	48
Figure 3.7. Particle size distribution of dust as affected by moisture contents of wood chips and hammer mill screen size.....	49
Figure 3.8. Particle size distribution of ground material and dust when wood chips at mc of 14.74% was ground through 1.20 mm hammer mill screen size.....	49
Figure 3.9. Bulk density (kg/m ³) of ground material and dust as affected by moisture content and hammer mill screen size (vertical bars represent the standard deviation at different moisture content and screen size).....	51
Figure 3.10. Particle density (kg/m ³) of ground material and dust as affected by moisture content and hammer mill screen sizes (vertical bars represent standard deviation at different moisture content levels and screen sizes).....	52
Figure 3.11. Ash content (% d.b.) of ground material and dust as affected by moisture content and hammer mill screens (vertical bars represent the standard deviation at each level of moisture content and screen size).....	53
Figure 3.12. Volatile content (% d.b.) of ground material and dust as affected by moisture content of wood chips and hammer mill screens (vertical bars represent the standard deviation at different moisture content and screen size).....	54
Figure 3.13. Relation between volatile content (% d.b.) and ash content (% d.b.) of dust.	54
Figure 3.14. Energy content (MJ/kg) of ground material and dust as affected by moisture content and hammer mill screens (vertical bars represent standard deviation at different moisture content and screens).....	55
Figure 3.15. Relation between energy content (MJ/kg) and ash content (% d.b.) of dust.	55

Figure 4.1. (a) Hot plate apparatus, (b) Metal ring and thermocouple (K type) (c) Ring filled with fresh dust sample and (d) Burned Dust.	66
Figure 4.2. Particle size distribution of fine (<90 μm), medium (90-180 μm) and coarse (180-420 μm) dust fractions	69
Figure 4.3. Particle size distribution of pine (unfractionated) and coal dust	69
Figure 4.4. Temperature profile of fine dust sample when hot plate was set at 290°C (<90 μm)..	73
Figure 4.5. Temperature profile when dust sample (<90 μm) ignited..	73
Figure 4.6. Example of TOD and TMWL from TGA data; curve is for determination of air-heated fine (< 90 μm) dust.....	75
Figure 4.7. Determination of T_{ch} by thermogravimetric analysis carried out in the presence of oxygen of fine (<90 μm) dust.....	75
Figure 4.8. Mass loss of three dust fractions heated in air atmosphere.	76
Figure 4.9. Mass loss of unfractionated pine dust and coal dust heated in air atmosphere.	76
Figure 4.10. Mass loss of dust fractions (fine, medium and coarse) heated in the oxygen atmosphere.	77
Figure 4.11. Mass loss of unfractionated pine and coal dust heated in the oxygen atmosphere....	77
Figure 4.12. Determination of apparent activation energy (<90 μm)	78
Figure 4.13. Ignition risk of pine dust fractions (fine dust, medium dust and coarse dust), unfractionated pine dust, lignite coal dust, biological materials dust (icing sugar, maize dust, wheat dust and animal waste) (Ramirez et al., (2010).	78
Figure 4.14. Determination of TRE and T_{max} by differential scanning calorimetry.....	80
Figure 4.15. DSC plots of three dust fractions of loblolly pine (fine, medium and coarse)	81
Figure 4.16. DSC plots of unfractionated loblolly pine dust and coal dust	81

List of Tables

Table 4.1 Geometric mean particle size of three pine dust fractions (fine, medium and coarse dust fraction), unfractionated pine dust and coal dust.	70
Table 4.2 Physicochemical properties of pine dust fractions (fine, medium and coarse).	71
Table 4.3 Physicochemical properties of pine dust fractions (fine, medium and coarse).	72
Table 4.4. Hot surface ignition temperature of dust fractions (fine, medium and coarse).....	74
Table 4.5. TGA parameters of fractionated pine dust samples (fine, medium and coarse dust fraction), unfractionated pine dust, lignite coal dust, bituminous coal dust and biological materials.	79
Table 4.6. Exothermic parameters of three fractions of pine dust	82
Table A.1 Amount of Dust Generated at different wood chip's moisture content and hammer mill screen sizes.....	96
Table A.2. Energy required to grind loblolly pine chips of different moisture contents through different haer mill screens	97
Table A.3. Moisture content (% w.b.) of ground loblolly pine at different moisture content levels and hammer mill screen sizes.....	98
Table A.4. Bulk Density kg/m^3 of ground loblolly pine at different levels of moisture content and hammer mill screen sizes.	99
Table A.5. Particle Density (kg/m^3) of ground loblolly pine at different levels of moisture content and hammer mill screen sizes.....	100
Table A.6. Ash Content (% d.b.) of loblolly pine chips at different levels of moisture content and hammer mill screen sizes	101
Table A.7. Volatile Content (% d.b.) of ground loblolly pine chips at different levels of moisture content and hammer mill screen sizes.....	102

Table A.8. Energy Content (kg/m^3) of ground loblolly pine chips at different levels of moisture content and hammer mill screen sizes.....	103
Table A.9. Moisture content (% d.b.) of loblolly pine dust at different levels of moisture content and hammer mill screen sizes.....	104
Table A.10. Bulk Density (kg/m^3) of loblolly pine dust at different levels of moisture content and hammer mill screen sizes	105
Table A.11. Particle Density (kg/m^3) of loblolly pine dust at different levels of moisture content and hammer mill screen sizes.....	106
Table A.12. Ash content (%d.b.) of loblolly pine dust at different levels of moisture content and hammer mill screen sizes	106
Table A.13. Volatile content (%d.b.) of loblolly pine dust at different levels of moisture content and hammer mill screen sizes.....	107
Table A.14. Energy content (% d.b.) of loblolly pine dust at different levels of moisture content and hammer mill screen sizes.....	107
Table B.1. Amount of dust generated (%) at different moisture content and screen size.....	108
Table B.2. Grinding energy at different moisture content and screen size	108
Table B.3. Desired MC of loblolly pine chips for experiment, actual MC of loblolly pine chips that was obtained, MC of ground loblolly pine and MC of dust.....	109
Table B.4. Average particle size (mm) of ground loblolly pine chips and loblolly pine dust.	109
Table B.5. Bulk density (kg/m^3) of loblolly pine chips and loblolly pine dust.....	110
Table B.6. Particle density (kg/m^3) of ground loblolly pine chips and loblolly pine dust.	110
Table B.7. Ash content (% d.b.) of ground loblolly pine chips and loblolly pine dust.....	111
Table B.8. Volatile content (% d.b.) of ground loblolly pine chips and loblolly pine dust.	111
Table B.9. Energy content (MJ/kg) of ground loblolly pine chips and loblolly pine dust.....	112
Table C.1. Physical properties of loblolly pine dust fractions (fine dust, medium dust, coarse dust), unfractionated loblolly pine dust and lignite coal	113
Table C.2. Chemical properties of loblolly pine dust fractions (fine dust, medium dust, coarse dust), unfractionated loblolly pine dust and lignite coal	114

Table C.3. TGA properties of loblolly pine dust fractions (fine dust, medium dust, coarse dust), unfractionated loblolly pine dust and lignite coal	115
Table C.4. Exothermic parameters of loblolly pine dust fractions (fine dust, medium dust, coarse dust), unfractionated loblolly pine dust and lignite coal	115
Table D.1. ANOVA results of dust generation (DG) as affected by moisture content and screen size	117
Table D.2. ANOVA results of energy required for grinding (ER) as affected by moisture content and screen size.....	118
Table D.3. ANOVA results of bulk density (BD) of ground material as affected by moisture content and screen size.....	118
Table D.4. ANOVA results of particle density (PD) of ground material as affected by moisture content and screen size.....	119
Table D.5. ANOVA results of ash content of ground material as affected by moisture content and screen size.	119
Table D.6. ANOVA results of volatile content (Vc) of ground material as affected by moisture content and screen size.....	120
Table D.7. ANOVA results of energy content (EC) of ground material as affected by moisture content and screen size.....	120
Table D.8. ANOVA results of bulk density of loblolly pine dust as affected by moisture content and screen size.....	121
Table D.9. ANOVA results of particle density of loblolly pine dust as affected by moisture content and screen size.....	121
Table D.10. ANOVA results of ash content of loblolly pine dust as affected by moisture content and screen size.	122
Table D.11. ANOVA results of volatile content of loblolly pine dust as affected by moisture content and screen size.....	122
Table D.12. ANOVA results of volatile content of loblolly pine dust as affected by moisture content and screen size.....	123
Table D.13. ANOVA results of moisture content (MC) of three dust fractions (fine, medium and coarse).	123
Table D.14. ANOVA results of bulk density of three dust fractions (fine, medium and coarse).124	
Table D.15. ANOVA results of particle density of three dust fractions	124
Table D.16. ANOVA results of ash content of three dust fractions (fine, medium and coarse)..	125

Table D.17. ANOVA results of volatile matter (vc) content of three dust fractions (fine, medium and coarse).	125
Table D.18. ANOVA results of energy content (EC) of three dust fractions (fine, medium and coarse).	126
Table D.19. ANOVA results of temperature of volatilization (TOD) of three dust fractions (fine, medium and coarse).	126
Table D.20. ANOVA results of temperature of maximum mass loss rate (TMWL) of three dust fractions (fine, medium and coarse).	127
Table D.21. ANOVA results of temperature of oxidation (T_{ch}) of three dust fractions (fine, medium and coarse).	127
Table D.22. ANOVA results of temperature of onset rapid exothermic reaction (TRE) of three dust fractions (fine, medium and coarse).	128
Table D.23. ANOVA results of maximum temperature during exothermic reaction (T_{max}) of three dust fractions (fine, medium and coarse).	128
Table D.24. ANOVA results of MC of loblolly pine dust and coal dust.	129
Table D.25. ANOVA results of bulk density (Bd) of loblolly pine dust and coal dust.	129
Table D.26. ANOVA results of particle density of loblolly pine dust and coal dust.	129
Table D.27. ANOVA results of ash content of loblolly pine dust and coal dust.	130
Table D.28. ANOVA results of volatile matter content of loblolly pine and coal dust.	130
Table D.29. ANOVA results of energy content (EC) of loblolly pine dust and coal dust.	131
Table D.30. ANOVA results of temperature of volatilization (TOD) of loblolly pine dust and coal dust.	131
Table D.31. ANOVA results of temperature of maximum mass loss rate of loblolly pine dust and coal dust.	132
Table D.32. ANOVA results of temperature of oxidation of loblolly pine and coal dust.	133
Table D.33. ANOVA results of temperature of rapid exothermic reaction (TRE) of loblolly pine dust and coal dust.	133
Table D.34. ANOVA results of maximum temperature during exothermic reaction (T_{max}) of loblolly pine dust and coal dust.	134

Chapter 1 Introduction

A major portion (36% of total energy) of the energy consumed in United States is obtained from crude oil with about 45% of the consumed crude oil imported from foreign countries (EIA, 2013). In addition to our over-reliance on crude oil and other fossil fuels (coal and natural gas), there are also issues of energy security due to price volatility of crude oil. Even though the current price of crude oil is \$108 per barrel, the crude oil price was as high as \$140 per barrel in 2008 (EIA, 2013).

Furthermore, the burning of petroleum products obtained from crude oil and the burning of other fossil fuels generates emissions that pollute the environment. These emissions contain gases such as carbon dioxide, methane, fluorinated gases, nitrous oxide and others that have been associated with unstable climatic conditions around the world. In 2011, the United States produced about 2299 million metric tons of carbon dioxide through the burning of petroleum products only (contributed to 44% of total carbon dioxide generation in the United States).

Therefore, there is a need for sustainable and environment friendly energy resources that can minimize our reliance on fossil fuels. These energy resources are often referred to as renewable energy resources (e.g. biomass, wind energy, solar energy and geothermal energy) because they are continuously replenished and therefore are abundant on earth. About 9% of the energy consumed (total of 100 quadrillion Btu energy) in United States was obtained from renewable resources in 2011 (EIA, 2013). Biomass is the only renewable energy resource that can provide the carbon needed in transportation fuels and chemicals. According to the Energy

Independency and Security Act (EISA, 2007), the United States has to replace 20% of its crude oil with renewable sources by the end of 2022. To achieve this target, the United States will need to produce 16 billion gallons of ethanol from lignocellulosic biomass, 15 billion gallons of ethanol from corn and 5 billion gallons of other biofuels such as biodiesel by 2022. Abundant forest resources in the United States can provide a significant amount of lignocellulosic biomass required to meet these goals. Loblolly pine is the dominant species in southern U.S. forests that grows on around 55 million acres of land (Murphy et al., 2012). Thereby, loblolly pine provides a promising feedstock that can be utilized to achieve the lofty target set by EISA (2007).

Before biomass can be transformed into energy, chemicals and byproducts, it must be harvested, collected and processed. Unfortunately, dust particles are generated during these pre-transformation unit operations. The two major consequences of dust generation are health and fire/explosions. This thesis focuses on the fire/explosion aspect of dust generation and specifically on the combustion and ignition risk of biomass dusts. The National Fire Protection Association (NFPA) defines combustible dusts as any fine particles with a diameter less than 420 μm (material can pass through a U.S. number 40 standard sieve) that present a fire or explosion hazard when dispersed and ignited in air (NFPA, 2011).

Several incidents of fire and explosion that were caused by combustible dusts have been documented. These incidents have resulted in economic and sometimes human losses. In a study carried out by the Chemical Safety and Hazard Investigation Board in 2003, there were 281 combustible dust explosions in the U.S. between 1980 and 2005 (CSB, 2004). As a result of these accidents, 119 people lost their lives while 718 were injured. About 25% and 23% of these accidents occurred in the wood and food processing industries, respectively (Blair, 2007). In 2008, a severe dust explosion occurred at the Imperial Sugar Plant in Port Wentworth, Georgia, resulting in 14 fatalities and causing injury to 36 workers while completely destroying the plant. The sugar plant lost resources worth about \$15 million and incurred a fine of about \$6 million for

violations of OSHA rules for combustible dusts. The company also had to pay over \$300 million to settle lawsuits (Vorderbrueggen, 2011). In April 2012, an explosion occurred at the Lakeland sawmill, British Columbia, Canada killing one worker and injuring more than 24 (CBCnews, 2013). Obviously, explosions due to combustible dusts continue to be an issue when dealing with bulk materials.

The goal of this study was to quantify the risk associated with combustion of dust generated during processing of loblolly pine chips. To achieve this goal, the following specific objectives were carried out:

- 1) Determine the effect of hammer mill screen size (1.20, 3.18 and 6.35 mm) and moisture content (5%, 15% and 25% on w.b.) on amount of dust generated and energy required to grind loblolly pine chips.
- 2) Quantify the physicochemical properties of ground material and dust collected from objective
- 3) Quantify the effect of particle size on physicochemical and ignition properties of fractionated dust from ground loblolly pine, and compare physicochemical and ignition properties unfractionated pine dust with lignite coal dust.

Chapter 2 Review of Literature

2.1 Energy Overview

Energy played a vital role in the development of civilization and in satisfying basic human needs. Furthermore, development of civilization has resulted in population explosion and causing increase in energy demand (Asif and Muneer, 2007) (Figure 2.1). For example, the United Nations Population Division has estimated that the human population will be around 8.1 billion by 2030. Approximately 700 quadrillion Btu energy will need to be available for these people (EIA, 2013). Most of this population rise has been observed to take place in developing countries such as India and China and hence, energy demand in these countries will be high in the future compared to developed countries (Asif and Muneer, 2007).

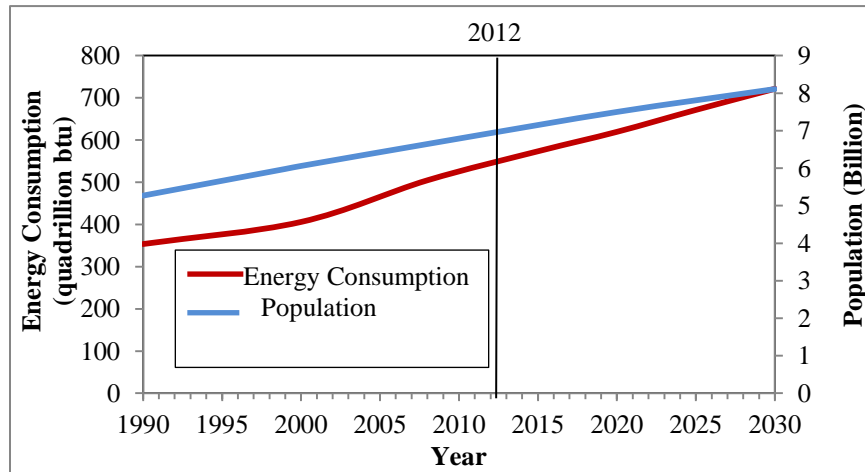


Figure 2.1. Rise in world energy consumption and human population (data EIA, 2013).

The United States is one of the leading energy consuming countries in the world utilizing 97.5 quadrillion Btu energy in 2011 which was about 18.31% (531.2 quadrillion) of total energy consumed in the world (EIA, 2013). The energy resources in the United States are petroleum, coal, natural gas, nuclear and renewables as shown in Figure 2.2 (EIA, 2013). However, renewable energy only accounts for 9% of the total US energy sources.

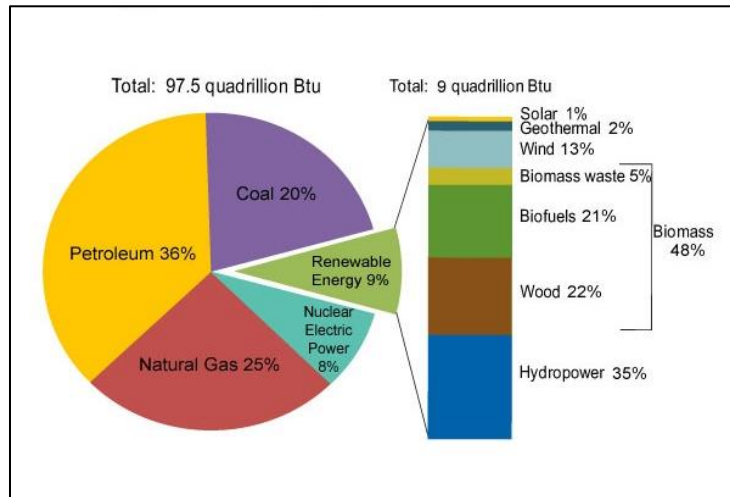


Figure 2.2. Energy Sources in the United States in 2011 (EIA, 2013).

2.1.1 Petroleum Products

Petroleum products (liquid fuels) are the primary energy source (36% of total energy consumption) in the United States consuming 18.8 million barrels per day (MMbd) in 2011. The United States highly depends upon foreign countries for petroleum products (about 45% of total petroleum consumption was imported in 2011). In order to reduce the dependency on imported foreign oil, domestic oil production has been increased over the past few years. In the year 2005, total oil import accounted for 60% of total petroleum products consumption and this reduced to 45% in 2011 (EIA, 2013). The country's long term goal is to reduce its oil import to 37% by 2035 (EIA 2013).

2.1.2 Coal and Natural Gas

Coal and natural gas are the other major sources of energy in the United States. The United States has the world's largest coal reserves which could last more than 200 years (EIA, 2013). These coal reserves are spread among 25 states. Five states (Wyoming, West Virginia, Kentucky, Pennsylvania, and Texas) accounted for 72% of total coal production in 2011 (EIA, 2013). About a billion short tons of coal were produced from U.S. mines in 2011 and 90% of which (about 900 million tons) was used for electricity generation (Figure 2.3). Although, major portion of electricity comes from coal powered plants, its contribution decreased since 2007 due to competition from natural gas and renewable energy resources. The United States also export 5% of its total coal production (EIA, 2013).

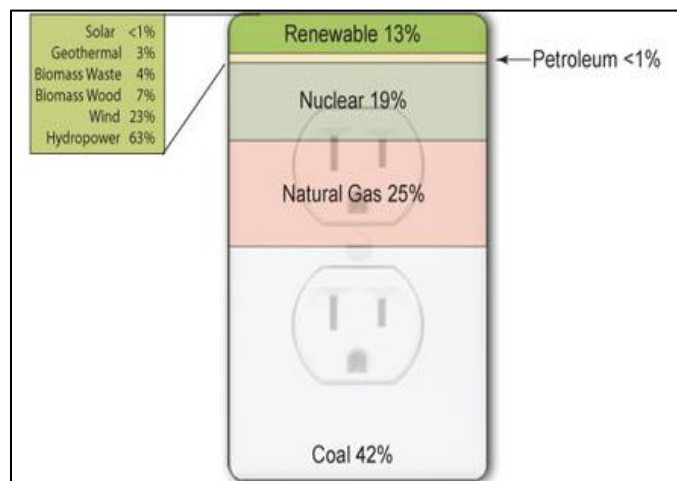


Figure 2.3. Electricity generation in the United States in 2011 (EIA, 2013).

The United States produced 23.0 trillion cubic feet of natural gas in 2011, which was 95% of its total natural gas consumption (EIA, 2013). The United States has abundance of natural gas thereby, facilitating higher production than consumption. The United States Energy Information Administration has estimated that natural gas production will increase to 3.1 trillion cubic feet in 2040. This is about 44% more than the natural gas production in 2011 (EIA, 2013).

2.1.3 Renewable Energy

Renewable energy sources include hydroelectric power, wind, biomass, geothermal and solar energy. The United States consumed 9 quadrillion Btu energy from renewable energy sources in 2011 which is equivalent to 9% of total energy consumed (Figure 2.3) (EIA, 2013).

About 13% of total U.S. electricity generated in 2011 was from renewable energy resources (EIA, 2013). Energy produced from water, hydroelectric power, is one of the primary renewable energy sources and accounted for about 63% of total electricity generated from renewables. However, the contribution of other renewable sources has been found to increase over the years. For example, wind energy increased from 6 billion kWh in 2000 to about 120 billion kWh in 2011 (EIA, 2013). Electricity generation from solar energy has also been found to increase from 0.64 million kWh in 2002 to 37.72 million kWh in 2011.

Ethanol and biodiesel are liquid fuels derived from biomass. The United States started the use of 10% ethanol (E 10) in most of the available gasoline from 2012. U.S. Environmental Protection Agency (EPA) has also approved 15% ethanol blend in new cars and light trucks. A large amount of ethanol production is from starch biomass such as corn and soybean. However, ethanol production from cellulosic biomass is minimal and it is far away to meet targets set by the Energy Independence and Security Act of 2007 (EISA 2007).

2.2 Fossil Fuels

Fossil fuels such as coal, oil and natural gas are non-renewable energy sources generated by anaerobic decomposition of organisms buried under the earth (Osueke and Ezugwu, 2011). The global view is that it took millions of years to form fossil fuels and hence they are not considered as renewables (Mckendry, 2002). Therefore, fossil fuel resources are limited but their demand is increasing daily. Researchers have different views on fossil fuel reserves and it is not known when fossil fuel reserves will be completely exhausted (Shafiee and Topal, 2009). For example, Salameh (2003) stated, “global oil supplies will only meet demand until global oil

production has peaked sometime between 2013 and 2020". Asif and Muneer (2007) documented that coal reserves in India, China, Russia and USA will be consumed in 315, 83, 1034 and 305 years, respectively. Further, estimates exist that liquid fuels have reached maximum production in Turkey and will be depleted by 2038 (Akpinar et al., 2008).

Although combustion of fossil fuels releases energy, greenhouse gases like carbon dioxide, methane, and nitrous oxide are also produced (Kennedy et al., 2010; Macedo et al., 2008). These greenhouse gases (GHGs) form a blanket around the earth which prevents heat from escaping, thereby causing an increase in temperature and climatic changes. Activities such as deforestation, industrial processes and agricultural activities also contribute to greenhouse gas emissions (Kennedy et al., 2010; Lal, 2004).

Renewable energy sources can contribute towards meeting the future energy demands of the world by reducing the significant proportion of fossil fuels. Renewables are environment friendly due to their potential to reduce greenhouse gas emissions. Several countries are increasing investment in renewable energy sources (Asif and Muneer, 2007; Wei et al., 2010). For example, the projected increase in renewable energy production in India, China and the United States is shown in Figure 2.4.

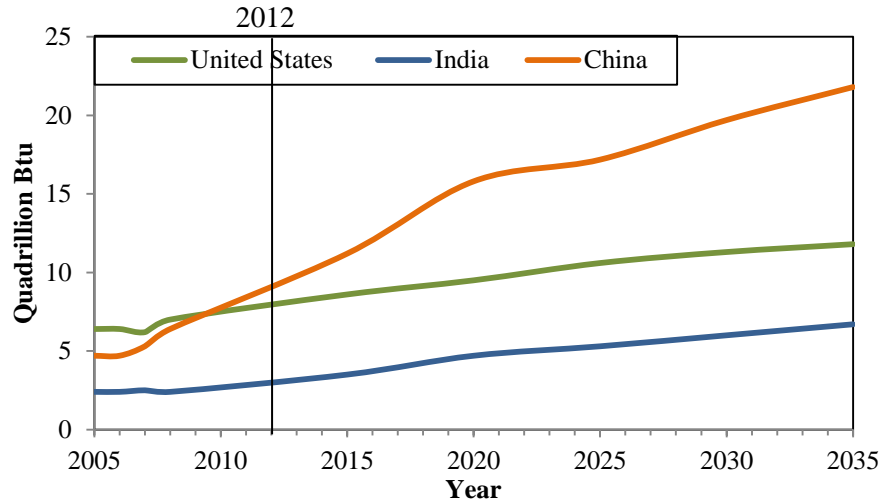


Figure 2.4. Renewable energy production in the United States, India and China (EIA, 2013).

2.3 Bioenergy

Bioenergy is energy derived from biomass which includes but not limited to dedicated energy crops, agricultural crops and trees, food, feed and fiber residues, aquatic plants, forestry and wood residues, industrial and municipal waste, processing byproducts and non-fossil organic material (ASABE S593.1, 2011). Biomass is produced through photosynthesis, during which plants produce the organic material by using CO₂ from atmosphere and water from ground in the presence of sunlight (Wei et al., 2010).

The United States has continued to increase bioenergy production because it provides energy security and does not add to the environmental problems caused by the use of fossil fuels. According to Energy Independence and Security Act of 2007, 21 billion gallons of cellulosic ethanol and advanced biofuels must be produced by the year 2022. Regular and sustainable supply of feedstock is mandatory to meet these targets. There is an abundance of feedstock in terms of forest trees and agricultural crops. According to “Billion Ton Study” the United States can produce 1.18 billion tons of non-grain biomass that can be used for biofuel productions (Perlack et al., 2005).

Forest trees are grown approximately on one third (749 million hectare) of the nation's total land (Simmons et al., 2008). About two third (204 million hectares) of forest land is classified as timberland which is a potential biomass source. Loblolly pine is one of the dominating species of southern forests and it occupies 51 million acre land (Murphy et al., 2012). According to Williams and Gresham, (2006), 15.2 Mg/ha of total biomass can be produced every year from loblolly pine tree by intensive management. This means a large amount (353.82 million tons per year) of loblolly pine tree is potentially available for bioenergy.

The United States has 181 million acres of land for agriculture. Grain and oilseeds are the major feedstocks that are currently used for producing ethanol, biodiesel and byproducts. Food and feed processing residues can also be used to generate energy. Agricultural land only provides 25% of total feedstock used for bioenergy industry (Simmons et al., 2008). This contribution can be increased by increasing land used for dedicated energy crops such as perennial and woody crops (Perlack et al., 2005).

Biomass can be transformed into heat and power, transportation fuels and chemical feedstock (Figure 2.5) by two main pathways, thermochemical conversion and biochemical conversion. Choice of conversion technique depends on various factors such as amount and type of feedstock, desired form of energy, economic and environmental conditions (McKendry, 2002).

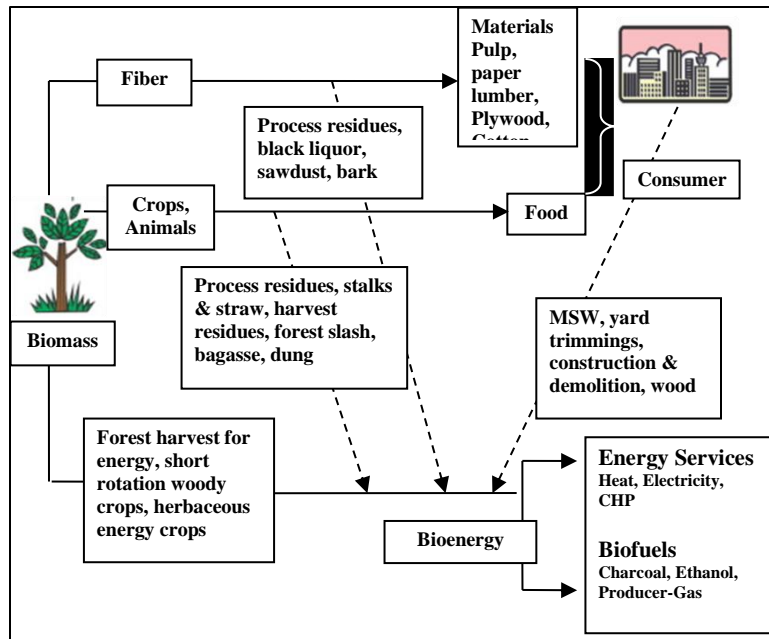


Figure 2.5. Flow chart showing conversion of biomass into bioenergy (Akpınar et al., 2008).

2.3.1 Thermochemical Conversion

Thermochemical conversion is considered more time efficient (in terms of seconds or minutes) compared to biochemical conversions (several days or weeks and even longer). Thermochemical conversion techniques are used to convert biomass into solid, liquid or gaseous products, are combustion, gasification, pyrolysis, and liquefaction (McKendry, 2002; Zhang et al., 2010).

2.3.1.1 Direct Combustion and Co-firing

Direct combustion of biomass was used for cooking and heating purposes in the past and is still being used in developed countries for power generation. Few examples of biomass power plants in the United States are: Alexandira (location: NH), Aspen Power (location: TX) and Cadillac (location: MI). Direct combustion produces heat (800-900°C) that are used to produce steam, mechanical power or electricity by using various equipment such as stoves, furnace, boilers, turbines etc. (Figure 2.6). Direct combustion is a very reliable technology due to its low

cost. Although, biomass of high moisture content (up to 50%) can be used for combustion, the process is not efficient at this high moisture content since the energy content of biomass varies inversely with moisture content. Fouling and corrosion problems are also associated with the combustion of biomass because of the presence of alkali metals and other elements (such as silicon, sulphur, chlorine, calcium and iron) in biomass ash (Zhang et al., 2010).

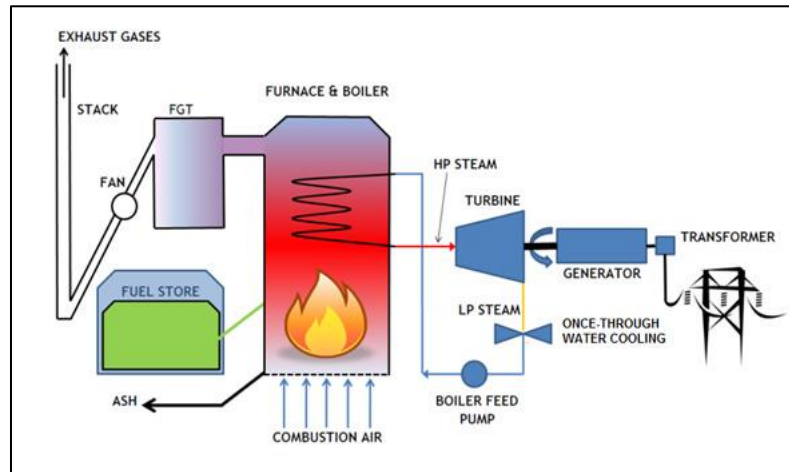


Figure 2.6. Schematic diagram of biomass power plant (Biomass, 2013).

Biomass can also be co-fired with coal for electricity generation. Examples of power plants in the United States where biomass is co-fired with coal are Schiller Station, Portsmouth, NH (co-fire fuel is wood), Boardman Plant, Boardman, OR (co-fire fuel is torrefied biomass), and Mount Poso Cogeneration Plant, Bakersfield, CL (co-fire fuel is agricultural and residential waste) (Nichols, 2012). Co-firing of biomass with coal also reduces the CO₂ emission. According to Mann and Spath (2001), 5 and 15 percent of biomass co-fired with coal can reduce CO₂ emissions by 5.4 and 18.2 percent, respectively. Co-firing of biomass is a cost effective technology and coal based power stations can be used with few modifications. Various types of biomass such as wood based, agricultural residues, dedicated energy crops and herbaceous materials can be co-fired with coal at different ratios (maximum up to 15%) (Zhang et al., 2010). Although, co-firing technology has been improving constantly, there are many problems resulting

from highly variable characteristics of biomass which includes high moisture content, volatile content, low calorific value and density compared to coal. Biomass also has high alkali content in ash which causes fouling, slagging and corrosion of reactors (McIlveen-Wright et al., 2007).

2.3.1.2 Pyrolysis

Pyrolysis is the thermal decomposition of biomass in the absence of oxygen. It converts biomass into the bio-char, bio-oil and gases at a high temperature (200-600°C) (Babu, 2008). Depending upon temperature and heating rate pyrolysis is divided into three types: fast pyrolysis, intermediate pyrolysis and slow pyrolysis. High temperature and high heating rate are essential to get high bio-oil yields and low temperature and low heating rates are preferred for more charcoal production (Zhang et al., 2010). Bio-oil can be used for power generation, as a feedstock for production of chemicals, and as a transportation fuel. In addition, bio-char can also be used as a soil amendment and carbon sequestration agent. High viscosity, thermal instability, corrosive nature (due to high acidity), and aging are major problems associated with bio-oil. A lot of techniques such as hydrodeoxygenation, catalytic cracking of pyrolysis vapors, emulsification, steam reforming and chemical extraction have been developed to overcome these issues (Zhang et al., 2007).

2.3.1.3 Gasification

Gasification involves conversion of biomass into combustible gases such as CO, CH₄, and H₂ at high temperature (800-1000°C) in the presence of oxygen. The process can be split into three stages: drying (>150°C), devolatilization (150-700°C) and gasification (800-1000°C). The mixture of H₂ and CO called 'syngas' can not only be used in power generation, but also in chemical production through Fischer-Tropsch synthesis (McKendry, 2002; Zhang et al., 2010). Gasifiers are characterized according to types of bed as fixed-bed and fluidized bed. Fixed-bed gasifiers further divided into two categories as updraft and down draft gasifiers, depending upon the types of flow. In the case of updraft, biomass is introduced from the top while in downdraft,

biomass is introduced from the bottom. Downdraft and updraft are most commonly used in past (Gómez-Barea and Leckner, 2010). Biomass gasification has many advantages such as low greenhouse emission, complete combustion, high thermal efficiency and compact equipments. However, it is not widely accepted for industrial uses because of its high initial investment (Zhang et al., 2007).

2.3.1.4 Liquefaction

Liquefaction is a technique to convert biomass into liquid form at low temperatures (280°C –420°C) and high pressures (5-20 MPa) in the presence of hydrogen and a catalyst. The process involves biomass breaking into smaller reactive molecules in water, which undergo polymerization to form oil mixtures of various ranges of molecular weight. Although, liquefaction is a costly process compared to pyrolysis, biomass of high moisture content can be processed without pre-drying (Qian et al., 2007).

2.3.2 Biochemical conversion

Biochemical conversion is the process of breaking down the carbohydrates in biomass into sugars in the presence of enzymes, acids, bases, solvents or other reagents. Catalyst and or microorganisms are then used to transform the sugars into biofuels (DOE, 2013). Although, biochemical process can operate on small scale with low maintenance, thermochemical conversion is highly preferred due to its ability to accept a wide range of biomass as feedstock (Jeguirim and Trouvé, 2009). The various biochemical conversion methods are described in details below.

2.3.2.1 Anaerobic Digestion

Anaerobic digestion is a type of biochemical conversion which involves decomposition of biomass (biomass of high moisture content, animal manure and food processing waste) in the absence of oxygen (Figure 2.7). Symbiotic groups of bacteria play a major role in this conversion

process. Some of the bacteria along with their roles have been discussed below. Hydrolytic bacteria hydrolyze the complex structure of biomass into sugars and amino acids. Fermentative bacteria change sugars and amino acids into acids. Acidogenic bacteria convert these acids into hydrogen and carbon dioxide. Methanogenic bacteria convert these products into biogas which is used for energy purposes such as cooking, heating and electricity production. The landfill methane gas is an example of anaerobic decomposition (Weiland, 2010).

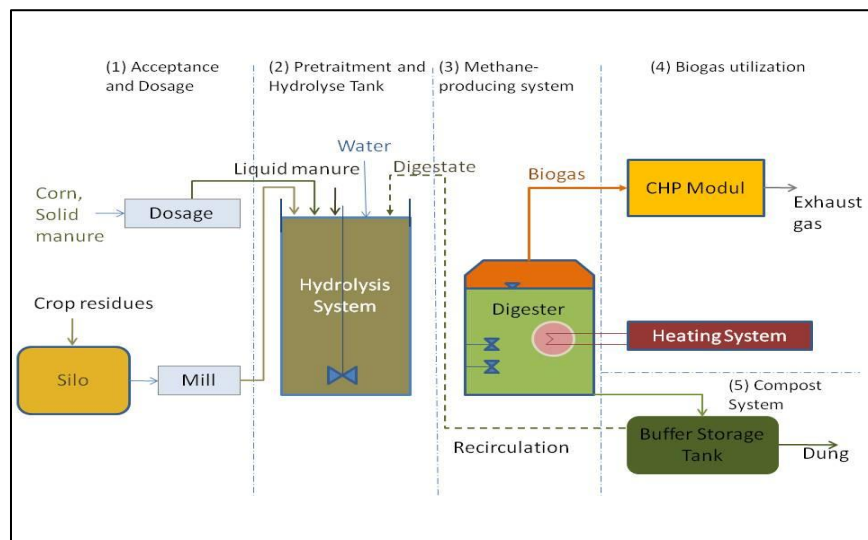


Figure 2.7. Schematic diagram of aerobic digestion (Biogas Technology, 2013).

2.3.2.2 Ethanol Production

Biochemical conversion is the main method to produce ethanol from biomass. Feedstock for ethanol production can be divided into three categories: 1) sugar-containing feedstock (sugar cane, sugar beet, sweet sorghum and fruits), (2) starch containing materials (corn, milo, wheat, rice, potatoes, cassava, sweet potatoes and barley), and (3) lignocellulosic biomass (wood, straw, and grasses) (Figure 2.8) (Balat and Balat, 2009). Sugar containing biomass are easily converted into ethanol by crushing, mixing with water and yeast and allowing the mixture to stay in large tanks in order to extract sugar. The yeast is used to transform the sugars into ethanol by breaking

them down which is followed by removal of impurities and water by distillation. Some ethanol is lost during distillation and high yield of ethanol can be achieved by secondary distillation. A high yield of ethanol can be obtained from starch materials but hydrolysis of the starch is required before fermentation of the resulting sugar into ethanol. Although, ethanol production from sugar and starch crops looks attractive, it creates a huge burden on agricultural land to produce more food crops (Naik et al., 2010).

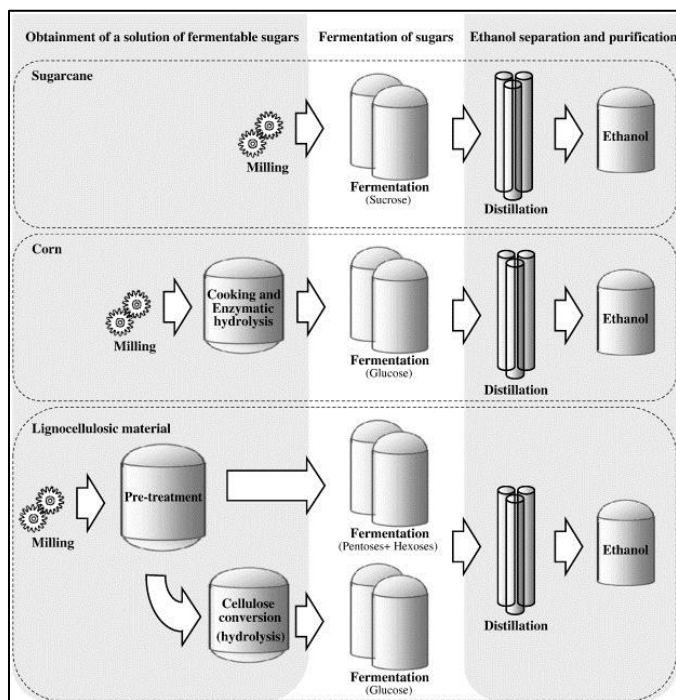


Figure 2.8. Schematic diagram of ethanol production (Mussatto, et a., 2010).

Cellulosic biomass is a cheap source of biomass for ethanol production because it is available in abundance. But economic and technological challenges are currently associated with ethanol production from lignocellulose crops due to chemical structure of lignocellulosic crops. Lignocellulosic biomass mainly consists of lignin, cellulose and hemicellulose. Cellulose and hemicellulose form about the two thirds of the cell wall of lignocellulosic feedstocks, are polysaccharides they can be converted into sugars by hydrolysis and then fermented into ethanol.

Hence, ethanol production of biomass depends only on cellulose and hemicellulose content. Cellulose is the main component of lignocellulosic biomass and it consists of long polymers of glucose. Inter linkages and hydrogen bonding in the cellulose makes it rigid. Hemicellulose consists of short and highly branched polymer of five-carbon (xylose and arabinose) and six carbon sugars (alactose, glucose, and mannose). Hemicellulose can be easily hydrolyzed into sugars due to its amorphous nature. The main problem is the rigid structure of lignocellulosic biomass in its conversion to ethanol. Biochemical conversion of lignocellulose involves pretreatment, hydrolysis, fermentation and product separation. Pretreatment is an important step in ethanol production because it is needed to break down the cellulosic and hemi-cellulosic structures (Figure 2.9). Lignocellulosic biomass cannot easily be hydrolyzed if pretreatment is not efficient. Different types of pretreatment methods such as physical (milling and grinding), physico-chemical (steam explosion/autohydrolysis, hydrothermolysis, and wet oxidation), chemical (alkali, dilute acid, oxidizing agents, and organic solvents), and biological processes have been used (Balat, 2011; Zhu and Pan, 2010; Mosier et al., 2005). Steam explosion is the most commonly used pretreatment method for ethanol production from lignocellulosic biomass (Parveen Kumar et al., 2009).

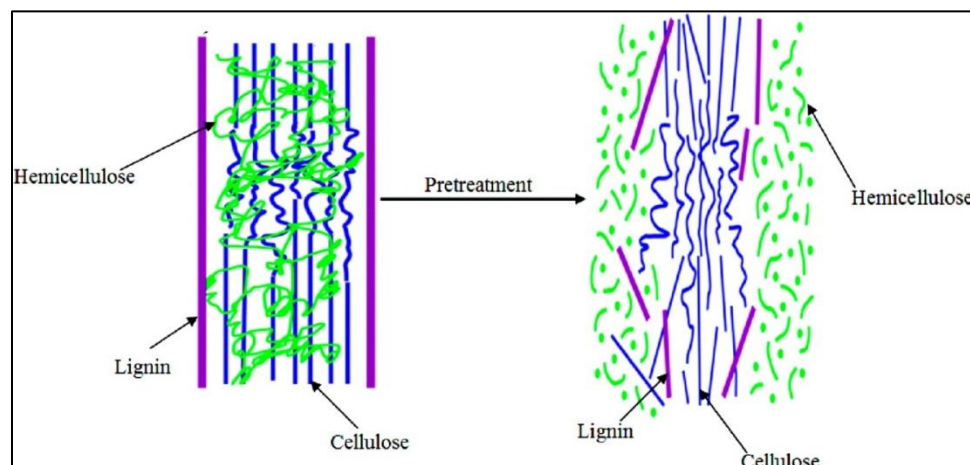


Figure 2.9. Pretreatment of lignocellulose crops for ethanol production (Kumar et al., 2009).

2.3.2.3. Biodiesel

Vegetable oil and animal fat can be transformed into biodiesel by transesterification process. Vegetable oil and animal fat are composed of triacylglycerol (TAG), which consists of long-chain fatty acids that are chemically bound to a glycerol (1,2,3-propanetriol) as shown in Figure 2.10. In transesterification process, TAG react with monohydric alcohol in the presence of catalyst at elevated temperature to form free fatty acids (FAAE) and glycerol (Figure 2.10) (Moser, 2011). It is a stepwise process in which the alcohol initially reacts with TAG to produce FAAE (bio-diesel) and diacylglycerols (DAG), DAG then reacts with alcohol to produce another molecule of FAAE and generates monoacylglycerols (MAG). Further reaction of MAG with alcohol yields glycerol and FAAE. Total yield of bio-diesel is obtained by the sum of FAAE produced at each step. Biodiesel can be directly used or mix with diesel to run the internal combustion engine. Biodiesel has many advantages compared to diesel such as low toxicity, inherent lubricity, superior flash point and low exhaust after burning. However, problems are associated with the use of biodiesel due to its high viscosity, low stability against oxidation and low volatility resulting in incomplete burning (Moser, 2011; Yusuf et al., 2011).

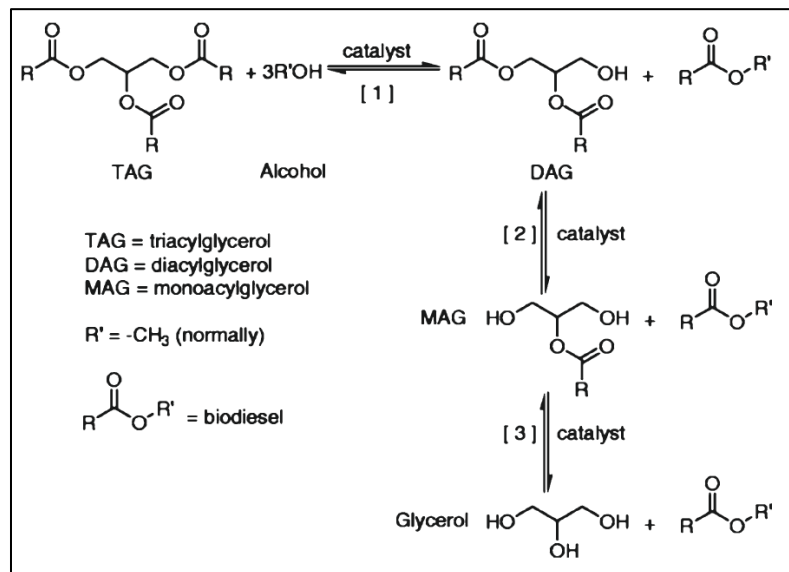


Figure 2.10. Chemical process to produce biodiesel from vegetable oil (Moser, 2011).

2.4 Biomass Logistics and Pre-processing

Biomass logistic is composed of unit operations, steps that are used to process and prepare the biomass after harvesting and before they get to the throat of bio-refinery plants (Figure 2.11). According to Energy Independence and Security Act, 2007, about 1 billion tons of biomass will be required to produce 36 billion gallons of biofuel by 2030. This requires a regular and adequate supply of biomass, a cost effective and optimal logistic system.

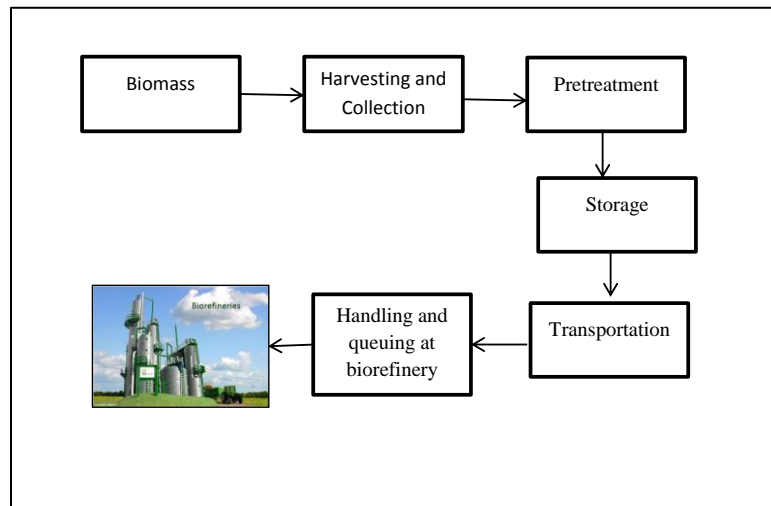


Figure 2.11. Flowchart representing a Biomass logistics system.

The major problem in biomass logistics is the low density and high moisture content of biomass which results in problems during transportation, storage and utilization. (Fasina, 2008; Petrou and Pappis, 2009; Sokhansanj et al., 2009). Additional energy is required to reduce the moisture in biomass destined for combustion because of the influence of high moisture content on efficiency of combustion (Hoffa et al., 1999; Lewandowski and Kicherer, 1997). Problems related to low bulk density can be solved by densification of biomass such as pelletization and briquetting (Tumuluru et al., 2010). However, densification involves energy intensive processes such as drying, grinding and compaction.

Handling and collection, preprocessing and storage of biomass require the use of equipment such as hammer mill, mechanical conveyors (screw augers, belt conveyor), cyclones, dryers, screening and classifying equipments. According to Echhoff (2003) and Abbasi and Abbasi (2007), these equipment cause dust generation when bulk material such as biomass are handled and processed. For example, fine particles present in the biomass are released in the form of dust during the free fall as shown in Figure 2.12.

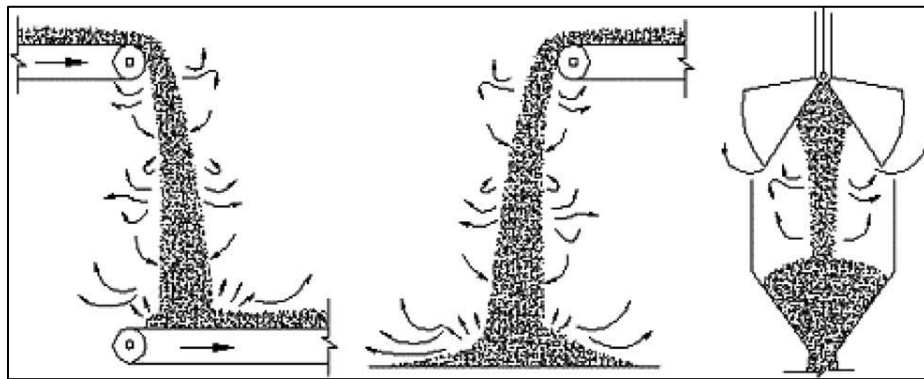


Figure 2.12. Dust generation during the handling of biomass (Wypch et al., 2005).

The amount of dust generated during biomass handling and processing depends on the feedstock, its moisture content and types of machines and equipment used for processing (Khan et al., 2008). However, only limited information is available with the research literature on the dust generation from biomass. Scholtz et al., (2009) observed that 14.8% of dust was generated during grinding of hay (*Medicago sativa L.*) through hammer mill. Madsen et al. (2004) studied the dustiness of straw, wood chips, and sawdust pellets and briquettes. Dust was generated by using rotating drum as air was passed through it. Number of particles (0.75-3.5 μm) in the air flow was measured and dustiness of biomass was expressed as number of particles/L of air. Straw was (100000-1500000/L air) dustiest biomass sample and wood pellets (150-1000/L of air) were less dusty compared to wood chips (5000-10000/L air) and sawdust briquettes (10000-15000/L air).

2.5 Health Problems from Dust

In addition to dust generation from processing equipment as described in the last section, dust can also be generated from harvesting and collection operations such as cutting, windrowing and bailing. The dust generated from these operations that contain microorganisms and endotoxins that cause health issues such as skin and eye irritation, lung and skin cancer and other respiratory problems (Clausnitzer and Singer, 2000).

A survey of dust exposure was conducted in 10 wood processing plants in the United States that included sawmill, plywood assembly plants, secondary wood milling operations, and factories producing finished wood products such as wood furniture and cabinets. Dust exposure was determined by dividing dust in to three fractions; respirable ($<10\mu\text{m}$), thoracic ($10\text{-}100\ \mu\text{m}$) and inhalable ($<100\ \mu\text{m}$). There were 2430 samples of different fractions were collected by using RespiCon Personal Particle Sampler. Overall, geometric mean (geometric standard deviation) exposure levels were found to be 1.44 (2.67), 0.35(2.65), and 0.18 (2.54) mg/m^3 for the inhalable, thoracic, and respirable fractions, respectively. Dust exposure level in the furniture manufacturing plants was significantly higher than those in sawmill and plywood assembly plants, wood milling plants, and cabinet manufacturing plants. However, only 1% of total samples were at or above the minimum exposure limit by OSHA ($5\ \text{mg}/\text{m}^3$) (Kalliny et al., 2008).

Madsen et al. (2004) reported the amount of microorganism in different types of biomass-- straws, wood chips, sawdust briquettes and pellets using various methods. High amount of actinomycetes, bacteria, muramic acid, endotoxin, LPS was observed in the straw dust compared to other biomass. Less amount of microorganism was observed in wood pellets and wood briquettes. The concentrations of endotoxin and fungi were high in straw and wood dust, respectively. For example, dust generated from straw contained 3610 EU/mg and dust obtained from wood chips contained 7.3×10^6 fungal spores/mg. It was also observed that $3\text{mg}/\text{m}^3$ of straw or wood dust contain enough amounts of endotoxin and fungi that can cause various health

problems. Hence, selection of biomass based on the presence of microorganism is very important to avoid health problems.

2.6 Combustible Dusts

As explained earlier, dust generation is a problem associated with handling and processing of biomass. Biomass dust is combustible in nature and can result in fires and explosion. National Fire Protection Association defined combustible dusts as follow:

NFPA, (2007) defined deflagrable wood dust as “wood particulate with a median diameter of 420 micrometers (m) or smaller in diameter (i.e., material passing through a U.S. No. 40 Standard sieve) having a moisture content of less than 25 percent (wet basis) that presents an explosion hazard when dispersed and ignited in air.”

NFPA 499 (NFPA, 2008a) defined combustible dust as “any finely divided solid material that is 420 micrometers (μm) or smaller in diameter (material passing through a U.S. No. 40 Standard sieve) that presents an explosion hazard when dispersed and ignited in air.”

NFPA 61 (NFPA, 2008b) defined agricultural dust as “any finely divided solid agricultural material that is 420 micrometers (μm) or smaller in diameter (material passing through a U.S. No. 40 Standard sieve).”

Calle et al. (2005) also mentioned that the dust particles have a diameter greater than 500 μm do not contribute significantly in dust explosions and this is close to the NFPA definition of dust. However, Echhoff, (2003) explained that fibers and flakes can also contribute significantly to dust explosions, though they cannot pass through a screen size of 420 micrometers (U.S. No. 40). Rate of burning of the material is directly proportion to the surface area. A spherical particle of 5 μm diameter when compressed into a flake having 0.2 μm thickness and about 20 μm length increases its surface area by 8 times. Hence, flakes of the same volume as sphere cannot pass through the same screen but can be burnt quickly due to increase in its surface area. NFPA 654

(NFPA, 2011) now corrected the definition of combustible dust as follows “a combustible particulate solid that presents a fire or deflagration hazard when suspended in air or some other oxidizing medium over a range of concentrations, regardless of particle size or shape.”

2.7 Ignition of Dusts

The three elements that are essential for combustible dusts to ignite are fuel (dust), oxygen and heat. These elements form what is known as fire triangle as shown in Figure 2.13. Fires and explosions due to the ignition of dusts or bulk materials are considered as one of the serious problems in processing industries (Eckhoff, 2000; Krause and Schmidt, 2001; Janes et al., 2008). Experiments and models were developed on ignition of combustible dusts and effects of various factors such as volume-surface ratio, size and shape of pores, volatiles and moisture on ignition have been studied (Gray et al., 2002; Schmidt et al., 2003; Wang et al., 1998).

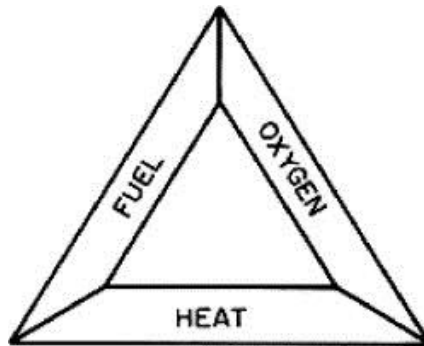


Figure 2.13. Components of fire triangle (fuel, oxygen and heat) (Gillman and Le May, 2007).

2.7.1 Ignition Sources

Energy or heat required for an ignition of dust is generally provided by an ignition source. The potential ignition sources that are found in processing plants include:

- 1) Open flames
- 2) Hot works such as welding and cutting
- 3) Hot surfaces

- 4) Burning dust
- 5) Mechanical impacts
- 6) Electric and electrostatic spark (Abbasi and Abbasi, 2007; Eckhoff, 2003; Taveau, 2012)

Hot surface is the most common ignition source for combustible dusts. Hot surface provides the required energy to initiate the ignition of dusts. Dust layer settled on the hot surface acts as insulation and minimizes heat loss. As a result, temperature of dust can increase to its ignition temperature thereby resulting in combustion. (Eckhoff, 2003).

Experimental work was done in past to find the relation between the depth of dust layer settled on hot surfaces and ignition temperature was determined. For example, minimum ignition temperatures of wheat flour dust layers with depth of 5 mm, 20 mm and 40 mm were 311 °C, 265 °C and 238 °C, respectively. Hence, minimum ignition temperature of dust increased with decrease in depth and similar results were obtained by Lebecki et al. (2003).

Shape and geometry of dust layer can also effect the ignition of combustible dusts. Joshi et al. (2012) studied the effect of geometry on the ignition behavior of bituminous coal dust deposited between two hot surfaces forming wedges of 60° and 90°. Three thermocouples were inserted along the plane of the wedge cross-section at various heights from the apex (lowermost, middle and top). Ignition of coal occurred at 190° C in the 60° wedge while it started at the 195° C in the 90° wedge. This indicated that the geometry of hot surfaces affects the ignition properties of dust settled on it.

Ignition properties of combustibles were also measured with the thermogravimetric apparatus and differential scanning calorimeter. As an example, Ramirez et al., (2010) studied the ignition properties of two powdered material (icing sugar and wheat flour) and five agricultural dusts (maize, wheat, barley, alfalfa, soybean, and icing sugar). TGA variables such as temperature of combustion onset (TIC), the temperature of maximum weight loss (TMWL) and

temperature of oxidation (T_{charac}) were determined. The minimum temperature required for the onset of an exothermic reaction (TOE), the maximum temperature reached during that exothermic reaction (TDE), and the temperature required for the onset of a rapid exothermic reaction (TRE) were calculated by using the DSC. Icing sugar was more susceptible to ignition due to its lowest TIC (212° C) and TMWL (220° C) but its melting hindered its ignition. Wheat dust and flour had the highest TIC and TMWL and they were less susceptible to ignition. The TOE of all material ranged from 80-100° C. Other dusts such as maize, wheat, soybean, barley and alfalfa have high risk of self-ignition and bread-making flour has a medium risk of self-ignition.

2.7.2 Factors affecting Ignition

Moisture Content

Moisture content of dust affects the ignition behavior of material. Material with high moisture ignites at higher temperature and more energy is required to ignite it. Moqbel et al. (2010) determined the ignition temperature of different types of solid wastes (food, cardboard, yard waste, glossy paper, newspaper, office paper, textile waste, mixed solid waste) at different moisture contents (10%, 20% and 40% on wet bases) by using a programmable furnace. Ignition temperature of all types of waste increased with moisture content. For example, ignition temperature of yard waste was 250, 295 and 333 °C at 10%, 20% and 30% moisture contents. Hence, high moisture content of dusts is favorable for reduced ignitability.

Particle Size

Rate of burning of material increases when material is divided into small particles because material subdivision leads to increase in surface area. In addition, more air is available for combustion, when particles are small. In general, particle size affects the ignition properties of dust (Chen et al., 1996; Eckhoff, 2003). Sweis (1998) determined that particle size increased the ignition temperature of oil shale. Ignition temperatures of dust at particle size 75.3 and 212.3 μm were 640° C and 680° C respectively.

Ash Content

Ash content is a measure of amount of inorganic components in material. Ash content of dust acts as heat sink because of its incombustible nature and it inhibits the ignition of material. Biomass has generally low ash content (about 0.1-8.4%, d.b.) compared to coal (4-30%, d.b.). Different types of material were used in combustible dust to reduce their ignitability. For an example, ignition onset temperature of wheat straw (ash content is 0.1% on d.b.) was increased when coal (ash content is 9.7% on d.b.) was added in different ratios. Ignition started at 260, 276 and 426 °C, when wheat straw to coal ratio was 100:0, 50:50 and 0:50, respectively (Vuthaluru, 2003).

Volatile Matter

Ignition of dusts highly depends upon their volatile matter because it acts as a fuel for ignition. Biomass has high volatile matter (48-86%) and thereby can be easily ignited. Dust generated from biomass handling will also be easily ignited. Ignition temperature of coal and biomass decreased with an increase in volatile matter as shown in Figure 2.14. Ignition temperature of wheat straw (volatile content: 72% d.b.), popular wood (volatile content: 75% d.b.), lignite (volatile content: 51% d.b.), bituminous (volatile content: 32% d.b.) and anthracite (volatile content: 9.8% d.b.) were 210, 290, 300, 450 and 490° C, respectively.

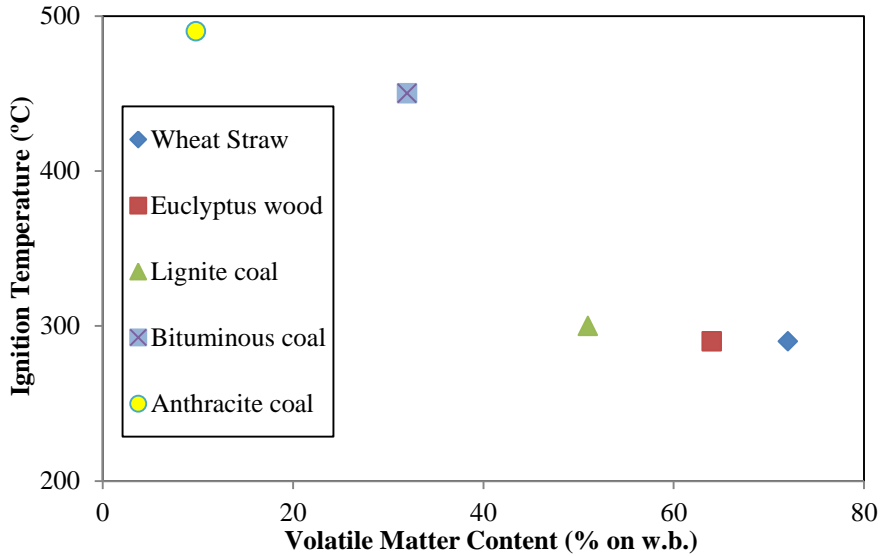


Figure 2.14. Effect of volatile content of material (coal and biomass) on ignition temperature (Grotkjær et al., 2003).

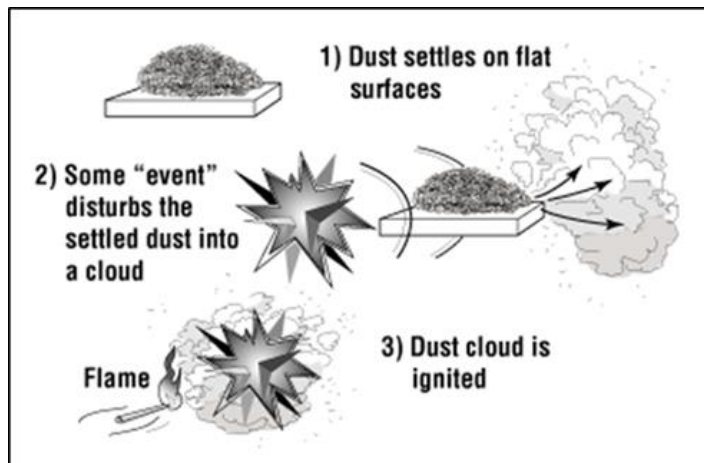


Figure 2.15. Dust explosion from ignited dust layer (Combustible Dusts, 2013).

2.8 Dust Explosion

As already discussed, dust generation is a problem with handling and processing of biomass. The dust particles settle on different parts of plant such as floor, equipments and can form a dust layer. Dust layer can be dispersed by an external source such as blow of air and as a

result, a dust cloud can be formed (Figure 2.15). If concentration of dust is high enough and it confined in a space, an explosions can occur when ignition source comes in contact with dust cloud. For example, a 1 mm layer of dust of bulk density 500kg/m^3 , when suspended in the space of 5 m^3 , can form the concentration of 100g/m^3 (Figure 2.16) (Amyotte and Eckhoff, 2010). The lower explosive limits of concentrations of sunflower flour, maize gluten, wheat processing waste are 125 g/m^3 , 100 g/m^3 , and 30 g/m^3 (Ramírez et al., 2009). Thereby it is possible for a 1mm layer (ignited) of biological material to cause an explosion in 5 m^3 rooms.

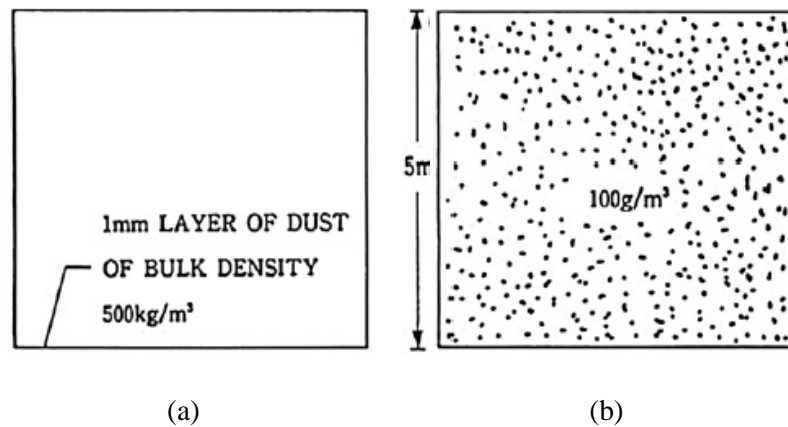


Figure 2.16. (a) A 1mm dust layer of biological material (bulk density is 500kg/m^3) (b) Dust forms a concentration of 100g/m^3 when dispersed in a room of 5 m^3 (Amyotte and Eckhoff, 2010).

However, dust layer can also be ignited when it directly comes into contact with ignition source. In this case, when dust layer suspended in air and forms the dust cloud, ignited dust itself acts as ignition source. The capability of ignited dusts to cause explosion has been studied by many researchers. Pinwasser (1986) reported that burning dust of a temperature of 700°C cannot cause ignition when fell through a dust cloud column (wheat flour). On the other hand, ignition of dust cloud occurred when smoldering dust of 25 mm and weighing 15 g, fell freely in column of 1 m length. Gummer and Lunn (2003) reported that smoldering dust can cause ignition when the

difference between the temperature of dust and the minimum ignition temperature of the dust cloud was high and burning dust was dispersed.

Hence, ignition of dust cloud by smoldering or burning of dust depends upon various factors such as temperature of burning dust, minimum ignition temperature of dust cloud, dispersion of nest, residence time of smoldering nest in dust cloud.

2.8.1 Factors effecting Dust Explosion Characteristics

Parameters such as minimum ignition energy (MIE), minimum ignition temperature (MIT), minimum explosion concentration (MEC), maximum explosion pressure (P_{\max}) and rate of explosion pressure rise $(\text{dip}/\text{dt})_{\max}$ are used to quantify dust explosion properties of material (Cashdollar, 2000; Nifuku et al., 2005). Minimum ignition energy is the amount of electrical energy required to ignite air/dust mixture at room temperature and atmospheric pressure. Minimum ignition temperature is the temperature of air at which combustion of dust particles begins. The minimum explosion concentration is the limiting value of concentration above which dust/air mixture can propagate a flame. Severity of the explosion depends upon maximum pressure and rate of pressure rise during the explosion (Echhoff, 2003). Dust explosion characteristics depend upon the physicochemical properties of dust and these are described below.

Particle Size

The particle size of dust affects its ignition and explosion properties. The rate of material burning increased with a decrease in surface area. The effect of particle size of Pittsburgh bituminous coal dust on MEC, P_{\max} and rate of pressure rise $(\text{dip}/\text{dt})_{\max}$ was determined by Cashdollar (1994). MEC increased with an increase in particle size but effect of small particles ($<100\mu\text{m}$) was negligible on MEC. No combustion occurred when a particle size was 200-300 μm existed. The maximum pressure and rate of pressure rise decreased with an increase in particle size. The maximum pressure during explosion was almost 6.5 and 6 bar when particle

size of dust was 10 and 100 μm , respectively. Rate of pressure rise was 80 and 60 bar.m/s, at a particle size of 10 and 100 μm , respectively (Cashdollar, 1994).

Particle size also affects the minimum ignition energy and minimum ignition temperature. Minimum ignition energy required to ignite magnesium dust cloud was about 4 and 230 mJ when the particle size was about 0-20 and 149-177 μm . The minimum ignition temperature was about 520° C and 650° C when particle size was 0-20 μm and 149-177 μm (Nifuku et al., 2007). Hence, the minimum ignition temperature and minimum ignition energy of dust cloud increased with an increase in particle size. Therefore, dust explosibility decreases with an increase in particle size.

Calle et al., (2005) characterized wood dust explosibility by developing a model based on chemical reaction, kinetics and thermodynamics. Severity of explosion was determined in terms of the maximum explosion rise and the rate of pressure rise. Experiment was also performed to compare the results. Wood dust was divided into four fractions according to size as 25-45, 45-71, 71-90 and 90-125 μm . Rate of pressure rise was 300 and 120 bar/sec when particle size were 25-45 and 90-125 μm respectively. Maximum pressure (about 7 bar) was almost same for four particle size fractions. The results obtained by model were close to experimental results.

Moisture Content

Moisture is generally present in combustible dusts depending on the hygroscopic nature of dusts, humidity in the atmosphere and internal moisture as in the case of biomass dust and has a strong influence on dust explosion characteristics (Khan et al., 2008 and Eckhoff, 2003). Since, severity of dust explosion depends upon the maximum explosion pressure and the rate of pressure rise during the explosion. Eckhoff (2003) explained the effect of moisture content in maize starch on rate of pressure rise. He concluded that the increase in moisture decreases the rate of rise in pressure during the explosion. Rate of pressure changed from 20 to 100 bars/s when moisture decreased from 25% to almost 0% (Eckhoff, 2003). Laar and Zeeuwen (1985) reported that the

minimum ignition temperature of maize starch increased with an increase in the moisture content. The minimum ignition temperatures at 13% and 0% moisture content were found to be 400 °C and 460 °C, respectively (Laar and Zeeuwen, 1985). The author also found that the minimum energy required to ignite the dust cloud of tapioca, maize starch and flour (wheat) increased with an increase in moisture content. The approximate MIE of tapioca changed from 20 to 200 mJ with an increase in the moisture from 1% to 7% (w.b.). MIE of flour varied approximately from 40 to 80 mJ with a change in moisture from 1% to 7% (w.b.). MIE of maize changed from 200 to 400 mJ when the moisture changed from 1% to 7% (Laar and Zeeuwen, 1985).

Dust Concentration

Dust concentration also affects dust explosion characteristics such as minimum ignition energy, minimum ignition temperature, explosion pressure and rise of pressure (Cashdollar, 2000). The effect of dust concentration of bituminous coal on maximum pressure and rate of pressure rise during explosion was studied by Cashdollar (1994). Maximum pressure (2 to 6.5 bar) and rate of pressure (10 to 30 bar.m/sec) increased with an increase in concentration (200 to 400 g/m³) of dust up to a dust concentration of about 400 g/m³ and after then become constant.

Chawla (1996) determined the amount of energy required for an explosion at different level of dust concentration of Pittsburgh coal. Ignition energy decreased with an increase in concentration of dust. When the concentration of dust was 50g/m³, about 5 kJ energy was required for explosion and 10 kJ ignition energy required when dust concentration was about 30 g/m³ (Chawla et al., 1996).

Nifuku et al. (2007) studied the effect of dust concentration and particle size of magnesium dust on its ignition temperature. It was observed that ignition temperature decreases with an increase in dust concentration. The lowest ignition temperature was 520°C when the dust concentration was about 100 g/m³ (Nifuku et al., 2007).

Chemical Properties of Dust

As already discussed, ash does not participate in ignition and explosion but it suppresses explosion of dust by absorbing heat released during explosion. High ash content material is used in combustible dusts to reduce the explosion risk (Abbasi and abbasi, 2007). Datidar and Amyotte (2002) studied the effect of fly ash (ash content is 90% on d.b.) on the explosibility of Pittsburgh pulverized coal (ash content is 6% on db). Explosion pressure reduced from 200 kPa to 100 kPa when concentration of fly ash increased from 75% to 80% and 200 kPa was the pressure limit to occur an explosion. Hence, a high percentage of fly ashes required to reduce the dust explosibility.

Volatile content in combustible dusts acts as fuel for explosion and also contributes to flame propagation. Effect of volatile content of coal dust on minimum explosion concentration was studied at three ignition energies (10, 5 and 2.5 kJ). MEC of dusts (<75 μm) of gilstonite coal (volatile content is 83%), Pittsburgh (volatile content is 34%), Oil shale (volatile content is 28%) and Pocahontas coals (volatile content is 16%) was determined. MEC of glistonite coal dust could be low (20 g/m^3) compared to other three coal types when 5 kJ energy was used for ignition and because of its high volatile content of glistonite coal. Pittsburgh and Pocathontas coal have MEC of 50 g/m^3 at 5kJ ignition energy although their volatile contents were different. They observed that when particle size of Pocathontas coal was small (<100 μm), they produce same amount of volatile content as Pittsburgh coal. Oil shale has higher minimum explosion concentration (160 g/m^3) compared to Pocathontas coal (30 g/m^3) at 5kJ ignition energy. High ash content in oil shale dust (ash content of Pocahontas coal, Oil Shale is 5 wt%, 70 wt%, respectively) act as heat absorber and hence required more explosion concentration to occur a dust explosion. Dust explosion risk is decreased if volatile content of dust is reduced. This principle is used to mitigate the dust explosion risk by adding material of high ash content.

Summary

Problems related to fossil fuels (coal, petroleum and natural gas) initiated a pursuit to look for alternative fuels. Renewable energy sources (biomass, solar energy, geothermal and wind energy) are abundant on the earth and can be transformed into energy by different methods and technologies. Biomass is one of important renewable energy resource which can be converted into heat, syn-gas, bio-oil, char, and ethanol by different techniques. A large amount of biomass is available in southern forests of United States in the form of loblolly pine tree to feed bioenergy industry. Dust can be generated during the harvesting, handling and processing of loblolly pine tree. High level of microorganisms, enzymes and endotoxins are observed in the biomass dust. Hence, working with the dust can cause the health problems such as eye irritation, respiratory problems, pulmonary diseases and allergies. Ignition and explosion risks are also associated with the bioenergy industries because of the combustible nature of dust from biomass. Physical properties of dusts such as particle size, moisture content affect ignition as well as explosion properties. High ignition and explosion risk is associated with the combustible dusts of small particle size and low moisture content. Chemical properties (ash content and volatile matter) of dust also influence their ignition and explosion behavior. Volatile matter content is very important property because it acts as a fuel for ignition. Ash content acts as a heat absorber and suppresses the ignitability and explosibility of dusts. Hence, it is important to understand the physicochemical and ignition properties of loblolly pine dust to avoid ignition and explosions accidents in the bioenergy industry centered on it.

Chapter 3 Physicochemical Properties of Ground Material and Dust

3.1 Abstract

Biomass conversion into energy is important to reduce the world's dependence on non-renewable energy resource because biomass is the only renewable resource of carbon that can be used to manufacture carbon-based liquid fuels, chemicals and products that are currently obtained from petroleum. Different types of equipment equipment such as grinders, mixers, dryers and conveyors during processing and handling of biomass. These equipment generate dusts when used on solid materials such as biomass. Dusts deposited around machinery and in processing plants can cause heating and ignition that can lead to explosion. Therefore, a study was conducted to quantify the effect of loblolly pine wood chip's moisture content and hammer mill screen size on the energy consumption and amount of dust generated during grinding. Physiochemical properties of the ground material and dust were also determined. Wood chips were conditioned to three different moisture contents (4.75%, 14.74% and 23.56% on w.b.) and ground through three different hammer mill screens (1.20, 3.18 and 6.35 mm). Grinding energy increased from 39.65 to 360.00 kJ/kg when the moisture content and screen size changed from 4.75% and 6.35 mm to 23.56% and 1.20 mm, respectively. The amount of dust generated decreased with increase in moisture content and screen size. About 21.50% of the dust was observed in ground material with wood chips at a moisture content of 4.75% was ground through the 1.20 mm hammer mill screen. From this study, moisture content and screen size were found to have a significant influence on physicochemical properties of ground material as well as dust obtained from loblolly pine.

3.2 Introduction

The world relies heavily upon fossil fuels such as petroleum products, coal and natural gas for its energy needs; Fossil fuel is however limited and may not be sufficient to meet the increasing energy requirement of the world in the near future. By the end of 2035, the world population is projected to increase to 8.1 billion which would require 700 quadrillion Btu of energy (EIA, 2013). In addition, fossil fuels produce greenhouse gases such as carbon dioxide, methane, water vapor, ozone, fluorocarbons and nitrous-oxide which are responsible for the rise in atmospheric temperature and various climatic changes (McKendry, 2002).

Renewable energy resources such as hydropower, wind, solar, geothermal, and bioenergy have the potential to reduce our reliance on fossil fuels and greenhouse gas emission. Bioenergy is the only renewable that can supply the carbon required to manufacture transportational fuels, chemicals and products. Bioenergy is obtained from plants and animal biomass which includes but is not limited to dedicated energy crops, agricultural crops and trees, food, feed and fiber residues, aquatic plants, forestry and wood residues, industrial and municipal waste, processing byproducts and non-fossil organic material (ASABE S593.1, 2011).

Most countries are increasing investment in the bio-based economy for energy security and environmental safety reasons. For example, United States has a target to produce 16 billion gallons of ethanol from cellulosic biomass by 2022. This is projected to reduce crude oil consumption by 20% (EISA, 2007). Currently, there are about 51 million acres of forestland is occupied by loblolly pine tree (Murphy et al., 2012). Therefore, a large amount of the required biomass in the United States will be obtained from loblolly pine tree. According to Williams and Greshman, (2006), 15.2 Mg/ha of total biomass can be produced from loblolly pine tree by intensive management. Therefore, a large amount (353.82 million tons per year) of the required biomass in the United States will be obtained from loblolly pine tree.

After harvesting, biomass have to be stored, processed and transported before they can be converted into energy, products and chemical (Mani et al., 2004). These unit operations will require the use of various equipment such as hammer mills, mechanical conveyors (screw augers, belt conveyor), cyclones, dryers, screening and classifying equipment. However, these types of equipment generate dust when they are used to handle and process bulk solid materials such as biomass (Abbasi and Abbasi, 2007; Eckhoff, 2003).

Biomass dust is combustible in nature. The National Fire Protection Association (NFPA) defines combustible dusts as any fine particles of diameter less than 420 μm (material can pass through the U.S. number 40 standard sieve) that present fire or explosion hazard when dispersed and ignited in air (NFPA, 2011). Combustible dusts are responsible for fires and explosions in the industries that handle or process the bulk material. The Chemical Safety and Hazard Investigation Board documented 281 fire and explosion accidents, caused by combustible dusts, in the United States between 1980 and 2005 in which 119 people lost their lives and 718 were injured (CSB, 2004).

Ignited dust is one of the main causes of fires and explosions in industries. Ignition requires the presence of fuel (dust), ignition source and oxygen (Abbasi and Abbasi, 2007). Hot surfaces, mechanical sparks, glowing cigarettes etc. can act as potential ignition sources. Ignition caused by hot surfaces (hot plates, bulbs, dryers, bearing, heated parts of equipments) is very common in processing plants because dust that settle on the hot surfaces act as insulation that inhibits heat loss and as a result the temperature of dust increases to the point of ignition (Eckhoff, 2003). Synnott et al. (1984) reported that the minimum ignition temperatures of flour of a depth of 5, 20 and 40 mm layers were 311°C, 265°C and 238°C, respectively. They found that the ignition temperature decreased with increase in depth of dust layer. Additionally, Joshi et al. (2010) determined the ignition temperature of bituminous coal dust settled between two hot surfaces forming wedges of 60° and 90°. They found that in a case of 90° wedge, ignition started at 195° C which was 5°C higher than 60° wedge.

An explosion can occur when all the five components (oxygen, dust, ignition source, dispersion of dust into air (mixing) and confinement) of the explosion pentagon are present and concentration of dust is high enough (Figure 3.1). Ignited dust can form a dust cloud when it is dispersed by mechanical action or blown by movement of air. Furthermore, ignited dust itself acts as ignition source for other dusts and can result in explosion (Eckhoff, 2003; Janes et al., 2008).

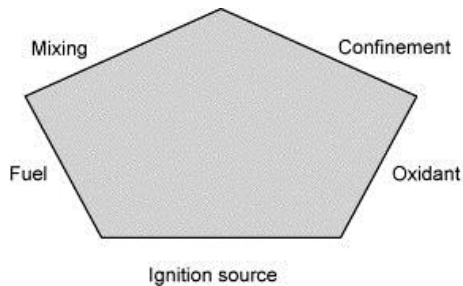


Figure 3.1. Dust explosion pentagon and its components (fuel, mixing, ignition source, oxidant, and confinement) (Abbasi and Abbasi, 2007).

Various researchers have indicated that ignition and explosion properties of dusts depend upon their physicochemical properties. Particle size of dust is one of the most important properties that affect ignition and explosion properties of dust because the total surface area exposed to oxygen increases as particle size decreases (Eckhoff, 2003; Abbasi and Abbasi, 2007). Small particles burn at low temperature and require less energy for ignition (Eckhoff, 2003). Nifuku et al. (2007) found that the minimum energy (MIE) required for the ignition of magnesium dust cloud was 40 and 120 mJ when the particle size was 0-20 and 149-177 μm , respectively. They also reported that the minimum ignition temperature (MIT) for magnesium dust was about 520°C and 650°C when particle size was 0-20 and 149-177 μm , respectively.

Dust with high moisture content ignites at high temperature and requires more energy to ignite because moisture in dusts acts as a heat sink with energy is wasted in vaporization of moisture. Laar and Zeeuwen, (1985) found that the minimum ignition temperature of maize

starch with 13% moisture and dry starch (almost 0%) were 460°C and 400°C, respectively. Similarly, the minimum energy required for ignition of maize starch increased from 200 mJ to 400 mJ when the moisture increased from 1% to 7%.

Since ash is incombustible in nature, it acts as an explosion inhibitor by absorbing the heat released during the explosion. Chawla et al. (1996) reported that dust concentration of 30 kg/m³ and 80 kg/m³ was required for ignition of oil shale and Pocahontas coal, respectively, the samples were exposed to the same amount of energy (5 kJ) was used. They attributed the differences in dust concentration to cause an explosion, to the high ash content of oil shale (70% d.b.) compared to Pocahontas coal (5% d.b.). In addition, volatile content in dusts is another important factor that affects the dust ignition. For example, ignition temperature of coal and biomass decreased with an increase in volatile content (Grotkjær et al., 2003). The ignition temperature of wheat straw (volatile content: 72% d.b.), popular wood (volatile content: 75% d.b.), lignite (volatile content: 51% d.b.), bituminous (volatile content: 32% d.b.) and anthracite (volatile content: 9.8% d.b.) were 210, 290, 300, 450 and 490 °C , respectively (Grotkjær et al., 2003).

Physicochemical properties are important to understand the ignition and explosion behavior of combustible dusts. However, limited information exists on the physicochemical properties of combustible dusts, and information in literature does not exist on loblolly pine dust in particular, considering its importance as a biomass resource in the United States. Therefore, the objectives of this study were to:

- 1) Determine the effect of hammer mill screen size (1.20 mm, 3.18 mm and 6.35 mm) and moisture content (5%, 15% and 25% on w.b.) on the amount of dust generated and energy required to grind loblolly pine chips.
- 2) Quantify the physicochemical properties of ground loblolly pine chips and dust collected from objective 1.

3.3 Materials and Methods

3.3.1 Wood Chips

Clean loblolly pine wood chips obtained from a forestland in south Alabama were used for this study. Moisture content of wood chips was determined according to ASTM standard E871-72 (ASTM E871-82, 2006) by placing 10 g sample in a conventional oven (Model No.-1370FM, Sheldon Manufacturing, Cornelius, OR) set at 105 °C for 24 hours. Initial moisture content of the chips (based on triplicates) was determined to be 53.2% on wet basis (w.b.).

3.3.2 Conditioning of Wood Chips

Wood chips were conditioned to a desired moisture levels (5%, 15% and 25% on w.b.) by drying in an oven (Excalibur Products, Sacramento, CA) at 45 °C and monitoring the mass of wood chips during the drying process. After drying, wood chips were kept in a closed container for 72 hours to allow moisture equilibration of the sample. The actual moisture contents of wood chips were determined after the 72 h equilibration period.

3.3.3 Grinding of Wood Chips

Wood chips were ground with a hammer mill (Model No.-10HBLPK, Sheldon Manufacturing, Tiffin, OH) using three different screen sizes (1.20, 3.18 and 6.35 mm). A known amount of wood chips was fed into the hammer mill manually. Energy required (kJ/kg) to grind the material was recorded with a watt meter (Model No.-A3314/01, EZ watt meter, Santa Ynez, CA) that was attached to hammer mill. The duration of grinding was also recorded. The energy required to run the hammer mill empty was also recorded before the material was introduced. Amount of dust in the ground material was obtained by passing the ground material through the 420 µm screen of a vibratory shaker (Model No.-K30-2-8S, Kason, Millburn, NJ) and weighing the mass of ground material that did not pass through the 420 µm screen. The amount of dust generated from wood chips ground through each screen was estimated as follows (equation 3.1).

$$\text{Quantity of dust} = \frac{M_{g1} - M_{g2}}{M_{g1}} \quad (3.1)$$

where

M_{g1} = Mass of ground material (kg)

M_{g2} = Mass of ground material that did not pass through the 420 μm screen (kg)

3.3.4 Moisture Content

Moisture content (MC) of dust and ground material was measured using a moisture content analyzer (Model No.-IR-200, Denver Instrument, Avrada, CO) according to ASTM standard E871-82 (ASTM E871-82, 2006) by placing 2 to 10 g of sample on the pan of the moisture content analyzer. This instrument provided moisture content on a wet basis.

3.3.5 Bulk Density

Bulk density (ρ_{bulk}) was measured by the Ohaus apparatus (Burrows Co., Evanston, IL) and according to the modified ASABE standard (ASABE S269.4, 2002). This measurement involved pouring the sample from a funnel into 1137 ml container. Bulk density was calculated from the ratio of mass of the material that filled in the container to the volume of the cylinder (equation 3.2).

$$\rho_{bulk} = \frac{\text{Mass}}{\text{Volume}} \quad (3.2)$$

3.3.6 Particle Density

The average volume of particles was estimated by a pycnometer (Model No.-AccuPyc 1330, Micromeritics Instrument Corp., Norcross, GA). by measuring the change in pressure when a known quantity of helium gas was passed through the pycnometer. Particle density (ρ_{part}) was

estimated from the ratio of the mass of material and volume measured by pycnometer (equation 3.3).

$$\rho_{part} = \frac{Mass}{Particle\ Volume} \quad (3.3)$$

3.3.7 Particle Size Distribution

Particle size distributions on volume basis of ground material and dust sample were determined with a digital image processing and size analysis system (Model No.- D-4278, Haan, Germany). Geometric mean diameter and geometric standard deviation were calculated from the data obtained from the equipment according to ASABE Standard S319.3 (2003).

$$d_{gw} = \log^{-1} \left[\frac{\sum_{i=1}^n (W_i \log \bar{d}_i)}{\sum_{i=1}^n W_i} \right] \quad (3.4)$$

$$S_{log} = \left[\frac{\sum_{i=1}^n W_i (\log \bar{d}_i - \log d_{gw})^2}{\sum_{i=1}^n W_i} \right]^{1/2} \quad (3.5)$$

$$S_{gw} = \frac{1}{2} d_{gw} \left[\log^{-1} S_{log} - (\log^{-1} S_{log})^{-1} \right] \quad (3.6)$$

where

d_{gw} is geometric mean diameter or median size of particles by mass (mm);

S_{log} is geometric standard deviation of log normal distribution by mass in 10-based logarithm (dimensionless);

S_{gw} is geometric standard deviation of particle diameter by mass (mm);

W_i is mass on i th sieve (g);

n is number of sieves plus one pan;

$\bar{d}_i = (d_i \times d_{i+1})^{1/2}$;

d_i is nominal sieve aperture size of the i th sieve (mm);

d_{i+1} is nominal sieve aperture size of the $i+1$ sieve (mm).

3.3.8 Ash Content

Ash content of the dust and ground material was determined using a Laboratory Analytical Procedure (LAP, 2005). According to this procedure, empty crucibles were placed in the muffle furnace (Model No.-F6020C, Thermoscientific, Dubue, Iowa) at 575 ± 25 °C for four hours. The crucibles were then removed and directly placed into the desiccator for at least one hour or until they cooled down to room temperature. Approximately 0.5 to 2 g, sample was placed into the tarred crucibles and the mass recorded to the nearest 0.1 mg. Crucibles with samples were placed in the muffle furnace and held at 105 °C for 12 minutes. The furnace was ramped to 250 °C at 10 °C/minute and held for 30 minutes. It was then increased to 575 °C at 20 °C/min and held for 180 minutes. After this, the temperature was allowed to drop to 105 °C before the crucibles were transferred to a desiccator to cool. Ash content was calculated on a dry basis using equation 3.7.

$$Ash(\%) = \frac{M_{ash} - M_{con}}{M_{od} - M_{con}} \times 100 \quad (3.7)$$

where

M_{ash} is the mass after heating (g)

M_{con} is the mass of the container (g)

M_{od} is the initial mass of dried biomass (g)

3.3.9 Volatile Matter

Volatile matter of dust and ground material was measured using the ISO 562 (ISO 562, 2010) method by exposing samples to a temperature of 900 ± 10 °C for 7 minutes in a volatile matter furnace (Model No.-VMF 10/6/3216P, Carbolite, Hope Valley, England). Volatile matter content (V_d) on dry basis was determined by using equation 3.8.

$$V_d = \left[\frac{100(M_3 - M_1)}{M_2 - M_1} - M_{ad} \right] \times \left(\frac{100}{100 - M_{ad}} \right) \quad (3.8)$$

where

M_1 is the mass, of the empty crucibles and lid (g)

M_2 is the mass, in grams, of the crucible and lid and the sample (g)

M_3 is the mass, in grams, of the crucibles after heating (g);

M_{ad} is the moisture content on wet basis (% w.b.)

3.3.10 Energy Content

Energy content of dust and ground material was estimated using a bomb calorimeter (Model No.-C200, IKA Works Inc. Wilmington, NC). Approximately 0.5 g sample was compressed with a press to form a pellet (Model No-C21, IKA Works Inc. Wilmington, NC). Final mass of the pellet was measured and placed in a steel container (decomposition vessel). The steel container was pressurized to 30 bars and sample was ignited with cotton thread connected to an ignition wire in a decomposition vessel. After the complete combustion of the sample, the energy content of sample was displayed by the calorimeter.

3.3.11 Data Analysis

Microsoft Excel (Microsoft Excel, Redmond, WA) was used for regression analysis and to plot graphs. The Analysis of Variance (ANOVA) procedures in the Statistical Analysis System (SAS, 2009) were used to determine the significant effect (95% of significance level) of moisture content and hammer mill screen size on dust generation, energy required for grinding and physicochemical properties of ground material and dust. The Tukey test was also performed to compare means of properties at different moisture contents and hammer mill screens. Each experiment was carried out in duplicates or triplicates.

3.4 Results and Discussion

3.4.1 Dust Generation during Grinding

In general, dust generation was significantly reduced ($p < 0.05$) with increase in moisture content of wood chips and hammer mill screen size (Figure 3.2). Approximately 21.50% of wood chips were converted into dust when the chips at MC of 4.7% were ground through a 1.20 mm screen. Since material remain in the grinding chamber until the impact of hammers reduced its size to pass through the screen, the number of times particles were struck by hammers increased with decrease in screen size. Therefore, more dust particles were generated when wood chips passed through the 1.20 mm screen. A similar result was reported by Kaliyan et al. (2009) who noticed an increase in dust generation with decrease in screen size when corn stover was ground with a hammer mill. Decrease in amount of dust generated with increase in moisture content was attributed to the lubricating action of moisture, which reduced the friction between wood particles as well as with the hammer mill surface. However, wood chips of high moisture content require more grinding time, resulting in more fine (dust) particles. Therefore, more dust particles were generated at a MC of 23.6% compared to a MC of 14.7% but the difference was not significant ($p > 0.05$).

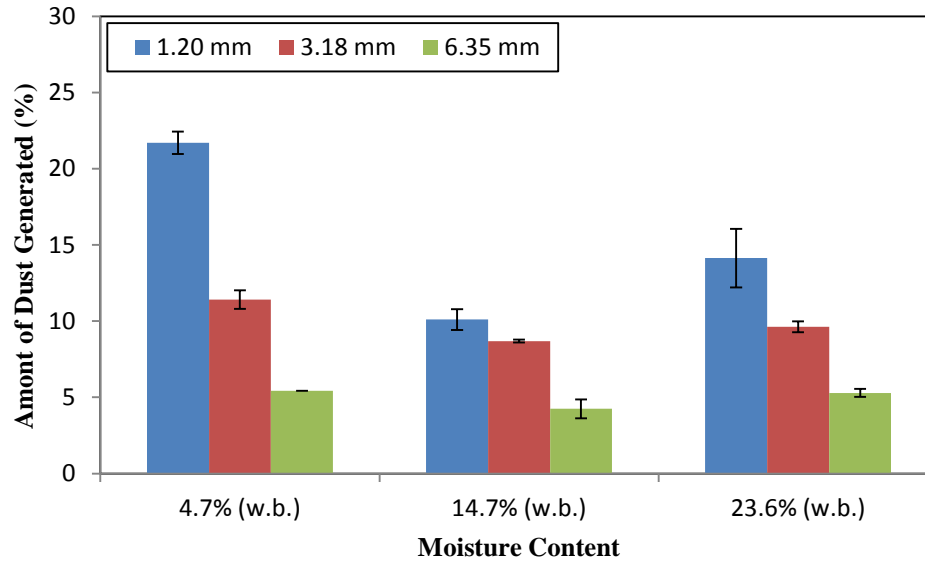


Figure 3.2. Effect of moisture content and screen size on the quantity (%) of dust produced (vertical bars represent standard deviation at each level of moisture content and screen size).

3.4.2 Energy Requirement for Grinding

Energy required (kJ/kg) to grind wood chips significantly ($p < 0.05$) increased with decrease in screen size and with increase in moisture content (Figure 3.3). Wood chips at initial moisture content of 23.6% required 360.00 kJ/kg energy to be ground through 1.20 mm screen whereas 40 kJ/kg energy was required to grind wood chips of 4.7% MC through 6.35 mm screen. Mani et al., (2004) determined the energy required for grinding wheat, barley straw, corn stover and switchgrass which was found to increase with reduction in screen size and increase in moisture content. Energy consumption for grinding wheat straw through 0.8, 1.6 and 3.2 mm hammer mill screens were 185, 133, and 4 kJ/kg, respectively at 8.30% (w.b.) moisture content and 163, 156 and 8.8 kJ/kg, respectively at 12.1% (w.b.) moisture content. The increase in shear strength due to rise in moisture content could result in higher energy consumption.

Energy required to grind pine wood chips was comparable to other studies (Esteban and Carrasco, 2006; Phanphanich and Mani, 2011). In this study 0.20-1.75% of energy content was used to grind loblolly pine wood chips through different hammer mill screens conditioned at

different moisture contents. Phanphanich and Mani, (2011) were reported that 1.2% of pine wood chip's calorific values was consumed during grinding of pine chips.

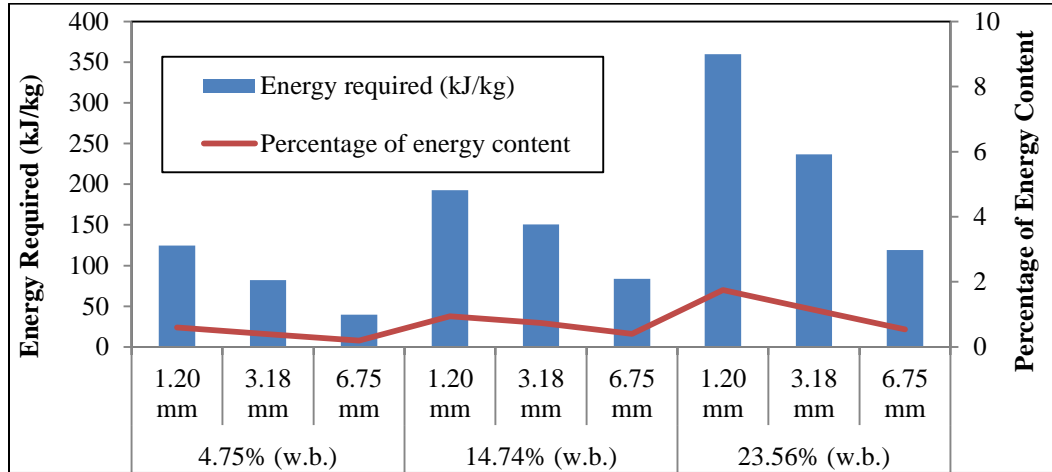


Figure 3.3. Effect of moisture content and screen size on the energy required (kJ/kg) for grinding.

3.4.3 Moisture Content

Ground material and dust had different moisture contents compared to that of wood chips. Moisture was lost during grinding from chips originally at 14.7% and 23.6% MC and this loss in moisture content increased with decrease in screen size. Reduction of moisture was due to the frictional heat produced during grinding. Scholtz et al. (2010) also observed a decrease in moisture content of hay (*Medicago Sativa L.*) from 11.5 % (w.b.) to 8.5% (w.b.) during grinding. However, moisture content of ground material and dust obtained at 4.7% MC was higher than that of the wood chips because of moisture absorption from atmosphere.

Since the moisture content of ground material and dust was different from the original moisture content of wood chips, the following designations are used in the rest of this chapter: low moisture content (LMC), medium moisture content (MMC) and high moisture content (HMC) were used to represent ground material and dust obtained from wood chips conditioned to 4.7%, 14.7% and 23.6% MC, respectively. Moisture contents of ground material and dust at different moisture levels are shown in Figure 3.4.

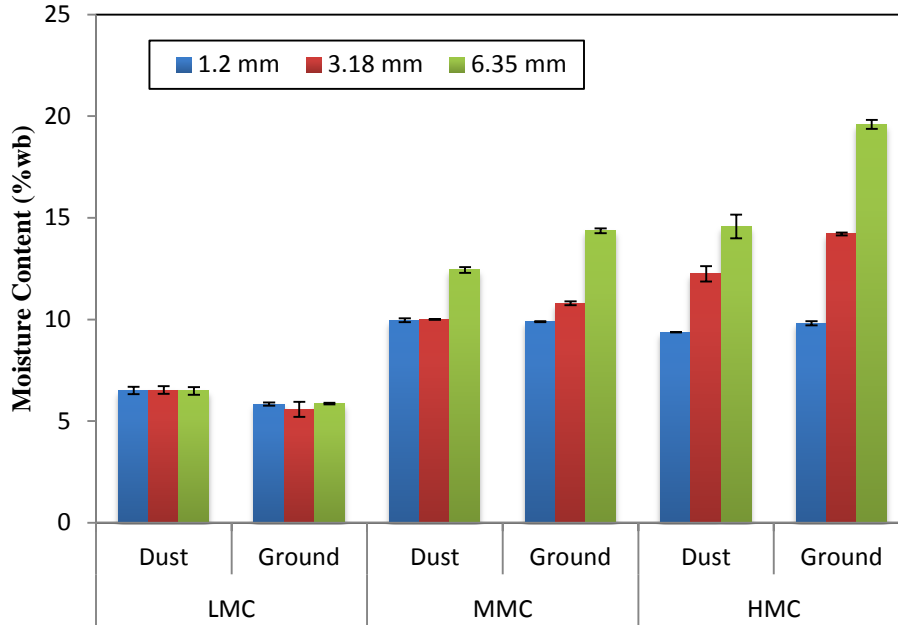


Figure 3.4. Moisture content (% w.b.) of ground material and dust at different wood chips moisture content levels and hammer mill screen sizes (vertical bars represents standard deviation at each level of moisture content and screen size).

3.4.4 Particle Size Distribution

Particle size distribution (Figure 3.5) and geometric mean particle size (Figure 3.6) of ground material changed with change in moisture contents of wood chips and the hammer mill screens. As expected, average particle size of ground material increased with an increase in screen size. Bimodal particle size distributions were also observed partly because of presence of fine (dust) particles. Similar trend was observed by Mani et al. (2004) during grinding of wheat, barley straw, corn stover and switchgrass. Coefficient of correlation between geometric particle size and moisture content of ground material was found to be 0.68 implying particle size of ground material increased with increase in moisture content. Similarly, Shaw et al. (2009) also found increase in average particle size of ground poplar wood chips and wheat straw with increase in moisture content.

Average size of dust was in the range of 0.25 mm to 0.40 mm. Particle size distribution of dust was almost similar at different moisture contents of wood chips and hammer mill screen

sizes (Figure 3.7). However, the distribution was narrow compared to the bimodal distribution of ground material (Figure 3.8).

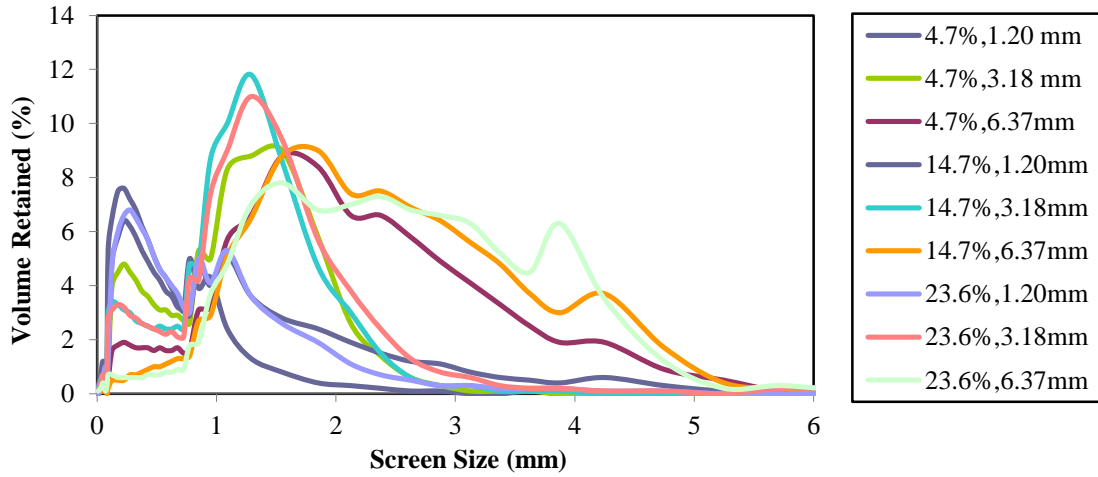


Figure 3.5. Particle size distribution of ground material as affected by moisture contents of wood chips and hammer mill screen size.

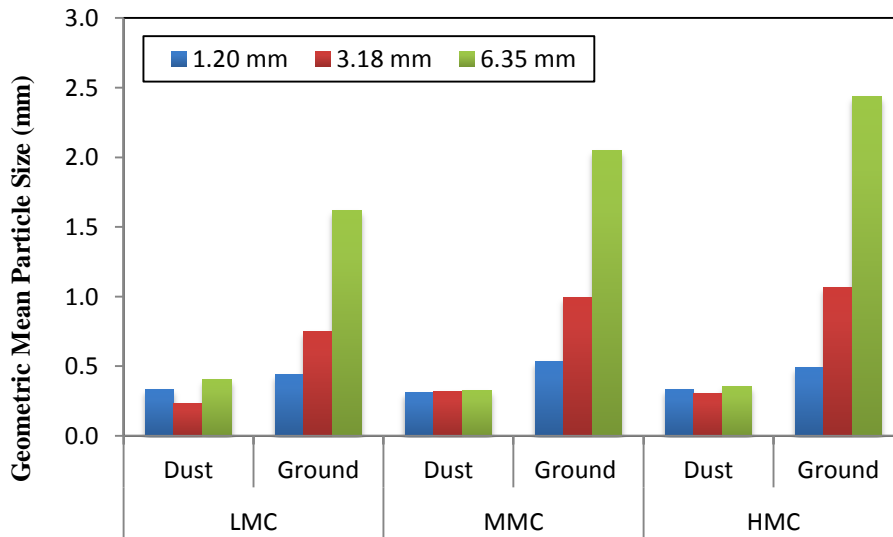


Figure 3.6. Geometric particle size of dust and ground material at different wood chips' moisture levels and hammer mill screens.

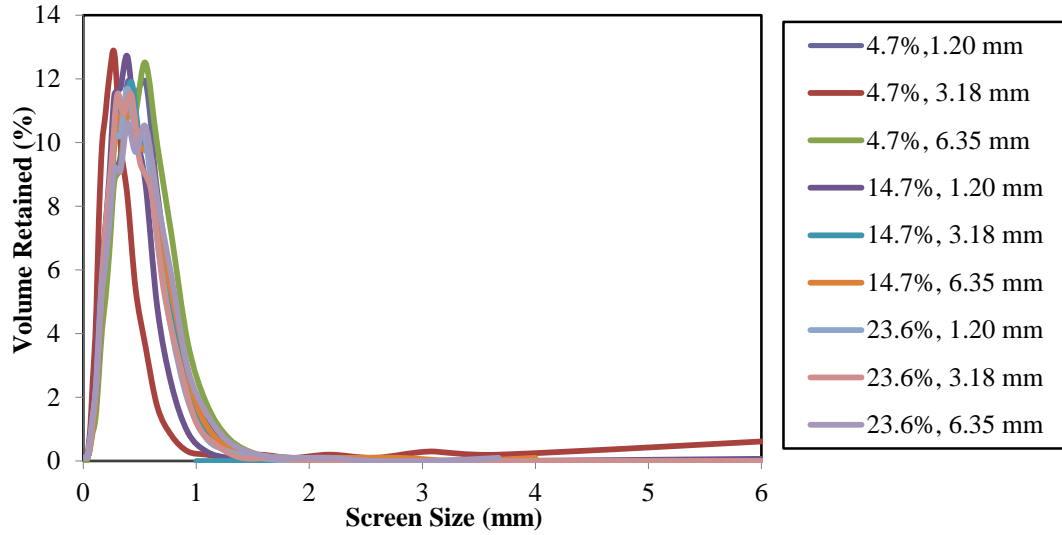


Figure 3.7. Particle size distribution of dust as affected by moisture contents of wood chips and hammer mill screen size.

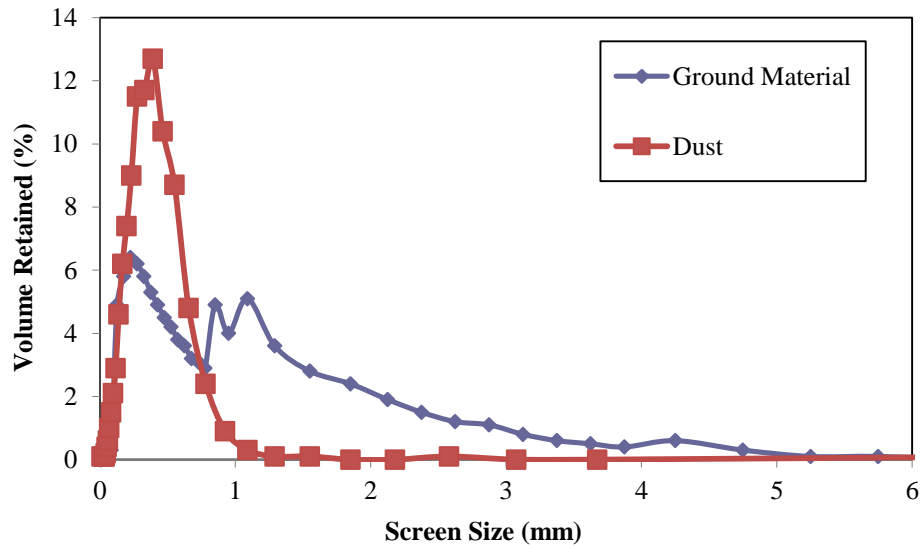


Figure 3.8. Particle size distribution of ground material and dust when wood chips at mc of 14.74% was ground through 1.20 mm hammer mill screen size.

3.4.5 Bulk Density

The bulk density of ground material significantly changed ($p < 0.05$) with change in wood chip moisture content and hammer mill screen size (Figure 3.9). Bulk density of ground material and dust ranged from 206.15 to 273.36 kg/m³ and 163.54 to 215.96 kg/m³, respectively. Since,

the particle size of ground material was larger when larger screens used, the increasing inter-particle voids resulted in decreased bulk density. Similar results were obtained by Mani et al. (2004), showed that bulk density of wheat straw ground at 3.1, 1.6 and 0.8 mm was 97, 107 and 121 kg/m³, respectively. Bulk density of ground material increased when moisture content changed from LMC to MMC and then decreased when moisture content changed from MMC to HMC Increase in moisture content causes increase in mass and increase in volume of material (Fasina, 2008; Mani et al., 2004). This means that when moisture content changed from LMC to MMC, increase in mass was more compared to increase in volume and when moisture content changed from MMC to HMC increase in volume was more compare to increase in mass.

Bulk density of dust also changed with moisture level in a similar way as the ground material. Bulk density of dust was significantly less ($p < 0.05$) compared to ground material (Figure 3.9) (Fasina, 2008). The overall effect of screen size on bulk density of dust was negligible ($p = 0.02$), but at HMC bulk density changed significantly with screen size. This change could be attributed to high variation in moisture content of dust with respect to screen size at HMC (9.37% MC at 1.20 mm to 14.57% MC at 6.35 mm) compared to LMC (MC variation was not significant) and MMC (9.96 % MC at 1.20 mm to 12.44% MC at 6.35 mm).

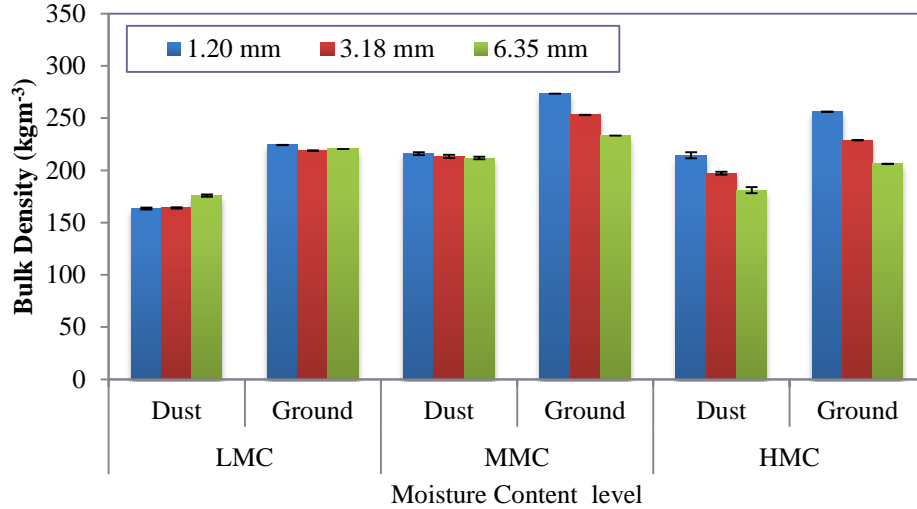


Figure 3.9. Bulk density (kg/m^3) of ground material and dust as affected by moisture content and hammer mill screen size (vertical bars represent the standard deviation at different moisture content and screen size).

3.4.6 Particle density

Particle density of ground material significantly changed ($p < 0.05$) by the moisture content of wood chips and effect of hammer mill screen size was not significant ($p = 0.04$). Particle density of ground material first decreased when moisture content increased from LMC to MMC and then increased when moisture content increased to HMC (Figure 3.10). Particle density of ground material and dust ranged from 1404.55 to 1469.55 kg/m^3 and 1514.40 to 1426.45 kg/m^3 . Initial decrease in particle density could be because of higher expansion in particle volume compared to increase in mass due to adding of moisture and the following increase could be attributed to higher mass change compared to volume expansion. In addition, particle density increased with decrease in screen size of hammer mill since intra particle voids decreased when material divided into small particles (Figure 3.10). Mani et al., (2004) observed the decrease in particle density of four types (wheat, barley straw, corn strowe and switchgrass) of ground biomass with respect to screen sizes of hammer mill. Particle density of wheat straw at 3.2, 1.6 and 0.8 mm screen of hammer mill was found to be 1030, 1260 and 1340 Kg/m^3 , respectively.

Particle density of dust was more compared to ground material but difference was not significant. Particle density of dust followed the same trend as ground material with respect to moisture content ($p < 0.05$) but effect of screen size was not significant ($p = 0.27$) (Figure 3.10).

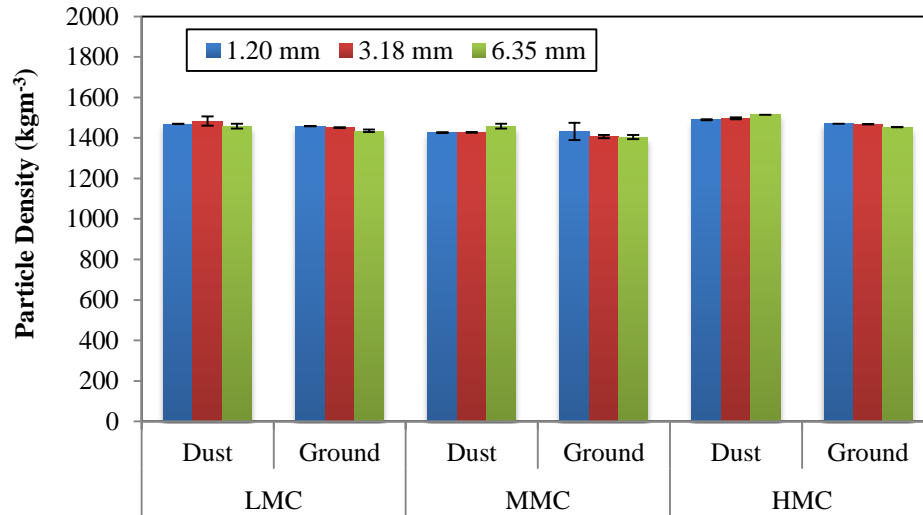


Figure 3.10. Particle density (kg/m^3) of ground material and dust as affected by moisture content and hammer mill screen sizes (vertical bars represent standard deviation at different moisture content levels and screen sizes).

3.4.7 Ash Content

Ash content of the ground material was not significantly influenced by moisture content ($p = 0.451$) and effect of screen size was marginally significant ($p = 0.0437$) (Figure 3.11). Ash content of dust was significantly more compared to ground wood chips ($p < 0.05$) and it increased with wood chip moisture content ($p < 0.05$) and hammer mill screen size ($p < 0.05$). Ash content is the measure of internal or external inorganic impurities in biomass. According to Bridgeman et al. (2007), inorganic particles are separated from lignocellulosic structure of biomass (reed canary grass and switchgrass) during grinding. These inorganic particles are more grindable and have smaller particle size compared to organic material. Therefore, more of the inorganic particles end up in the dust fraction. At high moisture content, wood chips took a long time to grind and more

inorganic particles were separated from organic particles. Therefore, dust collected at MMC and HMC had high ash content.

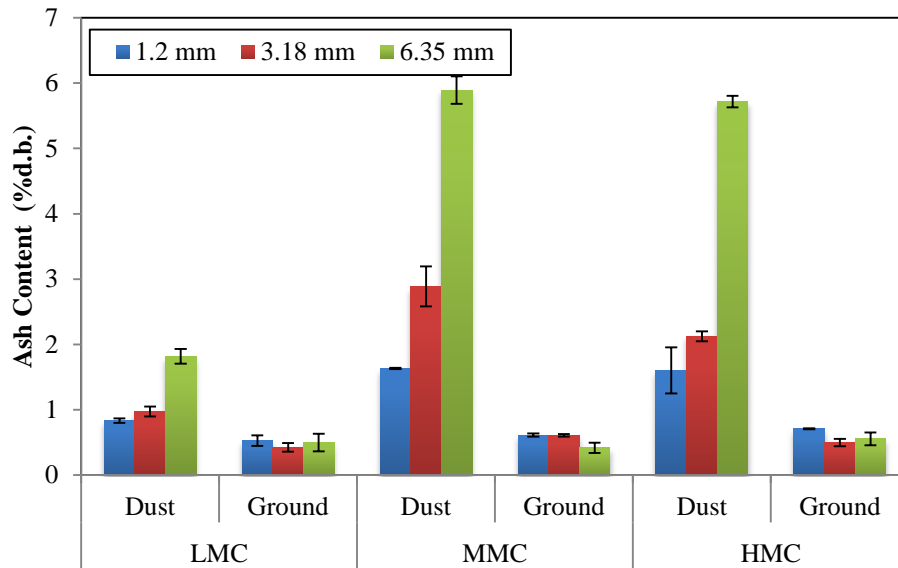


Figure 3.11. Ash content (% d.b.) of ground material and dust as affected by moisture content and hammer mill screens (vertical bars represent the standard deviation at each level of moisture content and screen size).

3.4.8 Volatile Matter

The volatile matter of ground material and dust are shown in Figure 3.12. Moisture content ($p=0.237$) and screen size ($P=0.453$) did not affect volatile matter of ground material. On the other hand, volatile matter of dust decreased significantly with increase in the wood chips' moisture content ($p<0.05$) and hammer mill screen size ($p=0.05$). In addition, dust had less volatile matter compared to ground material ($p<0.05$). As shown in Figure 3.13, volatile matter of dust is inversely related to its ash content. Similar results were reported by Gani and Naruse (2007) in which inverse relation between ash content and volatile matter was observed. Ash content and volatile matters of hinoki saw dust, rice straw and rice husks were found by authors to be 1.3, 20.4, 20.3 (% w.b.) and 97.4, 79.6, 78.4 (% w.b.) respectively (Gani and Naruse, 2007).

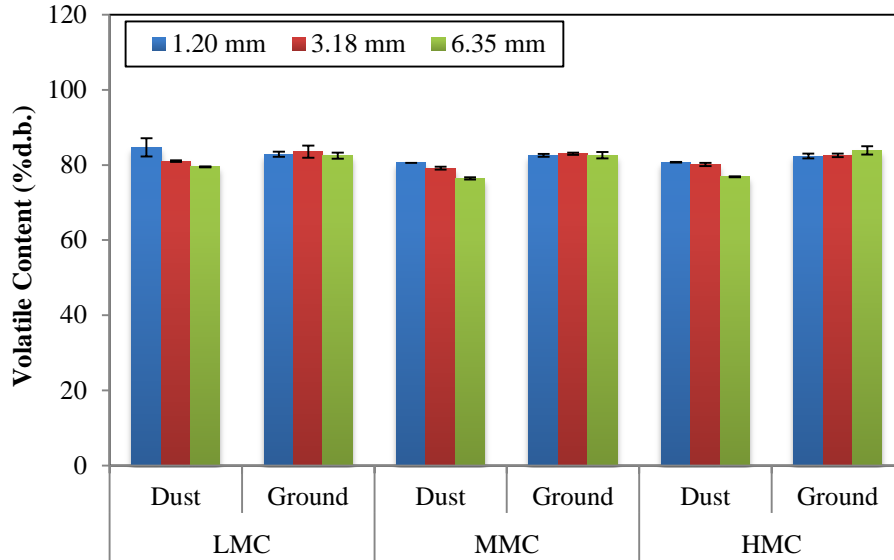


Figure 3.12. Volatile content (% d.b.) of ground material and dust as affected by moisture content of wood chips and hammer mill screens (vertical bars represent the standard deviation at different moisture content and screen size).

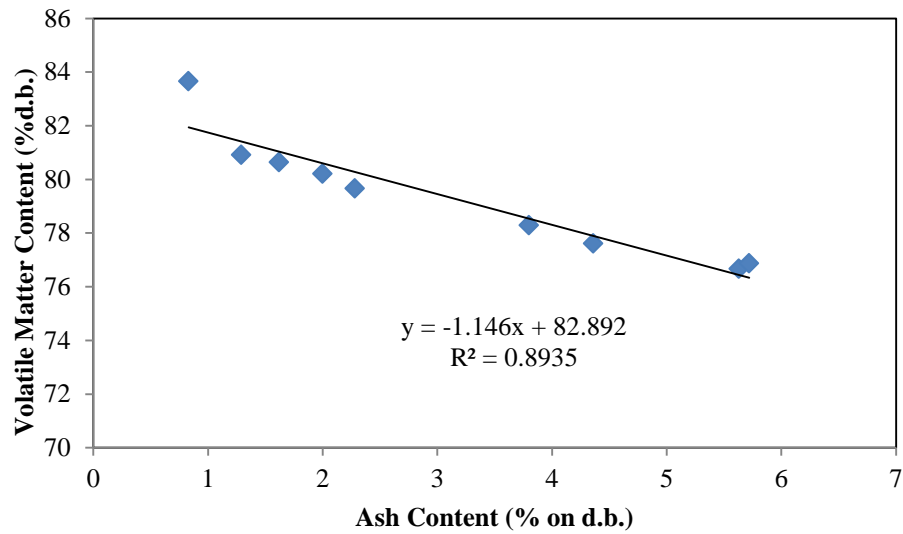


Figure 3.13. Relation between volatile content (% d.b.) and ash content (% d.b.) of dust.

3.4.9 Energy Content

Although statistical tests indicated significant effect of wood chips' moisture content ($p=0.03$) and hammer mill screen size ($p=0.02$) on energy content of ground material, no distinct

trend was observed (Figure 3.14). Energy content of ground material was higher compared to dust but difference was not significant (Figure 3.15). Energy content of dust decreased significantly ($p < 0.0020$) with increase in moisture content and effect of screen size ($p = 0.0528$) was not significant. Mani et al. (2004) and Ebling and Jenkins, (1985) also concluded that the energy content of biomass depends on ash content and volatile matter.

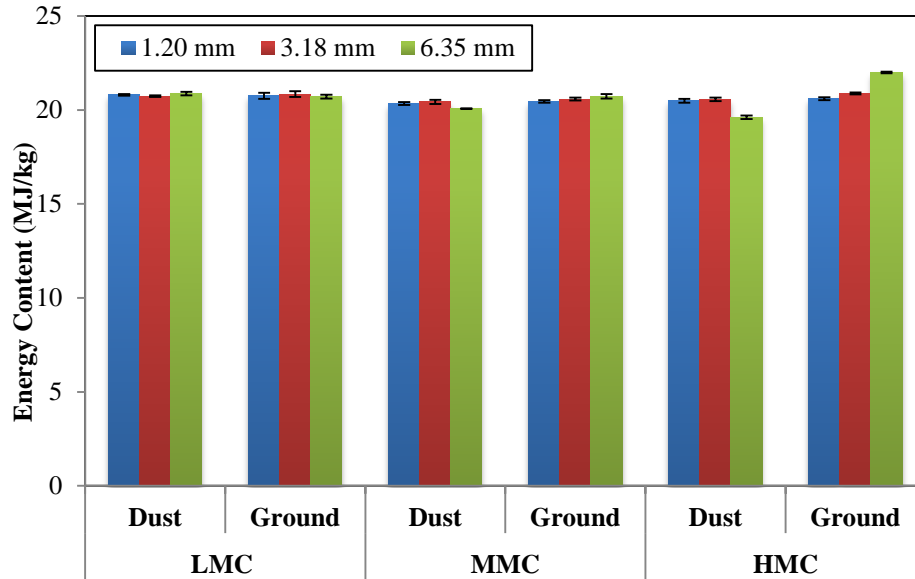


Figure 3.14. Energy content (MJ/kg) of ground material and dust as affected by moisture content and hammer mill screens (vertical bars represent standard deviation at different moisture content and screens).

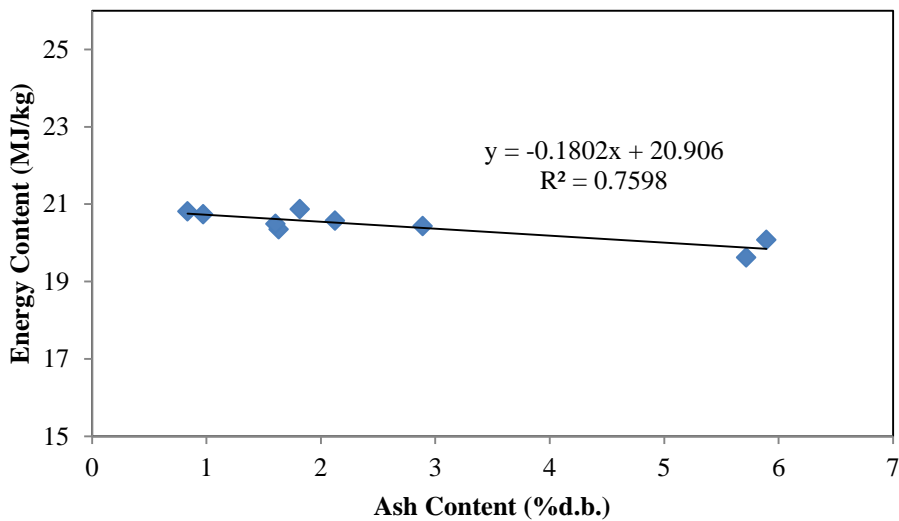


Figure 3.15. Relation between energy content (MJ/kg) and ash content (% d.b.) of dust.

3.5 Conclusion

The effect of hammer-mill screen and wood chip moisture content on energy consumption for grinding, dust generation and physicochemical properties of ground loblolly pine chips and dust was investigated. Energy required to grind wood chips was found to increase as moisture content increased and hammer-mill screen size decreased. About 39.65 kJ/kg energy was required to grind loblolly pine when wood chip moisture content was 23.56% and hammer mill screen of 1.20 mm whereas 360.00 kJ/kg energy was required to grind wood chips conditioned to 4.7% MC through a 6.35 mm screen. Dust generation decreased with increase in moisture content and hammer-mill screen size. Some moisture was lost during grinding and therefore, the moisture content of the ground material and dust was different from the moisture content of wood chips before grinding. Bulk density and particle density of ground material and dust also changed as moisture content and screen size varied. Influence of moisture content and screen size on chemical properties of ground material was less significant compared to dust. Ash content of dust was significantly ($p < 0.05$) influenced by wood chip moisture content and hammer-mill screens. Volatile and energy content of dust were inversely related to its ash content.

Chapter 4 Physicochemical and Ignition Properties of Dust

4.1 Abstract

Particle size of dust is an important parameter that affects its physical, chemical and ignition properties. To determine the effect of particle size on physiochemical and ignition properties of loblolly pine dust, chips were ground through a hammer mill and dust separated by passing ground material through a 420 μm screen on a vibratory shaker. The collected dust was then divided into three fractions (fine ($<90 \mu\text{m}$), medium (90-180 μm), coarse (180-420 μm). Physicochemical (moisture content, bulk and particle density, ash content, volatile matter and energy content) and ignition properties (hot surface ignition temperature, volatilization properties from TGA and exothermic parameters from DSC) of three fractions were determined. Physicochemical and ignition properties of unfractionated pine dust were also compared with coal dust. The results indicated that the fine fraction of dust had a high levels of bulk and particle density compared to medium and coarse dust fractions but the difference was significant ($p < 0.05$) only for bulk density. The fine dust fraction had significantly high inorganic content (1.70% d.b.) compared to medium and coarse fractions (1.27% and 0.76% on d.b., respectively). In contrast, medium and coarse fractions had high volatile and energy content. Pine dust had high moisture (8.16% on d.b.) and volatile content (82.36 % on d.b.) than coal dust. Contrarily, coal dust had high bulk-particle density, ash content and energy content versus pine dust. Fine dust had low hot surface ignition temperature than the medium and coarse dust. The effect of particle size on volatilization properties (temperature of volatilization, temperature of maximum mass loss rate

and temperature of oxidation) was not significant ($p < 0.05$). However, temperature of rapid exothermic reaction (242°C) of fine fraction was significantly lower than coarse and medium dust (253°C and 262°C). Pine dust had low hot surface ignition temperature, temperature of volatilization, temperature of rate of maximum mass loss and temperature of oxidation compared to coal dust. On the other hand, rapid exothermic reaction in coal dust started at a low temperature (235°C) than pine dust (241°C). According to hot surface ignition temperature and temperature of rapid exothermic reaction, ignition risk increased with decrease in particle size. The three pine dust fractions (fine, medium and coarse) and unfractionated pine dust had high risk of ignition while coal dust had low risk of ignition.

4.2 Introduction

Knowledge of the conditions that can result in dust ignition is important because ignition of bulk materials and dust is responsible for fires and explosions in industrial plants that process or handle bulk materials. Three conditions that have to be present for ignition to occur are air, fuel (dust) and an ignition source (Amyotte, 2006). Ignition sources that are typically present in processing plants include hot-ignition surface, mechanical and electrical sparks, open flames (welding and cutting flames) and ignited dusts (Abbasi and Abbasi, 2007).

Different types of experimental techniques have been used to measure the ignition properties of combustible dusts. Miron and Lazzara (1988) determined the effect of particle size on the hot plate ignition temperature of different dust samples (coal, three oil shales, lycopodium spores, corn starch, grain and brass powder). They found that the ignition temperature of these dusts (12 mm layer thickness) ranged from 160°C to 290°C and decreased with decrease in particle size (Miron and Lazzara, 1988).

Thermogravimetric analysis (TGA) is often used by various researchers to measure the ignitability of combustible dusts. TGA is a technique to measure the change in mass of the sample under programmed heating during the thermal decomposition of a material into the

volatiles. The higher the temperature at which material starts to decompose into volatiles, the lower is the ignition risk. Pilao et al. (2006) found maximum rate of mass loss of cork dust in the range of 380° C to 450°C. Liu et al. (2007) observed that the mass loss of coal dust started at 300° C and about 83% of the mass was lost by the time the material was heated to 600 °C.

Ramirez et al. (2010) measured the activation energy of different biological materials and used the data to determine the ignition risk by plotting the activation energy against the oxidation temperature. Activation energy of icing sugar, maize, wheat, barley, alfalfa, bread-making flour, soya and lycopodium dust ranged from 61.7 to 67.7 kJ/mole and their oxidation temperatures ranged from 239°C to 332°C. All of these dusts except lycopodium dust were at high risk of ignition because their activation energies and oxidation temperatures were less than 90 kJ/mole and 300°C, respectively.

Differential scanning calorimeter (DSC) has been used by researchers to measure ignition properties of combustible dusts by determining heat flow as a function of temperature during heating (Lu et al., 2009; Ramirez et al., 2010). In addition, temperature at which endothermic or exothermic reactions begin was obtained from the heat flow curves (Lu et al., 2009; Ramirez et al., 2010). Lu et al. (2009) studied the ignition characteristics of dusts obtained from three types of crystalline benzoyl peroxides. The heat released during the decomposition reaction of 98%, 75% and 50% crystalline benzoyl peroxides was equal to 1047.78, 957.04 and 771.16 J/g, respectively. Furthermore, they found that endothermic reaction (103°C) and exothermic reaction (110°C) started at almost the same temperatures for three types of samples. Ramirez et al. (2010) found that rapid exothermic reaction in icing sugar, maize, wheat, barley, alfalfa, bread-making flour, soya and lycopodium dust starts at 4°C, 242°C, 252°C, 257°C, 240°C, 271°C, 245°C and 213°C, respectively.

Ignition properties of combustible dusts depend upon their physical properties. Particle size is one of the most important physical properties that affect ignitability of dust particles.

Since, surface area of a material increases when it is ground into smaller particles and more oxygen from the atmosphere is available to react with particles when the particle size is small. In addition, small particles react with oxygen at a faster rate (Chamberlain and Hall, 1973; Ren et al., 1999; Cashdollar, 2000; Eckhoff, 2003;). Similarly, Ren et al. (1999), reported an increase in the rate of oxidation as particle size decreased up to a critical particle size that ranged from 138 to 387 μm for different types of coal (Ren et al., 1999). Sweis (1998) determined that the ignition temperature of oil shale particles of size 75.3 and 212.3 μm was 640 °C and 680 °C, respectively and increased with increase in particle size. Bowes and Townshend (1961) obtained the hot plate ignition temperature of beech sawdust after fractionating into four sizes (853-422, 422-251, 251-124 and <124 μm). The fine fraction (<124 μm) ignited at 335° C, the lowest temperature of ignition compared to the other fractions. The ignition temperature of other fractions (853-422, 422-251, 251-124 μm) were 350°C, 345°C and 340°C, respectively.

Chemical properties of dusts such as ash and volatile matter also influence the ignition behavior of dust. For example, the volatile matter of dust acts as fuel for the ignition process. Dust with high volatile content has low ignition temperature as compared to those with low volatile content. For example, Grotkjær et al. (2003) found that the ignition temperature of wheat straw (volatile content at 72% d.b.), lignite coal (volatile content at 51% d.b.), and anthracite coal (volatile content at 32% d.b.) were about 210°C, 300°C and 490°C, respectively. Additionally, the author found that ash content in the combustible dust did not affect its ignition potential but acts as a heat absorber (Grotkjær et al., 2003). High ash content materials such as fly ashes (ash content of 90% on d.b.) are often mixed with combustible dusts to reduce their ignitability (Dastidar and Amyotte, 2002).

Physicochemical properties of biomass change when fractionated into different particle size because of its chemical and structural heterogeneity. Miranda et al. (2012) determined the ash content of barks of Norway spruce (*Piceaabies* (L.) Karst) and Scots pine (*Pinussylvestris* L.)

after fractionating into six sizes (<0.180, 0.180-0.250, 0.250-0.450, 0.450-0.850, 0.850-1.00 and 1.00-2.00 mm). They found that for both samples, fine fractions had high ash content compared to coarse dust. Ash content of the fine fractions (<0.180 mm) of the bark for Norway spruce and Scot pine were 5.3%, and 17.3% (d.b.), respectively with the ash content of the coarse fractions of both samples was about 3.2% (d.b.). Similar results were obtained by Birdgemann et al. (2007) for the ash content of ground reed canary grass (RCG) and switchgrass (SG) after fractionating into two sizes (<90 μm and >90 μm).

Physicochemical properties are important to understanding of the ignition behavior of dusts. These physiochemical properties change with particle size. However, limited research has been conducted to find the relationship between physiochemical and ignition properties of loblolly pine dust. Therefore, the objective of this study was to determine the effect of particle size on the physicochemical and ignition properties of loblolly pine dust after fractionating dust into three groups (<90, 90-180, 180-420 μm).

4.3 Materials and Methods

4.3.1 Sample Preparation and Physicochemical Properties Determination

Clean loblolly pine wood chips were obtained from south Alabama forests. The initial mean moisture content of wood chips was 52.21% (w.b.). The wood chips were the air-dried to 10.03% (w.b.). The moisture contents of wood chips were determined according to ASTM standard (E871-82) (ASTM, 2006). This process involved placing of 10 g of sample in a forced convection oven set at a temperature of 105 °C for 24 hours.

The dried wood chips were thereafter ground using hammer mill (Model No.-10HBLPK, Sheldon Manufacturing, Tiffin, OH) fitted with a 1.20 mm screen and or a 3.17 mm screen. Dust was separated by passing the ground material through the 420 μm screen on a vibratory shaker (Model No.-K30-2-8S, Kason, Millburn, NJ). A sieve shaker (Model No.-RX-20, Ro-Top, OH)

was used to separate the dust samples into three fractions: (a) coarse fraction-particles retained on a 180 μm screen, (b) medium fraction-particles which passed through a 180 μm screen but retained on a 90 μm screen and (c) fine fraction-particles that passed through a 90 μm screen. A similar procedure was used to obtain dust from pulverized lignite coal sample that was obtained from Alabama Power electrical generating plant in Gorgas, AL.

The methodology used in determination of the physiochemical properties of the fractions are same as those described in chapter 3 for moisture content, bulk density, particle density, particle size and distribution, ash content, volatile matter content and energy content.

4.3.2 Particle Size Distribution

Particle size distribution on a volume basis for the dust samples was measured with a digital image particle analysis system (Model No.-D-4278, Haan, Germany). Particle size distribution of fine the dust (<90 μm) obtained by camsizer was wide compared to medium and coarse dust. Particle sizee distribution of then obtained by using a sieve shaker (Model No.-RX-20, Ro-Top, OH) and seven screens ranging in size from 0.045 to 1.25 mm plus a pan. Geometric mean diameter and geometric standard deviation were obtained according to ASABE Standard S319.3 (2003) and equations 4.1- 4.3.

$$d_{gw} = \log^{-1} \left[\frac{\sum_{i=1}^n (W_i \log \bar{d}_i)}{\sum_{i=1}^n W_i} \right] \quad (4.1)$$

$$S_{\log} = \left[\frac{\sum_{i=1}^n W_i (\log \bar{d}_i - \log d_{gw})^2}{\sum_{i=1}^n W_i} \right]^{1/2} \quad (4.2)$$

$$S_{gw} = \frac{1}{2} d_{gw} \left[\log^{-1} S_{\log} - (\log^{-1} S_{\log})^{-1} \right] \quad (4.3)$$

where

d_{gw} is the geometric mean diameter or median size of particles by mass (mm);

S_{\log} is the geometric standard deviation of the log normal distribution by mass in 10-based logarithm (dimensionless);

S_{gw} is the geometric standard deviation of particle diameter by mass (mm);

W_i mass on i th sieve (g);

n is number of sieves plus one pan;

$$\bar{d}_i = (d_i \times d_{i+1})^{1/2};$$

d_i is nominal sieve aperture size of the i th sieve (mm);

d_{i+1} is nominal sieve aperture size of the $i+1$ sieve (mm).

4.3.3 Moisture Content

Moisture content of dust samples was measured with a moisture content analyzer (Model No.-IR-200, Denver Instrument, Avrada, CO) by placing 10 g of sample in the pan of the moisture content analyzer (ASTM E87182 standard, 2006). The analyzer was programmed to perform this analysis at a temperature of 105 °C. Results were displayed on screen after the completion of test and then documented in Microsoft Excel worksheet.

4.3.4 Bulk Density

Bulk Density (ρ_{bulk}) of dust samples were measured with the Ohaus apparatus (Model No-BurrowsCo., Evanston, IL) according to ASABE Standard S269.4 (ASABE S269.4, 2002). Samples were poured from a funnel into a 1137 mL container. Samples were then leveled using a steel rod with the sample mass measured and recorded. Bulk density of dust samples were calculated according to equation 4.4.

$$\rho_{bulk} = \frac{Mass}{Volume} \quad (4.4)$$

4.3.5 Particle Density

Mean particle volume of dust samples was obtained with a helium pycnometer (Model No.-AccuPyc 1330, Micromeritics Instrument Corp., Norcross, GA). A known amount of mass (about 2 g) was placed in the sample container of the instrument to measure the particle volume. Particle density was calculated from the ratio of sample mass in the sample container to the volume measured by the pycnometer.

4.3.6 Energy Content

Energy content of dust samples was measured using a bomb calorimeter (Model No.-C200, IKA Works Inc., Wilmington, NC). Approximately 0.5 g of sample was compressed with a press to form pellet (Model No.-C21, IKA Works Inc., Wilmington, NC) and then placed in a steel container. Cotton thread connected to an ignition wire was used to ignite the sample after the sample in the container was pressurized to 30 bars.

4.3.7 Ash Content

Ash content of the dust samples was determined according to the NREL Laboratory Analytical Procedure (LAP, 2005). A sample of about 2 g was placed in crucibles and then transferred into a muffle furnace (Model No.-F6020C, Thermoscientific, Dubue, IO). The furnace was programmed to heat up to 105°C, ramped to 250°C at 10°C/minute and held at this temperature for 30 minutes, followed by increasing to 575°C at 20°C/min and held for 180 minutes and then finally lowering temperature back to 105°C. Crucibles were then placed in the desiccator for 1 hour and allowed to cool to room temperature. The mass of the samples was measured to 0.1 mg by using a weighing balance. Ash content on the dry basis was calculated according to equation 4.5.

Ash content of coal dust was determined by using ASTM standard (ASTM D 3174-04, 2004). Based on a standard, coal dust sample of about 1 g was first heated to 450 °C at a rate of

10 °C/min. It was then heated so that a final temperature of 700 °C was attained by the end of the second hour and then heated for additional 2 hours.

$$Ash(\%) = \frac{M_{ash} - M_{con}}{M_{od} - M_{con}} \times 100 \quad (4.5)$$

M_{ash} is the mass of ash (g)

M_{con} is the mass of the container (g)

M_{od} is the mass of dried biomass (g)

4.3.8 Volatile Matter

Volatile matter of dust was measured according to ISO 562 (ISO 562, 2010). About 1g ± 0.1 of sample was placed in a crucibles. The crucibles were placed in a volatile matter furnace (Model No.-VMF 10/6/3216P, Carbolite, Hope Valley, England) at 900°C ± 10°C for 7 min. Crucibles were then removed from the furnace and placed in a desiccator until they cooled to room temperature. The final mass of the crucibles with sample was measured. Volatile content was calculated as follows.

$$Vd = \left[\frac{100(M_3 - M_1)}{M_2 - M_1} - Mad \right] \times \left(\frac{100}{100 - Mad} \right) \quad (4.6)$$

where

M_1 is the mass of the empty crucibles with lid (g);

M_2 is the mass of the crucibles with lid after placing sample in the crucibles (g);

M_3 is the final of the crucibles with lid after heating (g);

M_{ad} is the moisture content of the sample before heating (% w.b.)

4.3.9 Hot Surface Ignition Temperature

Hot surface ignition temperature of dust samples was determined according to ASTM-E2021 (2010) by using a commercial hot plate (Model No.-VmWare, Thorofore, NJ). The apparatus consisted of a commercial hot plate, metal plate (200 mm diameter and 20 mm thickness), a metal ring (12.7 mm diameter and 100 mm depth) and thermocouples (Figure 4.1).

The metal plate placed on commercial hot plate and metal ring was placed on the metal plate. A type K bare thermocouple (0.20 to 0.25 mm) was fixed radially across the metal ring and another thermocouple was attached to the metal hotplate. The temperatures from the two thermocouples were recorded by a data logger (Fuji Electric Systems Co, Ltd, Tokyo, Japan) at an interval of 5 seconds. To carry out the test, the desired temperature was set on the temperature controller of the hot plate. The metal ring was then filled with the dust sample when the temperature of hot plate reached the desired temperature. Surface of dust sample was leveled with the top part of metal ring. Temperature of the hot plate and dust layer was monitored and recorded continuously. If ignition did not occur, the test was repeated with fresh dust but with a set temperature that is 5°C higher than the previous test. Process was repeated until ignition of the dust sample occurred. Hot surface ignition was taken as the average of temperature of ignition and the maximum temperature at which dust did not ignite (5°C lower than the ignition temperature).

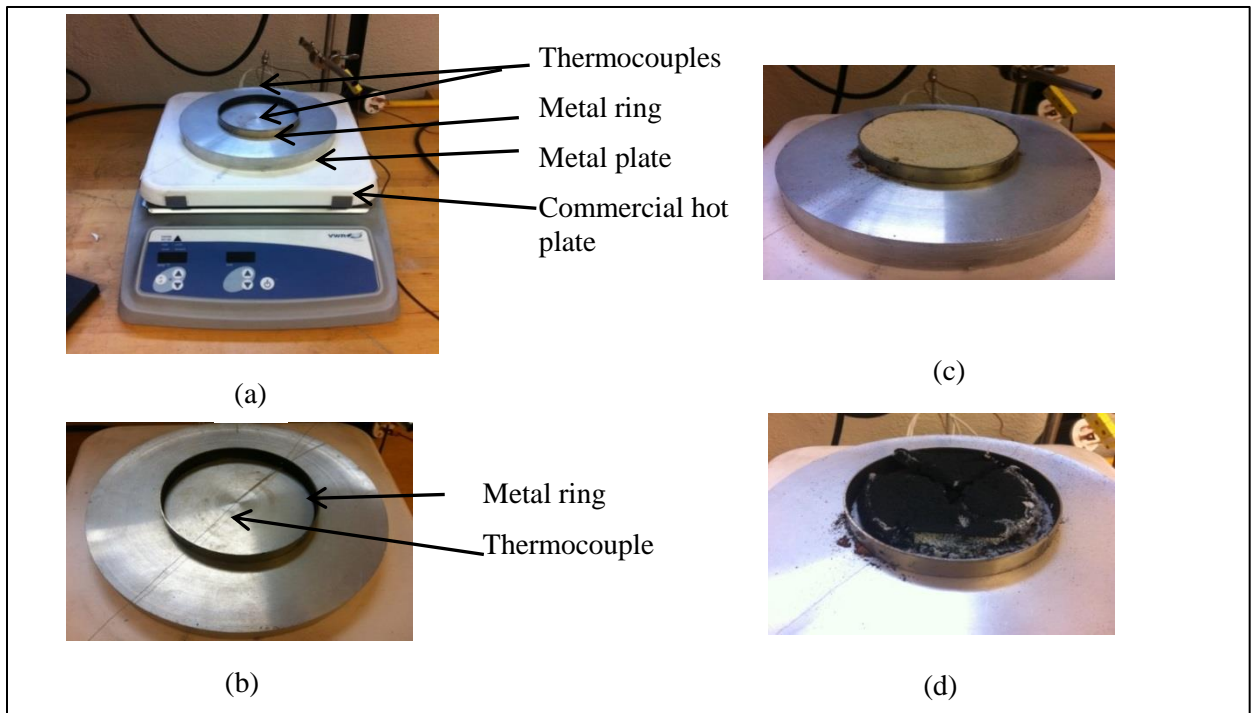


Figure 4.1. (a) Hot plate apparatus, (b) Metal ring and thermocouple (K type) (c) Ring filled with fresh dust sample and (d) Burned Dust.

4.3.10 Volatilization Properties

A TGA (Model No.-Pyris 1 TGA, PerkinElmer, Shelton, CT) was used to quantify the volatilization properties by monitoring mass loss of 5 mg of dust samples when subjected to programmed heating from 30°C to 800°C at 5°C min⁻¹ under air and oxygen atmospheres. A single oxidation temperature could not be obtained when sample was heated under air and therefore, oxygen was used to determine oxidation temperature (T_{ch}). The onset temperature of volatilization (TOD) and the temperature of maximum rate of mass loss (TMWL) were determined by analyzing the data recorded by software provided by apparatus manufacturer. The TOD indicates the starting temperature at which some of the components began to volatilize. The TMWL is the temperature at which maximum volatile matter is produced. The lower the temperature, readily the material is ignited. The oxidation temperature (T_{char}) was obtained by heating sample under the oxygen stream.

The apparent activation energy (E_a) of each sample was determined using equations 4.7-4.11 and from the data obtained from thermogravimetric analysis under the air stream. A linear equation was fitted to plot of $\ln\left(\frac{dm}{dt}\right)$ versus $\frac{1}{T}$ (equation 4.11) in a Microsoft Excel 2010 (Microsoft Excel, Redmond, WA). The E_a was obtained from the slope ($\frac{E_a}{R}$) of the linear fit. The activation energy was plotted against the oxidation temperature to estimate the risk of ignition associated with various dust samples (Ramirez et. al, 2010).

The equation for loss of mass (dm/dt) was

$$\frac{dm}{dt} = kf(x) \quad (4.7)$$

with degree of the conversion process can be defined as

$$f(x) = (1 - \alpha)^n \quad (4.8)$$

Arrhenius equation to determine k

$$k = Aexp^{-E/RT} \quad (4.9)$$

$$\frac{dm}{dt} = Aexp^{-E/RT}(1 - \alpha)^n \quad (4.10)$$

$$\ln\left(\frac{dm}{dt}\right) = \ln(A) + n * \ln(1 - \alpha) - \frac{E}{RT} \quad (4.11)$$

where R is the universal gas constant, (8.314 J/mol K), T is the temperature (K), and A and E are kinetics parameters pre-exponential factor (1/s) and activation energy (J/mol), respectively.

4.3.11 Exothermic Reaction Parameters

Differential Scanning Calorimetry (Model No.-Q200, TA Instruments, New Castle, DE) was used to estimate the exothermic reaction parameters by measuring heat flow when a sample was heated using air from 30°C to 500°C at a rate 20°C/min. About 0.5 mg of material was placed in 50 µl crucible. The plot of heat flow (Q) versus temperature was analyzed with software provided by manufacturer to estimate the following exothermic reaction parameters- onset temperature for rapid exothermic reaction (T_{RE}) and, the maximum temperature reached during the exothermic reaction (T_{max}). Exothermic energy was also determined by calculating the area under curve from the plot of heat flow versus temperature with the help of software provided by manufacturer.

4.2.12 Data Analysis

The Analysis of Variance (ANOVA) procedures in the Statistical Analysis System (SAS, 2009) were used to determine the significant effect (95% of significance level) of particle size on physiochemical and ignition properties of loblolly pine dust. The Tukey test was also performed to compare means of properties of three fractions of dust and unfractionated pine dust and coal dust. Each experiment was carried out in duplicates or triplicates. Microsoft Excel (Microsoft Excel, 2010, Redmond, WA) was used for regression analysis and to plot graphs.

4.4 Results and Discussion

4.4.1 Particle Size Distribution and Moisture Content

Particle size distributions of the three fractionated dust samples are shown in Figure 4.2. There was skewness in the distributions of fractionated dust samples (Figure 4.2) as well as

unfractionated pine dust and coal dust (Figure 4.3). Geometric particle size of three loblolly pine dust fractions (fine, medium and coarse) ranged from 68 μ m-202 μ m. Coal dust had a wide particle size distribution compared to unfractionated loblolly pine dust. Geometric particle size of coal dust was also larger than the unfractionated loblolly pine dust (Table 4.1).

Moisture contents of three dust fractions were not significantly different ($P > 0.05$). Moisture content of unfractionated loblolly pine dust was higher compared to coal dust (Table 4.3)

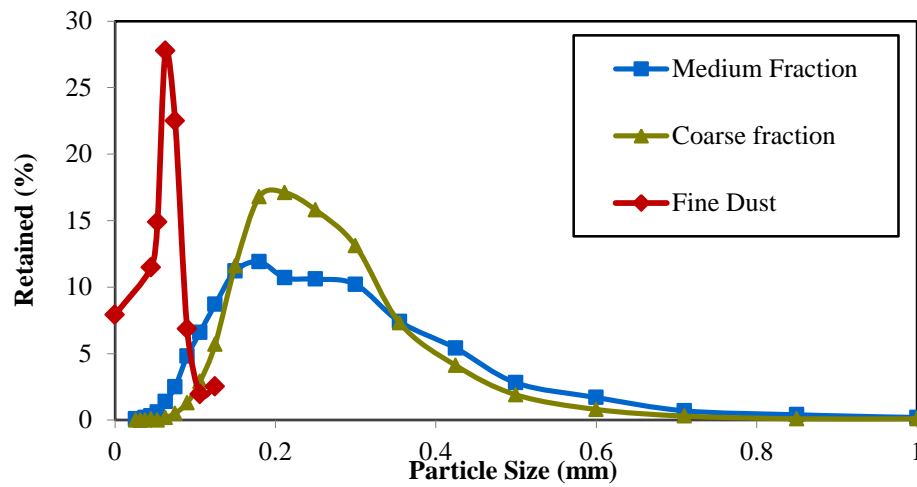


Figure 4.2. Particle size distribution of fine (<90 μ m), medium (90-180 μ m) and coarse (180-420 μ m) dust fractions

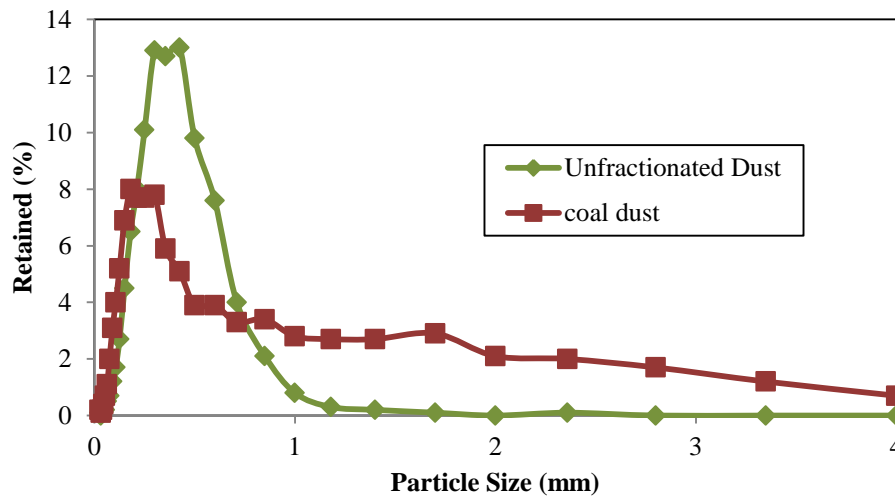


Figure 4.3. Particle size distribution of pine (unfractionated) and coal dust

Table 4.1 Geometric mean particle size of three pine dust fractions (fine, medium and coarse dust fraction), unfractionated pine dust and coal dust.

Properties	Fine Dust (<90µm)	Medium Dust (90-80) µm	Coarse Dust (180-420 µm)	Unfractionated Dust(<420 µm)	Coal Dust (<420 µm)
Particle Size (µm)	68.18±18.03	189.45±123.15	201.80±86.34	291.05±169.83	320.41±374.37

4.4.2 Bulk and Particle Density

Bulk densities of three types of fractions (fine, medium and coarse) were shown in the Table 4.2. Bulk density of the dust sample decreased significantly ($p>0.05$) with increase in particle size. This is because of decrease in internal particle voids as particle size decreased. Mani et al. (2004) also found that the bulk density of material decrease with an increase in the geometric mean diameter (Mani et al., 2004). Particle density of dust did not change significantly with a change in particle size ($p>0.05$). Bulk and particle density of coal was higher than the loblolly pine dust because of the high mineral content (ash) in coal compared to biomass (Vassilev et al., 2010). Similar results were obtained by Demribas et al. (2004) and they reported that an average bulk density of biomass was about 500 kg/m^3 while an average bulk density of coals was about 1300 kg/m^3 (Table 4.3).

4.4.3 Ash Content

Ash content of dust samples significantly increased ($P=0.0012$) with decrease in particle size (Table 4.2) with the fine fraction of dust having ash content of 1.70% while the coarse dust samples has ash content of 0.76% . Similar results were obtained by Miranda et al. (2012), Liu and Bui (2011) and Bridgeman et al. 2007 for switchgrass and reed canary grass. This was because that the inorganic particles were more grindable and they were separated from

lignocellulose structure of crops during grinding As expected, ash content of pine dust (1.08% on dry basis) was lower than the coal dust (19.22% on dry basis) because of higher levels of inorganic compounds in coal (Demirbas, 2004).

4.4.4 Volatile Matter

Volatile matter did not change significantly ($P=0.489$) with change in particle size (Table 4.2). Pine dust had high volatile content (82.36% on d.b.) compared to coal dust (31.00% on d.b.) because in general biomass have the higher hydrogen to carbon and oxygen to carbon ratios compared to coal (Jenkins et al., 1998). Volatiles are due to the decomposition of hydrogen, oxygen and carbon contents when a sample is heated at high temperature (Table 4.3).

4.4.5 Energy Content

Energy content of fractionated dust was not significantly ($P=0.6363$) affected by particle size. Energy content of dust fractions varied from 20.25 to 20.28 MJ/kg. Energy content of biomass dust (20.01 MJ/kg) was significantly less than coal dust (26.94 MJ/kg). This is due to high oxygen content in biomass compared to coal (Demirbas, 2004). These values were comparable to the values obtained by Carter, (2012) (Table 4.2 and Table 4.3).

Table 4.2 Physicochemical properties of pine dust fractions (fine, medium and coarse).

Samples	Moisture Content (%w.b.)	Bulk Density (kg/m^3)	Particle Density (kg/m^3)	Ash Content (% d.b.)	Volatile Material (% d.b.)	Energy Content (MJ/kg)
Fine Dust (<90 μm)	9.20 _a	208.33 _b	1443.55 _a	1.70 _c	82.19 _a	20.28 _a
Medium Dust (90-180 μm)	9.46 _a	179.14 _a	1448.29 _a	1.27 _b	82.07 _a	20.25 _a
Coarse Dust (180-420 μm)	8.73 _a	168.92 _a	1423.65 _a	0.76 _a	83.94 _a	19.68 _a

Subscripts with the different letters in row are significantly different ($p<0.05$).

Table 4.3 Physicochemical properties of pine dust fractions (fine, medium and coarse).

Samples	Moisture Content (% w.b.)	Bulk Density (kg/m³)	Particle Density (kg/m³)	Ash Content (% d.b.)	Volatile Matter (% d.b.)	Energy Content (MJ/kg)
Unfractionated Pine Dust (<420 µm)	8.16 _b	196.21 _a	1457.99 _a	1.08 _a	82.36 _b	20.01 _a
Lignite Coal Dust (<420 µm)	5.76 _a	521.48 _b	1513.31 _b	19.22 _b	31.00 _a	26.94 _b

Subscripts with the different letters in row are significantly different (p<0.05).

4.4.6 Hot Surface Ignition Temperature

Figure 4.4 and Figure 4.5 show the typical temperature profile obtained during the hot surface test. In the example shown the dust (fine dust) did not ignite when the hot plate was set to a temperature of 290°C (Figure 4.4) and hence there was a horizontal line. However, at a hot plate temperature of 295°C, the dust combusted and hence the rapid increase in temperature (Figure 4.5).

Results of the hot plate test showed that fine dust sample (< 90 µm) ignited at 295°C with smoke and flame being observed at this temperature. However, fine dust did not ignite at hot plate temperature of 290°C. Medium and coarse dust fractions were ignited at 300°C and 305°C, respectively. Hot plate ignition temperature therefore increases with an increase in particle size. We suspect this because of smaller particles of fine fraction causes faster volatile matter production (Chen et al. 1996). Ignition temperature of coal dust (295°C-300°C) was higher than the pine dust (295°C). This is because of the high volatile content of pine dust that caused the dust to react faster and ignited at low temperature (Demirbas, 2004). Ignition temperature of coal dust was lower compared to that obtained by Reddy et al. (1988). They found that the ignition temperatures of Prince and Pittsburgh coals were 250°C and 270°C, respectively. It could be because they used 10 mm layer of dust and these coal samples also have slightly higher volatile

content compared to coal sample used for present work (volatile contents of Prince coal and Pittsburgh coal were 34.35% and 36.4% respectively).

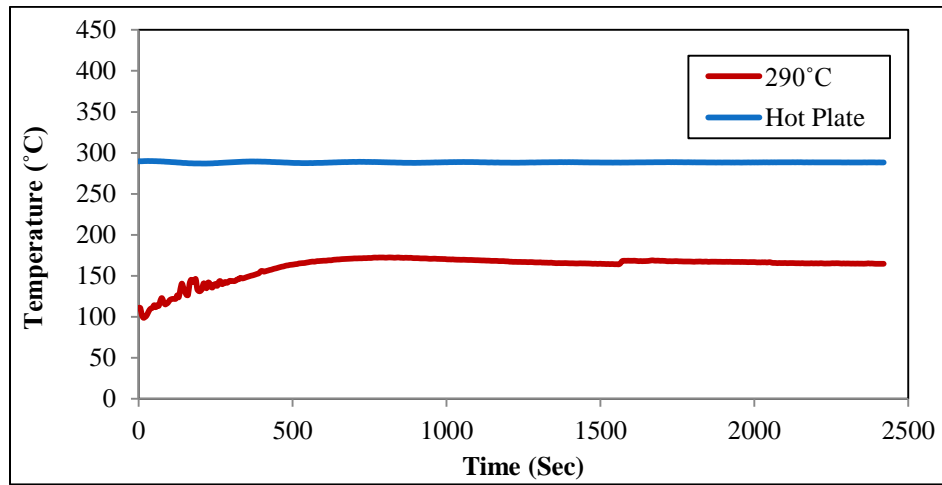


Figure 4.4. Temperature profile of fine dust sample when hot plate was set at 290°C (<90 μm).

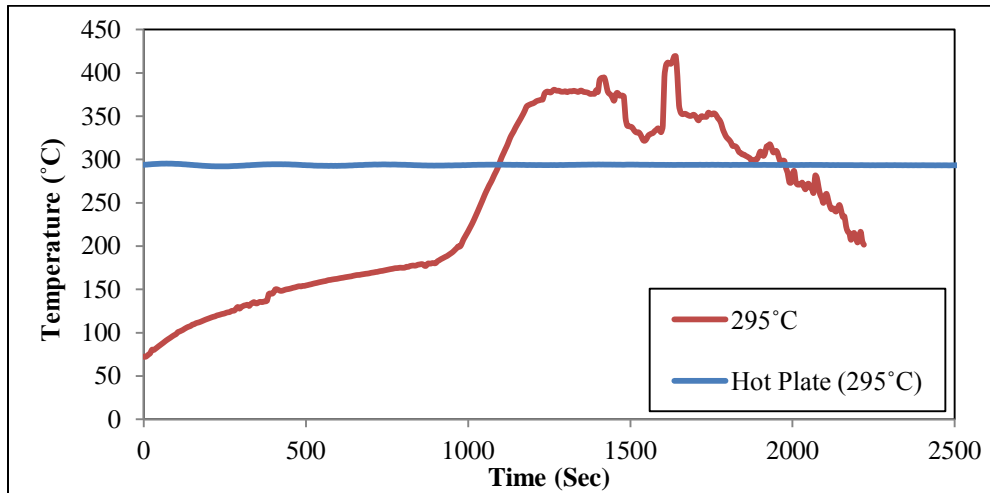


Figure 4.5. Temperature profile when dust sample (<90 μm) ignited. Hot plate was set at 295°C.

Table 4.4. Hot surface ignition temperature of dust samples

Properties	Fine dust (<90 μm)	Medium Dust (90-180 μm)	Coarse Dust (180-420 μm)	Unfractionated Pine Dust (<420 μm)	Lignite Coal Dust (<420 μm)
Ignition temperature ($^{\circ}\text{C}$)	290-295	295-300	300-305	290-295	295-300

4.4.7 Volatilization Properties

The typical, observed mass loss curves for dust samples heated in air and oxygen atmosphere are shown in Figures 4.6 and 4.7. There was an initial mass loss (about 10% of total mass) that was obtained between 30 $^{\circ}\text{C}$ to 100 $^{\circ}\text{C}$ which is attributed to release of moisture from the dusts. The thermal decomposition of dust started at about 220 $^{\circ}\text{C}$ followed by a rapid mass loss at about 324 $^{\circ}\text{C}$ that ends at about 500 $^{\circ}\text{C}$. Beyond 500 $^{\circ}\text{C}$, mass loss was negligible and the final mass recorded by TGA approximately equals to the ash content of the sample.

Particle size of dust did not affect significantly the volatilization properties (Table 4.3). The onset temperature of volatilization and the maximum mass loss rate temperature were obtained from the derivative of mass loss curve as shown in Figure 4.6. Loblolly pine dust had significantly low onset temperature of volatilization (TOD), temperature of maximum rate of mass loss (TMWI) and temperature of oxidation compared to coal dust because of the high volatile content of pine dust (82.36% d.b.) compared to coal dust (31.00% d.b.) (Figure 4.9). Similar results were obtained by Vuthaluru (2004) for coal and wood waste showed that their respectively onset ignition temperature were 260 $^{\circ}\text{C}$ and 426 $^{\circ}\text{C}$.

Using equation 4.11 apparent activation energy (E_a) of fine, medium and coarse dust fraction was 69.89, 67.05 and 71.25 kJ/mole, respectively. These values are comparable to activation energy (72.98 kJ/mol) of wood waste obtained by Sadhukhan et al., (2008). The plot of E_a versus T_{chr} was used to measure the ignition risk for the dust fractions (Figure 4.13). Coal dust

had lower risk of ignition as compared to pine dust. Similar plot was obtained by Ramirez et al., (2010) to examine the ignition risk associated with biological materials (icing sugar, maize dust and wheat dust). The risk of ignition of icing sugar, maize dust, and wheat dust were also shown in Figure 4.13 (Table 4.5).

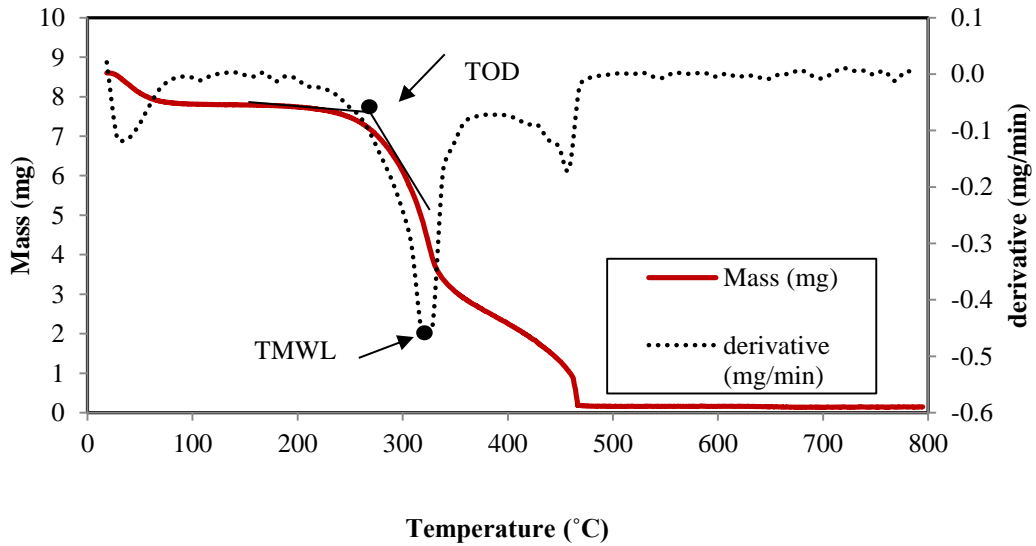


Figure 4.6. Example of TOD and TMWL from TGA data; curve is for determination of air-heated fine (< 90µm) dust.

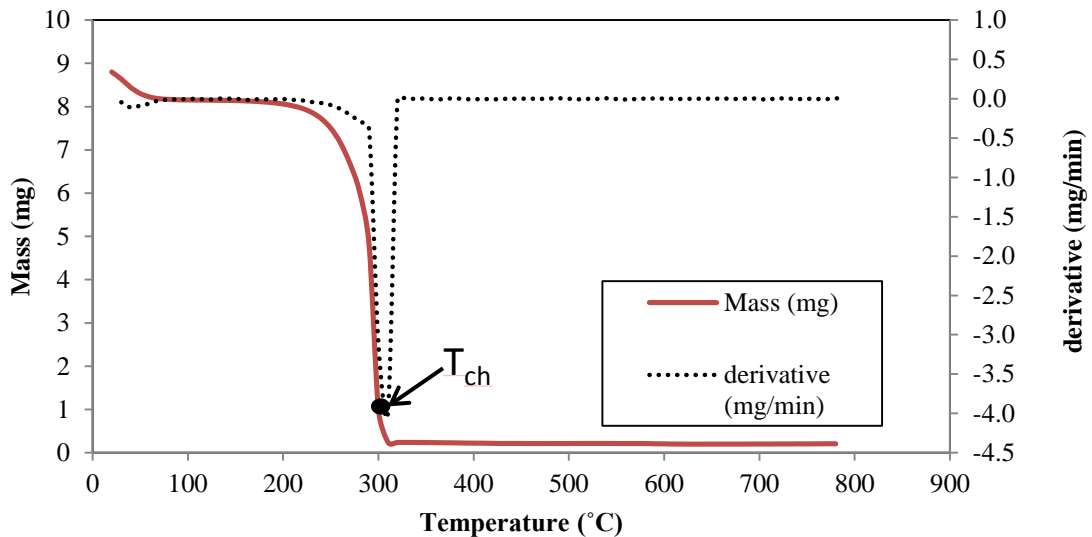


Figure 4.7. Determination of T_{ch} by thermogravimetric analysis carried out in the presence of oxygen of fine (<90µm) dust.

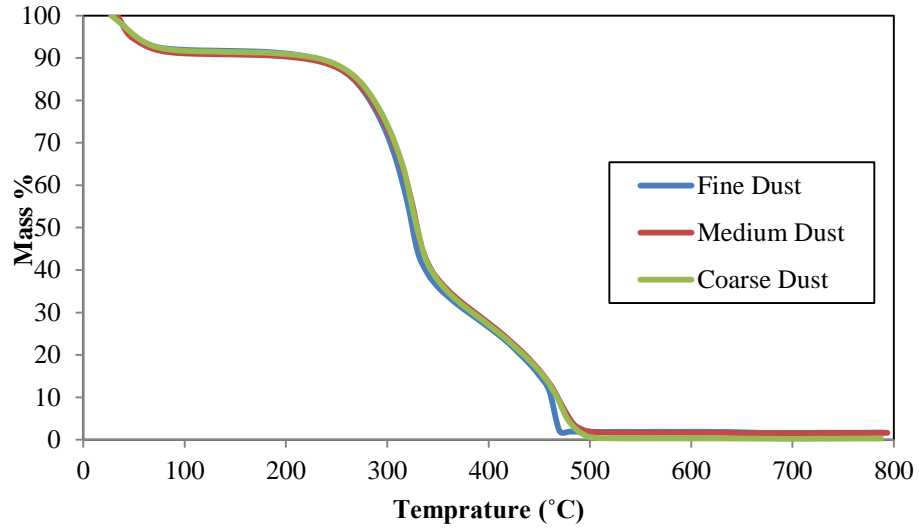


Figure 4.8. Mass loss of three dust fractions heated in air atmosphere (fine, medium and coarse).

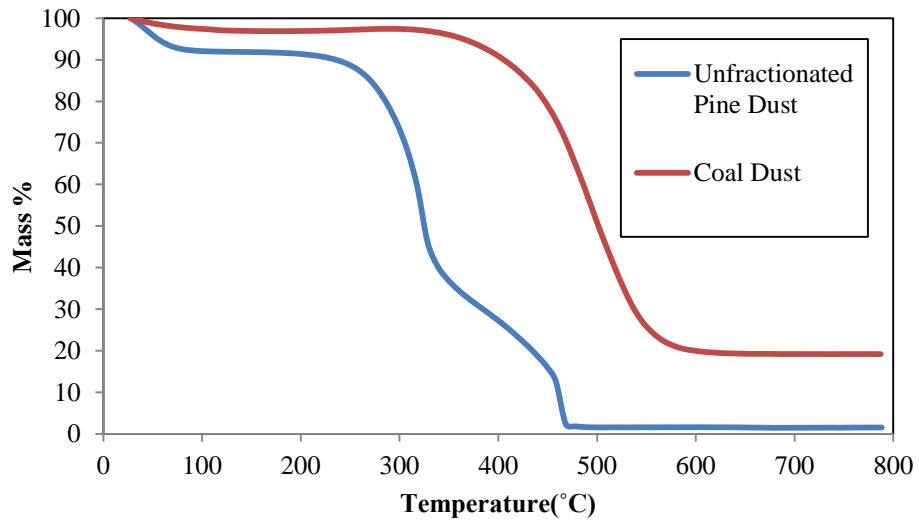


Figure 4.9. Mass loss of unfractionated pine dust and coal dust heated in air atmosphere.

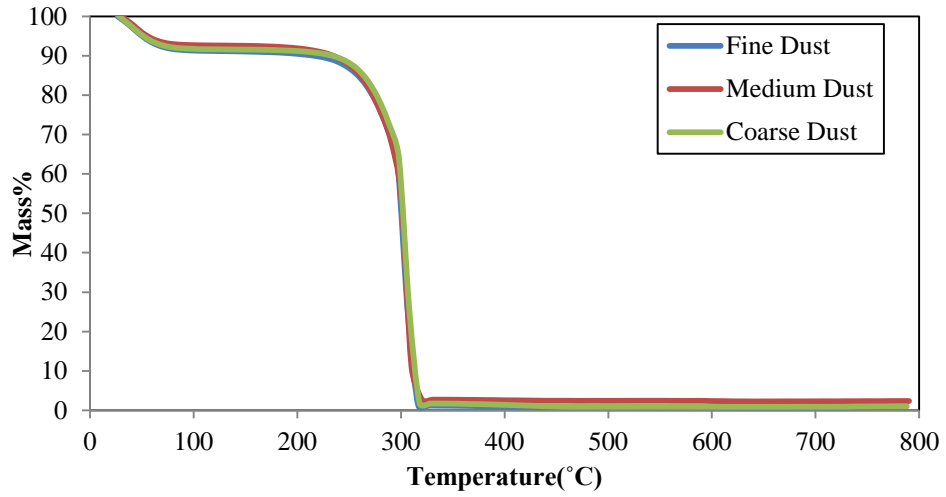


Figure 4.10. Mass loss of dust fractions (fine, medium and coarse) heated in the oxygen atmosphere.

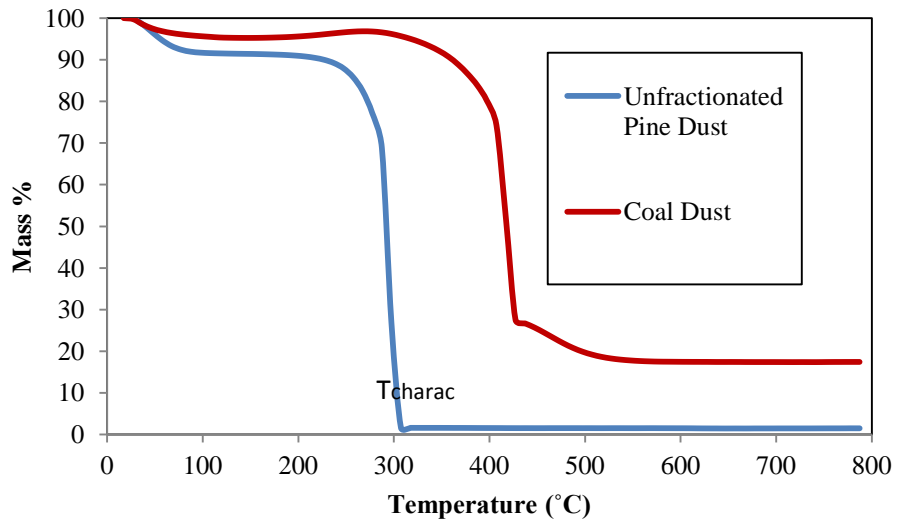


Figure 4.11. Mass loss of unfractionated pine dust and coal dust heated in the oxygen atmosphere.

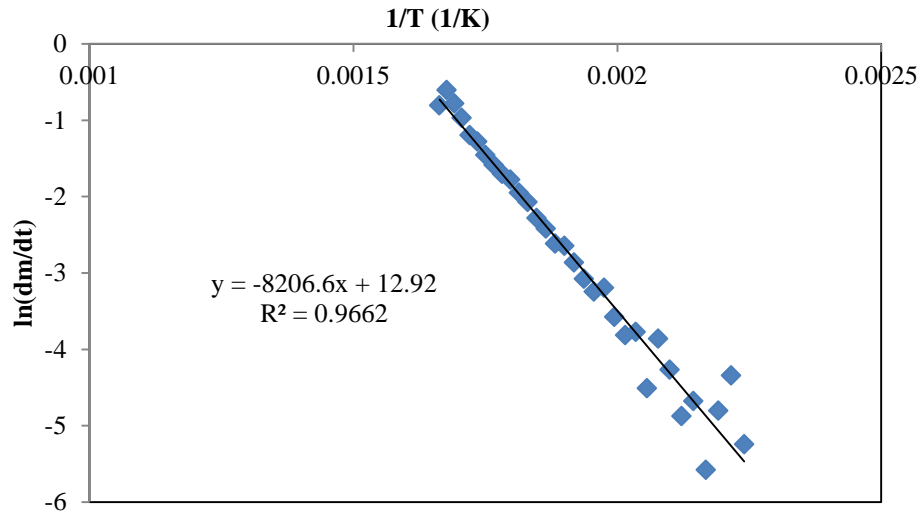


Figure 4.12. Determination of apparent activation energy (<90 μm) .

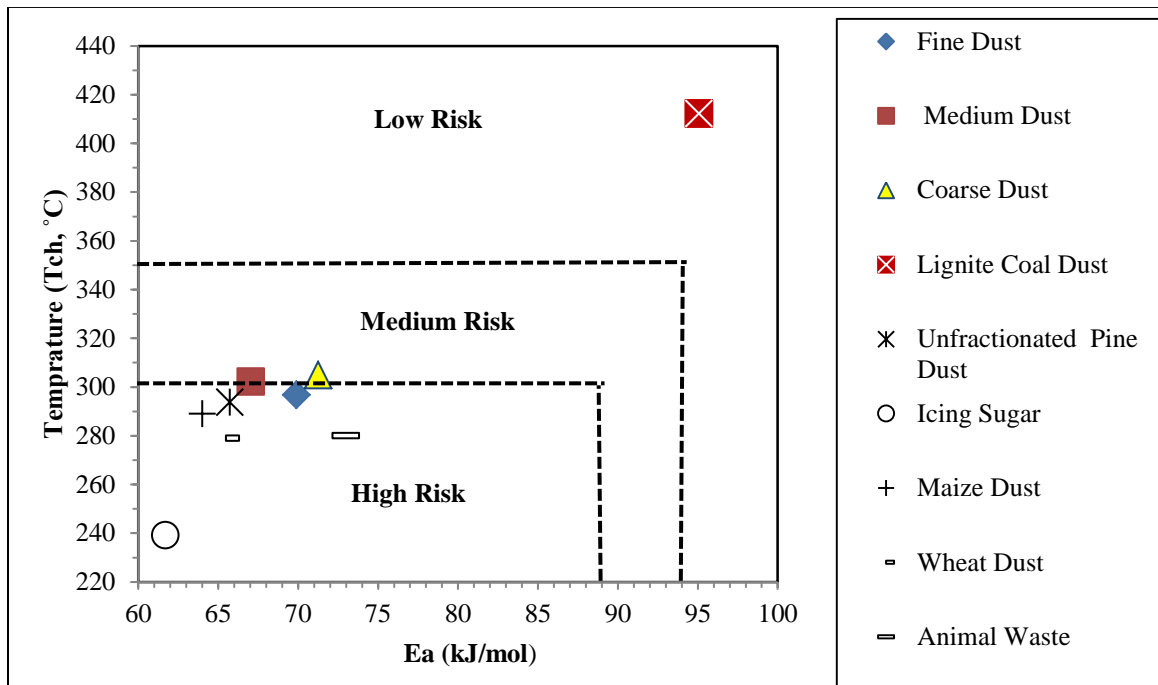


Figure 4.13. Ignition risk of pine dust fractions (fine dust, medium dust and coarse dust), unfractionated pine dust, lignite coal dust, biological materials dust (icing sugar, maize dust, wheat dust and animal waste) (Ramirez et al., (2010).

Table 4.5. TGA parameters of fractionated pine dust samples (fine, medium and coarse dust fraction), unfractionated pine dust, lignite coal dust, bituminous coal dust and biological materials.

Properties	TOD (°C)	TMW (°C)	T_{char}(°C)	E_a (kJ/mole)
Fine Dust (<90µm)	272 _a	325 _a	299 _a	70
Medium Dust (90-80) µm	264 _a	324 _a	304 _a	69
Coarse Dust (180-420 µm)	268 _a	325 _a	301 _a	71
Unfractionated Pine Dust (<420 µm)	273 _e	324 _e	293 _e	65
Lignite Coal Dust (<420 µm)	409 _f	489 _f	417 _f	95
Icing Sugar	212	220	239	62
Wheat Dust	268	279	279	65
Maize Dust	252	283	289	64
Animal Waste	300	180	280	73
Bituminous Coal Dust	392	407	261	80

Subscripts with the same values are not significantly different ($p < 0.05$) and a, b, c compare three fractions (fine, medium and coarse) with each other while e and f compare unfractionated pine and lignite coal dust.

Data for icing sugar, wheat dust, maize dust, bituminous dust have been used from Ramirez et al. (2010)

4.4.8 Exothermic Parameters (DSC)

The heat flow curve for the dust fraction was shown in Figure 4.14, when dust samples were heated from 30°C to 550°C at a rate of 20°C/minute. The negative value of heat flow indicated endothermic reaction that peaked about 100°C due to evaporation of moisture from dust

sample. After the loss of moisture, reaction of dust sample with oxygen started which produce oxo-compounds and released heat.

DSC parameters of dust for all three fractions (242-262°C) were also similar (Figure 4.15). Rapid exothermic reaction of fine dust started at low temperature compared to other dust fractions (Table 4.6). The rapid exothermic reaction in other biological materials such as maize wheat, barley, alfalfa and bread-making flour start also started in the range of 242-271°C (Ramirez et al., 2010). Rapid exothermic coal dust (235°C) started at low temperature compared to pine dust (241°C) because of its high carbon content (Figure 4.16). These values were comparable to values obtained by Ramirez et al. (2010) for three coal samples (Subbituminous coal, bituminous coal and Semi-anthracite coal). Maximum temperature of coal dust during the exothermic reaction was high compared to pine dust because of the higher energy content of coal dust.

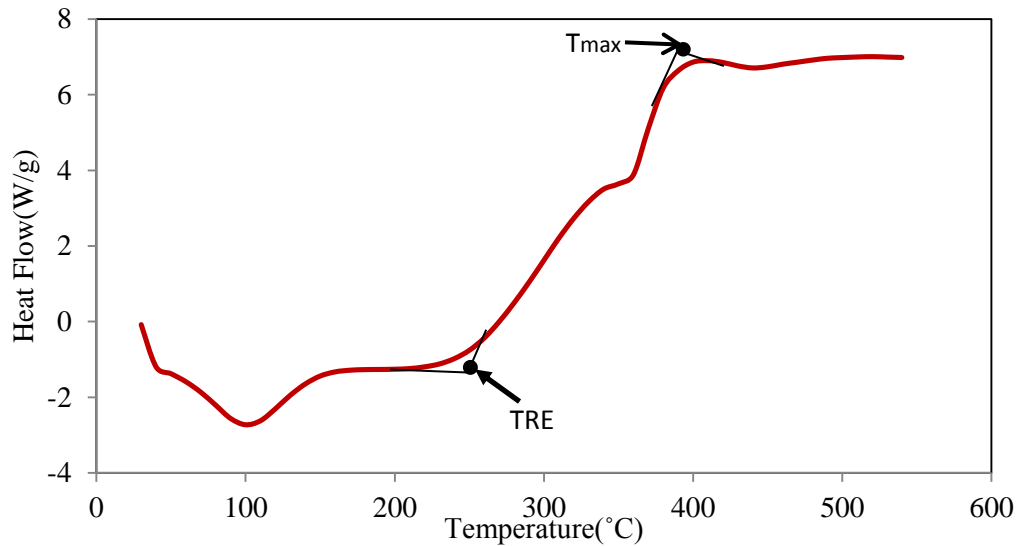


Figure 4.14. Determination of TRE and T_{max} by differential scanning calorimetry

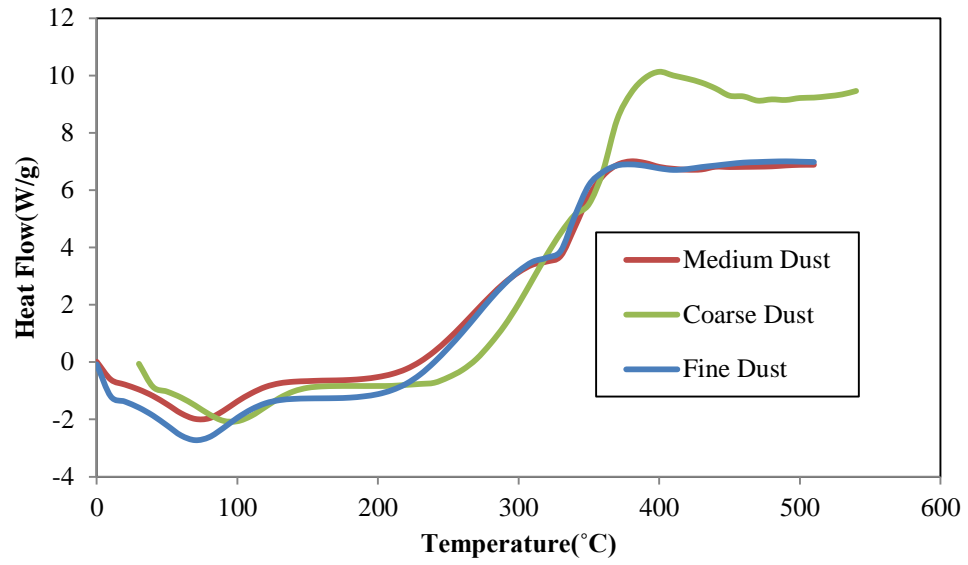


Figure 4.15. DSC plots of three dust fractions of loblolly pine (fine, medium and coarse)

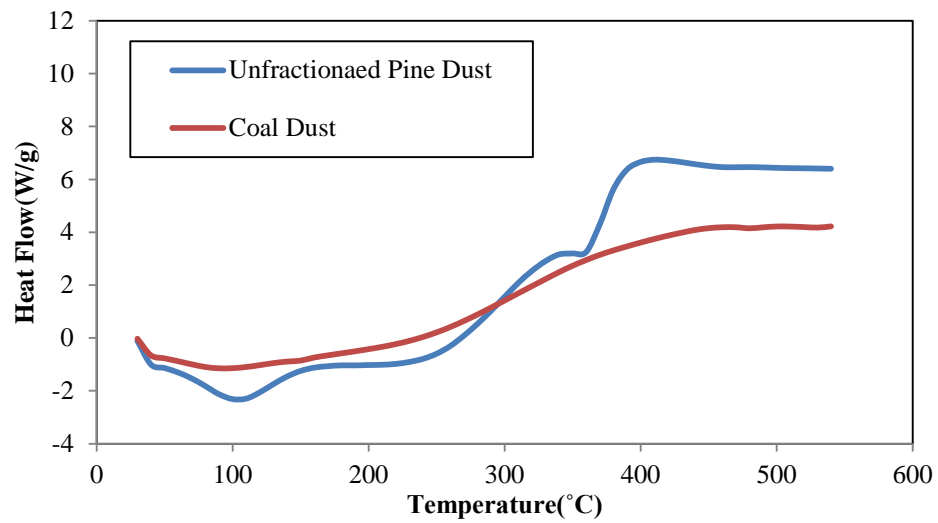


Figure 4.16. DSC plots of unfractionated loblolly pine dust and coal dust

Table 4.6. Exothermic parameters of three fractions (fine, medium and coarse dust) of pine dust

Properties	TRE (°C)	T _{max} (°C)	Exothermic Energy (kJ/kg)
Fine Dust (<90µm)	242 _a	397 _a	1114
Medium Dust (90-180) µm	253 _b	405 _a	1710
Coarse Dust (180-420 µm)	262 _b	398 _a	1100
Unfractionated Pine Dust (<420µm)	241 _f	400 _e	1231
Lignite Coal Dust (<420µm)	235 _e	453 _f	441
Icing Sugar	410	480	-
Wheat Dust	252	283	-
Maize Dust	242	386	-
Animal Waste	-	370	-
Bituminous Coal Dust	240	323	-

Subscripts under the values show the comparison of means according to Tukey test (P<0.05) and a, b, c compare three fractions (fine, medium and coarse) with each other while e and f compare unfractionated pine and lignite coal dust.

Data for icing sugar, wheat dust, maize dust, bituminous dust have been used from Ramirez et al. (2010)

4.5 Conclusion

Particle size affected the physical, chemical and ignition properties of loblolly pine dust. Bulk density of dust increased with a decrease in particle size. Particle density of dust remained nearly uniform with change in particle size. The fine dust fraction contained more ash content (1.70% on d.b.) compared to coarse and medium dust fractions (1.27% and 0.76% d.b., respectively). Volatile content and energy content of the three fractions were not significantly different (p>0.05). TGA and DSC parameters of the three types of dust fractions were similar. All

dust fractions were at the high to medium risk of ignition according to the activation energy and oxidation temperature results. Coal had high bulk and particle density, ash content and energy content compared to loblolly pine dust. High ash content and low volatile content of the pine dust affected its ignition properties. Ignition temperature of pine dust was between 290 °C and 295 °C which was lower compared to coal dust (295-300°C). Pine dust had a low onset temperature of volatilization (273°C) and temperature of maximum rate of mass loss (324°C) compared to coal. However, rapid exothermic reaction in coal started at a lower temperature (235°C). Pine dust was at high risk of ignition compared to coal based on the plot of activation energy and oxidation temperature results.

Chapter 5 Summary and Future Recommendation

5.1 Summary

The moisture content of wood chips and hammer-mill screen size significantly affected the amount of dust generated and energy required for grinding. When wood chips of three different moisture contents (w.b.) (4.7%, 14.7% and 23.6%) were ground through different hammer mill screens (1.20, 3.18 and 6.35 mm), about 5%-21% of wood chips were converted into dust. About 2% of the energy content of loblolly pine chips was utilized during the grinding. In general, the amount of dust generated decreased with increase in moisture content and screen size. Furthermore, energy required for grinding increased with increase in moisture content and decrease in screen size. Physicochemical properties of ground loblolly pine chips and dust were significantly affected by chip moisture content and hammer mill screen size. Except for particle density and energy content, physicochemical properties of loblolly pine dust were significantly different than ground chips. The ash content of dust was up to six times that of ground material. Physicochemical properties of loblolly pine dust were significantly affected by its particle size. Loblolly pine dust had high moisture content and volatile matter compared to coal dust. However, bulk and particle density, ash and energy content of coal dust was higher compared to coal dust. Similar to other biological materials, loblolly pine dust was at high risk of ignition compared to coal dust. The hot surface temperature, temperature of volatilization and temperature of onset

rapid exothermic reaction indicated that the susceptibility of the ignition increased with decrease in particle size.

In conclusion, the amount of dust generation during grinding of loblolly pine chips depends upon its moisture content and selection of screen size of grinder. Moisture content and screen size of grinder also affect physicochemical properties of biomass dust. Fine fraction of dust is at high risk of ignition compared to coarse dust fractions and should be handled carefully.

5.2 Future Recommendation

This study delivers the useful information regarding the physicochemical and ignition properties of dust from loblolly pine chips. Still, more work can be completed to better understand the problems related to biomass dusts.

Tests should be carried out to determine the amount of microorganisms and endotoxins and their growth in the dust obtained from loblolly pine chips to avoid the health problems. It would be very useful and time saving if physicochemical properties of dusts can be predicted from ground biomass. A model should be developed to find the relation between physicochemical properties of different types of ground biomass and their dusts. In the present study, only the effect of particle size on ignition properties of dusts was determined. Moisture content of biomass is another important property of biomass dust that influences their ignition properties. Therefore, additional test should be completed on ignition properties of dusts should by conditioning at different moisture contents (w.b.) ranging from 10% to 25% . Different types of biomass such as switch-grass, crop residues, eucalyptus tree and municipal waste are being used to produce bio-energy. However, limited information is available regarding the ignition properties of dust from biomass. It is crucial to determine the ignition properties of dust of different types of biomass to

avoid the explosion and ignition risk in bioenergy industry. In the future work, ignition properties of different types of biomass should be determined by following similar procedure.

References

Abbasi, T., and S. A. Abbasi. 2007. Dust explosions—Cases, causes, consequences, and control. *Journal of Hazardous Materials* 140(1–2):7-44.

Akpınar, A., M. İ. Kömürcü, M. Kankal, İ. H. Özölçer, and K. Kaygusuz. 2008. Energy situation and renewables in Turkey and environmental effects of energy use. *Renewable and Sustainable Energy Reviews* 12(8):2013-2039.

Amyotte, P. R. 2006. Solid inertants and their use in dust explosion prevention and mitigation. *Journal of Loss Prevention in the Process Industries* 19(2–3):161-173.

Amyotte, P. R., and R. K. Eckhoff. 2010. Dust explosion causation, prevention and mitigation: An overview. *Journal of Chemical Health and Safety* 17(1):15-28.

ASABE Standard S269.4. 2003. Cubes, pellets, and crumbles—definitions and methods for determining density, durability, and moisture content. ASABE, St. Joseph, MI.

ASABE Standard S319.3, 2003. Method of determining and expressing fineness of feed materials by sieving. *American Society of Agricultural and Biological Engineers*.

ASABE S593.1. 2011. Terminology and Definitions for Biomass Production, Harvesting and Collection, Storage, Processing, Conversion and Utilization. *American Society of Agricultural and Biological Engineers*.

Asif, M., and T. Muneer. 2007. Energy supply, its demand and security issues for developed and emerging economies. *Renewable and Sustainable Energy Reviews* 11(7):1388-1413.

ASTME871-82. Reapproved 2006. Standard Test Method for Moisture Analysis of Particulate Wood Fuels.

ASTM E2021-09. 2010. Standard Test Method for Hot-Surface Ignition Temperature of Dust Layers. *ASTM*.

- Babu, B. V. 2008. Biomass pyrolysis: a state-of-the-art review. *Biofuels, Bioproducts and Biorefining* 2(5):393-414.
- Balat, M., and H. Balat. 2009. Recent trends in global production and utilization of bio-ethanol fuel. *Applied Energy* 86(11):2273-2282.
- Balat, M. 2011. Production of bioethanol from lignocellulosic materials via the biochemical pathway: A review. *Energy Conversion and Management* 52(2):858-87
- Biogas Technology, 2013. Schematic Diagram of Biogas Plant. Available at <http://www.bebgmbh.de> . Accessed 2 March 2013.
- Biomass, 2013, Learning Goal and Explanation. Available at . www.is3felipee-portfolio.blogspot.com. Accessed 10 March 2013.
- Blair, A.S. 2007. Dust explosion incidents and regulations in the United States. *Journal of Loss Prevention in the Process Industries*. 20:523-529.
- Bowes, P. C. and S. E, Townshend. 1962. Ignition of combustible dusts on hot surfaces. *British Journal. Applied Physics*.13: 105-114.
- Bridgeman, T. G., L. I. Darvell, J. M. Jones, P. T. Williams, R. Fahmi, A. V. Bridgwater, T. Barraclough, I. Shield, N. Yates, S. C. Thain, and I. S. Donnison. 2007. Influence of particle size on the analytical and chemical properties of two energy crops. *Fuel* 86(1–2):60-72.
- Carter, C. L. 2012. Physicochemical Properties and Thermal Decomposition of Torrefied Woody Biomass and Energy Crop. MS thesis. Auburn, Alabama: Auburn University, Biosystems Engineering Department.
- Cashdollar, K. L. 1994. Flammability of metals and other elemental dust clouds. *Process Safety Progress* 13(3):139-145.
- Cashdollar, K. L. 2000. Overview of dust explosibility characteristics. *Journal of Loss Prevention in the Process Industries* 13(3–5):183-199.
- Callé, S. , L. Klabá, D. Thomas, L. Perrin, and O. Dufaud. 2005. Influence of the size distribution and concentration on wood dust explosion: Experiments and reaction modelling. *Powder Technology* 157(1–3):144–148
- CBCnews. 2012. Wood dust suspected in B.C. sawmill blasts: Available at <http://www.cbc.ca>. Accessed 10 September 2012.
- Chamberlain, E. A. C., and D. A. Hall. 1973. The ambient temperature oxidation of coal in relation to the early detection of spontaneous heating *The Mining Engineer*:387–397.

- Chawla, N., P. R. Amyotte, and M. J. Pegg. 1996. A comparison of experimental methods to determine the minimum explosible concentration of dusts. *Fuel* 75(6):654-658.
- Chen, Y., S. Mori, and W.-P. Pan. 1996. Studying the mechanisms of ignition of coal particles by TG-DTA. *Thermochimica Acta* 275(1):149-158.
- Clausnitzer, H., and M. J. Singer. 2000. Environmental influences on respirable dust production from agricultural operations in California. *Atmospheric Environment* 34(11):1739-1745.
- Combustible Dusts, 2013. Combustible Dusts. Available at <http://www.ccohs.ca>. Accessed 1 April, 2013.
- CSB, 2004 West. Investigation Report. *Dust Explosion*. West Pharmaceutical Services, Inc., U.S. Chemical Safety and Hazard Investigation Board (CSB). Available at <http://csb.gov/index.cfm>. Accessed 10 April, 2013.
- Dastidar, A. G., and P. R. Amyotte. 2002. Explosibility boundaries for fly ash/pulverized fuel mixtures. *Journal of Hazardous Materials* 92(2):115-126.
- Demirbaş, A. 2001. Biomass resource facilities and biomass conversion processing for fuels and chemicals. *Energy Conversion and Management* 42(11):1357-1378.
- Demirbas, A. 2004. Combustion characteristics of different biomass fuels. *Progress in Energy and Combustion Science* 30(2):219-230.
- DOE. 2013. Biochemical Conversion. United States Department of energy. Available at www.eere.energy.gov. Accessed 17 December 2012.
- Ebling, J., and B. Jenkins. 1985. Physical and chemical properties of biomass fuels. *Transactions of the ASAE (American Society of Agricultural Engineers)* 28(3):5.
- Eckhoff, R. K. 2000. Design of electrical equipment for areas containing combustible dust: Why dust standards cannot be extensively harmonised with gas standards. *Journal of Loss Prevention in the Process Industries* 13(3-5):201-208.
- Eckhoff, R. K. 2003. *Dust Explosion in the Process Industries*. 3 ed. Gulf Professional Publications, 2003.
- EIA. 2013. United States Energy Information Administration. Available at <http://www.eia.gov>. Accessed 10 March, 2013.
- Energy Independence and Security Act of 2007, H.R.6, in: 110th United States Congress, 1st Session, (Ed.), H.R.6, Congressional Record, Washington D.C.
- Esteban, L. S. and J. E. Carrasco. 2006. Evaluation of different strategies for pulverization of forest biomasses. *Powder Technology*. 166 (3):139-151.
- Fasina, O. O. 2008. Physical properties of peanut hull pellets. *Bioresource Technology* 99(5):1259-1266.

- Gani, A., I. Naruse. 2007. Effect of cellulose and lignin content on pyrolysis and combustion characteristics for several types of biomass. *Renewable Energy*. 32(4): 649–661.
- García-Torrent, J., Á. Ramírez-Gómez, E. Querol-Aragón, C. Grima-Olmedo, and L. Medic-Pejic. 2012. Determination of the risk of self-ignition of coals and biomass materials. *Journal of Hazardous Materials* 213–214(0):230-235.
- Gillman, T. H., and I. Le May. 2007. Mechanical and electrical failures leading to major fires. *Engineering Failure Analysis* 14(6):995-1018.
- Gomez, L. D., C. G. Steele-King, and S. J. McQueen-Mason. 2008. Sustainable liquid biofuels from biomass: the writing's on the walls. *New Phytologist* 178(3):473-485.
- Gómez-Barea, A., and B. Leckner. 2010. Modeling of biomass gasification in fluidized bed. *Progress in Energy and Combustion Science* 36(4):444-509.
- Gray, B. F., M. J. Sexton, B. Halliburton, and C. Macaskill. 2002. Wetting-induced ignition in cellulosic materials. *Fire Safety Journal* 37(5):465-479.
- Grotkjær, T., K. Dam-Johansen, A. D. Jensen, and P. Glarborg. 2003. An experimental study of biomass ignition. *Fuel* 82(7):825-833.
- Gummer, J., G.A Lunn. 2003. Ignitions of explosive dust clouds by smouldering and flaming agglomerates. *Journal of Loss Prevention in the Process Industries*. 16(1):27–32.
- Hoffa, E. A., D. E. Ward, W. M. Hao, R. A. Susott, and R. H. Wakimoto. 1999. Seasonality of carbon emissions from biomass burning in a Zambian savanna. *Journal of Geophysical Research: Atmospheres* 104(D11):13841-13853.
- IEA.2013. International Energy Agency. Available at <http://www.iea.org>. Accessed 2 February, 2013.
- ISO 562, 2010. Hard coal and coak. Determination of volatile matter. *International Standards*.
- Janes, A., D. Carson, A. Accorsi, J. Chaineaux, B. Tribouilloy, and D. Morainvillers. 2008. Correlation between self-ignition of a dust layer on a hot surface and in baskets in an oven. *Journal of Hazardous Materials* 159(2–3):528-535.
- Janes, A., J. Chaineaux, D. Carson, and P. A. Le Lore. 2008. MIKE 3 versus HARTMANN apparatus: Comparison of measured minimum ignition energy (MIE). *Journal of Hazardous Materials* 152(1):32-39.
- Jeguirim, M., and G. Trouvé. 2009. Pyrolysis characteristics and kinetics of *Arundo donax* using thermogravimetric analysis. *Bioresource Technology* 100(17):4026-4031.
- Jenkins, B. M., L. L. Baxter, T. R. Miles Jr, and T. R. Miles. 1998. Combustion properties of biomass. *Fuel Processing Technology* 54(1–3):17-46.

- Jokela, E. J., P. M. Dougherty, and T. A. Martin. 2004. Production dynamics of intensively managed loblolly pine stands in the southern United States: a synthesis of seven long-term experiments. *Forest Ecology and Management* 192(1):117-130.
- Joshi, K. A., V. Raghavan, and A. S. Rangwala. 2012. An experimental study of coal dust ignition in wedge shaped hot plate configurations. *Combustion and Flame* 159(1):376-384. *Journal of Loss Prevention in the Process Industries*. 20(4-6): 691-697.
- Kaliyan, N., R. V. Morey, M. D. White, and D. G. Tiffany. 2009. A Tub-Grinding/Roll-Press Compaction System to Increase Biomass Bulk Density: Preliminary Study. *ASABE*.
- Kalliny, M. I., J. A. Brisolará, H. Glindmeyer, and R. Rando. 2008. A Survey of Size-Fractionated Dust Levels in the U.S. Wood Processing Industry. *Journal of Occupational and Environmental Hygiene* 5(8):501-510.
- Kennedy, C., J. Steinberger, B. Gasson, Y. Hansen, T. Hillman, M. Havránek, D. Pataki, A. Phdungsilp, A. Ramaswami, and G. V. Mendez. 2010. Methodology for inventorying greenhouse gas emissions from global cities. *Energy Policy* 38(9):4828-4837.
- Khan, N., M. Bradley, and R. Berry. 2008. Best Practice Guide for Handling of Biomass Fuels and Coal-Biomass Mixes. *The Wolfson Centre for Bulk Solids Handling Technology*(4).
- Krause, U., and M. Schmidt. 2001. The influence of initial conditions on the propagation of smouldering fires in dust accumulations. *Journal of Loss Prevention in the Process Industries* 14(6):527-532.
- Kumar, P., D. M. Barrett, M. J. Delwiche and P. Stroeve. 2009. Methods for Pretreatment of Lignocellulosic Biomass for Efficient Hydrolysis and Biofuel Production. *American Chemical Society*. 48 (8):3713–3729.
- Laar, G. F. M. v., and J. P. Zeeuwen. 1985. On the minimum ignition energy of dust/air mixture. *Archivum Combustion* 5:145-149.
- Lal, R. 2004. Agricultural activities and the global carbon cycle. *Nutrient Cycling in Agroecosystems* 70(2):103-116.
- LAP. 2005. Determination of Ash in Biomass by Laboratory Analytical Procedure *National Renewable Energy Laboratory NREL/TP-510-42622* .
- Lebecki, K., Z. Dyduch, A. Fibich, and J. Śliż. 2003. Ignition of a dust layer by a constant heat flux. *Journal of Loss Prevention in the Process Industries* 16(4):243-248
- Lewandowski, I., and A. Kicherer. 1997. Combustion quality of biomass: practical relevance and experiments to modify the biomass quality of *Miscanthus x giganteus*. *European Journal of Agronomy* 6(3–4):163-177.
- Liu, X., and X. T. Bi. 2011. Removal of inorganic constituents from pine barks and switchgrass. *Fuel Processing Technology* 92(7):1273-1279.
- Liu, Y., J. Sun and D. Chen, 2007. Flame propagation in hybrid mixture of coal dust and methane. *Journal of Loss Prevention in the Process Industries* 20 (4–6):691–697.

- Lu., K., T. Chin and K. Hua, 2009. Investigation of the decomposition reaction and dust explosion characteristics of crystalline benzoyl peroxides. *Journal of Hazardous Material*. 161(1): 246-256.
- Macedo, I. C., J. E. A. Seabra, and J. E. A. R. Silva. 2008. Green house gases emissions in the production and use of ethanol from sugarcane in Brazil: The 2005/2006 averages and a prediction for 2020. *Biomass and Bioenergy* 32(7):582-595.
- Madsen, A. M., L. Martensson, T. Schneider, And L. Larsson. 2004. Microbial Dustiness and Particle Release of Different Biofuels. *Annals of Occupational Hygiene* 48(4):327-338.
- Mani, S., L. G. Tabil, and S. Sokhansanj. 2004. Grinding performance and physical properties of wheat and barley straws, corn stover and switchgrass. *Biomass and Bioenergy* 27(4):339-352.
- Mann, M., and P. Spath. 2001. A life cycle assessment of biomass cofiring in a coal-fired power plant. *Clean Products and Processes* 3(2):81-91.
- McIlveen-Wright, D. R., Y. Huang, S. Rezvani, and Y. Wang. 2007. A technical and environmental analysis of co-combustion of coal and biomass in fluidised bed technologies. *Fuel* 86(14):2032-2042.
- McKendry, P. 2002. Energy production from biomass (part 2): conversion technologies. *Bioresource Technology* 83(1):47-54.
- Mettanant, V., P. Basu, and J. Butler. 2009. Agglomeration of biomass fired fluidized bed gasifier and combustor. *The Canadian Journal of Chemical Engineering* 87(5):656-684.
- Microsoft Excel, 2010. Microsoft Office 2010 Redmond, WA
- Miranda, I., J. Gominho, I. Mirra, and H. Pereira. 2012. Chemical characterization of barks from *Picea abies* and *Pinus sylvestris* after fractioning into different particle sizes. *Industrial Crops and Products* 3.
- Miron, Y., and C. P. Lazzara. 1988. Hot-surface ignition temperatures of dust layers. *Fire and Materials* 12(3):115-126.
- Moqbel, S., D. Reinhart, and R.-H. Chen. 2010. Factors influencing spontaneous combustion of solid waste. *Waste Management* 30(8-9):1600-1607.
- Moser, B. 2011. Biodiesel Production, Properties, and Feedstocks. In *Biofuels*, 285-347. D. Tomes, P. Lakshmanan, and D. Songstad, eds: Springer New York.
- Mosier, N., C. Wyman, B. Dale, R. Elander, Y. Y. Lee, M. Holtzapple, and M. Ladisch. 2005. Features of promising technologies for pretreatment of lignocellulosic biomass. *Bioresource Technology* 96(6):673-686.
- Murphy, L. N., William J. Riley, and William D. Collins. 2012. Local and Remote Climate Impacts from Expansion of Woody Biomass for Bioenergy Feedstock in the Southeastern United States. *J. Climate* 25:7643-7659.

- Mussatto, S. I., G. Dragone, P. M. R. Guimarães, J. P. A. Silva, L. M. Carneiro, I. C. Roberto, A. Vicente, L. Domingues, and J. A. Teixeira. 2010. Technological trends, global market, and challenges of bio-ethanol production. *Biotechnology Advances* 28(6):817-830.
- Naik, S. N., V. V. Goud, P. K. Rout, and A. K. Dalai. 2010. Production of first and second generation biofuels: A comprehensive review. *Renewable and Sustainable Energy Reviews* 14(2):578-597.
- NFPA. 2007. Standard on Explosion Protection by Deflagration Venting *National Fire Protection Association NFPA 68*.
- NFPA. 2008a. Recommended practice for the classification of hazardous (classified) locations for electrical installations in chemical process areas *National Fire Protection Association NFPA 499*.
- NFPA. 2008b. Standard for the prevention of fires and dust explosions in agricultural and food processing facilities. *National Fire Protection Association NFPA-61*.
- NFPA. 2011. Revised Dust Standard- Safety Engineering Networks. *National Fire Protection Association*.
- Nichols, D., J. Zerbe. 2012. Cofiring Biomass and Coal for Fossil Fuel Reduction and Other Benefits—Status of North American Facilities in 2010. *United States Department of Agricultural and Forest Service*.
- Nifuku, M., H. Tsujita, K. Fujino, K. Takaichi, C. Barre, M. Hatori, S. Fujiwara, S. Horiguchi, and E. Paya. 2005. A study on the ignition characteristics for dust explosion of industrial wastes. *Journal of Electrostatics* 63(6–10):455-462.
- Nifuku, M., S. Koyanaka, H. Ohya, C. Barre, M. Hatori, S. Fujiwara, S. Horiguchi, and I. Sochet. 2007. Ignitability characteristics of aluminium and magnesium dusts that are generated during the shredding of post-consumer wastes. *Journal of Loss Prevention in the Process Industries* 20(4–6):322-329.
- Oseuke, C.O. and C. A. K. Ezugwu. 2011. Study of Nigeria Energy Resources and Its and Its Consumption. *International Journal of Scientific & Engineering Research*. 2 (12):ISSN 2229-5518.
- Perlack, R. D., L. L. Wright, A. F. Turhollow, R. L. Graham, B. J. Stokes, and D. C. Erbach. 2005. Biomass as Feedstock for a Bioenergy and Bioproducts Industry The Technical Feasibility of a Billion-Ton Annual Supply, United States Department of Energy, Oak Ridge, TN. *United States Department of Energy, Oak Ridge, TN*.
- Petrou, E. C., and C. P. Pappis. 2009. Biofuels: A Survey on Pros and Cons. *Energy & Fuels* 23(2):1055-1066.
- Phanphanich, M., and S. Mani. 2011. Impact of torrefaction on the grindability and fuel characteristics of forest biomass. *Bioresour. Technology* 102(2):1246-1253.
- Pialo, R. E. Ramalhoa, C. Pinho. 2006. Overall characterization of cork dust explosion. *Journal of Hazardous Material* 133(1-3): 183-195.

- Pinkwasser, T. 1986. On the Ignition capacity of Free-falling Smouldering Fires. *Euromech Colloquium 208, Explosions in Industry*.
- Pinkwasser, T. 1986. On the Ignition capacity of Free-falling Smouldering Fires. *Euromech Colloquium 208, Explosions in Industry*.
- Qian, Y., C. Zuo, J. Tan, and J. He. 2007. Structural analysis of bio-oils from sub-and supercritical water liquefaction of woody biomass. *Energy* 32(3):196-202.
- Ramírez, Á., J. García-Torrent, and P. J. Aguado. 2009. Determination of parameters used to prevent ignition of stored materials and to protect against explosions in food industries. *Journal of Hazardous Materials* 168(1):115-120.
- Ramírez, Á., J. García-Torrent, and A. Tascón. 2010. Experimental determination of self-heating and self-ignition risks associated with the dusts of agricultural materials commonly stored in silos. *Journal of Hazardous Materials* 175(1-3):920-927.
- Reddy, P. D., P. R. Amyotte, and M. J. Pegg. 1998. Effect of Inerts on Layer Ignition Temperatures of Coal Dust. *Combustion and Flame* 114(1-2):41-53.
- Ren, T. X., J. S. Edwards, and D. Clarke. 1999. Adiabatic oxidation study on the propensity of pulverised coals to spontaneous combustion. *Fuel* 78(14):1611-1620.
- Sadhukhan, A. K., P. Gupta, T. Goyalb, and R. K. Saha. 2008. Modelling of pyrolysis of coal-biomass blends using thermogravimetric analysis. *Bioresource Technology* 99 (17):8022-8026.
- Salameh, M. G. 2003. Can renewable and unconventional energy sources bridge the global energy gap in the 21st century? *Applied Energy* 75(1-2):33-42.
- SAS. 2009. SAS User's Guide: Statistics. Ver. 6a. Cary, N.C.: SAS Institute, Inc
- Schmidt, M., C. Lohrer, and U. Krause. 2003. Self-ignition of dust at reduced volume fractions of ambient oxygen. *Journal of Loss Prevention in the Process Industries* 16(2):141-147.
- Scholtz, G., HJ van der Merwe, and T. Tylutki. 2009. Sample preparation of Medicago sativa L. hay for chemical analysis. *South African Journal of Animal Science*. 39(1): 73-76.
- Shafiee, S., and E. Topal. 2009. When will fossil fuel reserves be diminished? *Energy Policy* 37(1):181-189.
- Shaw, M. D., C. Karunakaran, and L. G. Tabil. 2009. Physicochemical characteristics of densified untreated and steam exploded poplar wood and wheat straw grinds. *Biosystems Engineering* 103(2):198-207.
- Simmons, B. A., D. Loque, and H. W Blanch. 2008. Next-generation biomass feedstocks for biofuel production. *Genome Biology* 9(12):9.
- Sokhansanj, S., S. Mani, A. Turhollow, A. Kumar, D. Bransby, L. Lynd, and M. Laser. 2009. Large-scale production, harvest and logistics of switchgrass (*Panicum virgatum* L.) – current technology and envisioning a mature technology. *Biofuels, Bioproducts and Biorefining* 3(2):124-141.

- Sweis, F. K. 1998. The effect of admixed material on the ignition temperature of dust layers in hot environments. *Journal of Hazardous Materials* 63(1):25-35.
- Synnott, E. C., J. B. Glynn, and T. C. Duane. 1984. Minimum ignition temperature of a self-raising flour on a standard hot-plate. *Journal of Food Engineering* 3(2):151-160.
- Taveau, J. 2012. Secondary dust explosions: How to prevent them or mitigate their effects? *Process Safety Progress* 31(1):36-50.
- Tumuluru, J. S., C. T. Wright, K. L. Kenney, and J. R. Hess. 2010. A Technical Review on Biomass Processing: Densification, Preprocessing, Modeling, and Optimization. *2010 ASABE Annual International Meeting*.
- Vassilev, S. V., D. Baxter, L. K. Andersen, and C. G. Vassileva. 2010. An overview of the chemical composition of biomass. *Fuel* 89(5):913-933.
- Vordebrueggen, J.B. 2011. Imperial sugar refinery combustible dust explosion investigation. *Process Safety Progress* 30(1): 66-81.
- Wang, H., B. Z. Dlugogorski, and E. M. Kennedy. 1998. Low-temperature oxidation of coal at elevated pressures. *Journal of Loss Prevention in the Process Industries* 11(6):373-381.
- Wei, M., S. Patadia, and D. M. Kammen. 2010. Putting renewables and energy efficiency to work: How many jobs can the clean energy industry generate in the U.S. *Energy Policy* 38(2):919-931.
- Weiland, P. 2010. Biogas production: current state and perspectives. *Applied Microbiology and Biotechnology* 85(4):849-860.
- Williams, T. M., and C. A. Gresham. 2006. Biomass accumulation in rapidly growing loblolly pine and sweetgum. *Biomass and Bioenergy* 30(4):370-377.
- Wypych, P., D. Cook, and P. Cooper. 2005. Controlling dust emissions and explosion hazards in powder handling plants. *Chemical Engineering and Processing: Process Intensification* 44(2):323-326.
- Yusuf, N.N.A.N., S.K. Kamarudin and Z. Yaakub. 2011. Overview on the current trends in biodiesel production. *Energy Conversion and Management*. 52 (7):2741–2751.
- Zhang, L., C. Xu, and P. Champagne. 2010. Overview of recent advances in thermo-chemical conversion of biomass. *Energy Conversion and Management* 51(5):969-982.
- Zhang, Q., J. Chang, T. Wang, and Y. Xu. 2007. Review of biomass pyrolysis oil properties and upgrading research. *Energy Conversion and Management* 48(1):87-92.
- Zhu, J. Y., and X. J. Pan. 2010. Woody biomass pretreatment for cellulosic ethanol production: Technology and energy consumption evaluation. *Bioresource Technology* 101(13):4992-5002.

Appendix A -Amount of Dust Generated, Energy Required for Grinding and Physicochemical Properties Data

Table A.1 Amount of Dust Generated at different wood chip’s moisture content and hammer mill screen sizes

Moisture Level (% w.b.)	Screen Size (mm)	Dust Generated (%)	Mean (%)	Standard Deviation (%)
		21.18		
4.7	1.2	22.22	21.70	0.74
		11.84		
14.7	1.2	10.98	11.41	0.61
		5.43		
23.6	1.2	5.43	5.43	0.00
		9.62		
4.7	3.18	10.59	10.11	0.69
		8.75		
14.7	3.18	8.62	8.69	0.09
		4.69		
23.6	3.18	3.81	4.25	0.62
		11.32		
4.7	6.35	16.95	14.14	3.98
		9.37		
14.7	6.35	9.88	9.63	0.36
		5.47		
23.6	6.35	5.11	5.29	0.25

Table A.2. Energy required to grind loblolly pine chips of different moisture contents through different hammer mill screens

Moisture Level (% w.b.)	Screen Size (mm)	Energy Required to Run Empty Hammer-mill (kJ)	Grinding Energy (kJ/kg)	Mean Grinding Energy (kJ/kg)	Standard Deviation of Grinding Energy (kJ/kg)
		1800.00	138.46		
4.7	1.20	1368.00	110.77	124.62	19.58
		2088.00	223.1		
14.7	1.20	1944.00	162.25	192.68	43.02
		2808.00	368.78		
23.6	1.20	2520.00	351.22	360.00	12.42
		1440.00	71.29		
4.70	3.18	1368.00	92.90	82.10	15.28
		2304.00	118.76		
14.70	3.18	1872.00	182.54	150.65	45.09
		3240.00	238.02		
23.60	3.18	2736.00	235.38	236.7	1.86
		864.00	31.30		
4.70	6.35	792.00	48.00	39.65	11.81
		1446.48	101.93		
14.70	6.35	1094.40	65.21	83.57	25.97
		1584.00	128.22		
23.6	6.35	1656.00	110.34	119.28	12.64

Table A.3. Moisture content (% w.b.) of ground loblolly pine at different moisture content levels and hammer mill screen sizes

Moisture Level (% w.b.)	Screen Size (mm)	Moisture Content (% w.b.)	Mean (% w.b.)	Standard Deviation (%w.b.)
4.7	1.20	5.88	5.83	0.08
		5.74		
		5.88		
14.7	1.20	9.9	9.89	0.02
		9.87		
		9.9		
23.6	1.20	9.8	9.82	0.11
		9.93		
		9.72		
4.7	3.18	5.81	5.58	0.37
		5.77		
		5.15		
14.7	3.18	10.9	10.80	0.09
		10.72		
		10.78		
23.6	3.18	14.17	14.21	0.07
		14.29		
		14.16		
4.7	6.35	5.86	5.86	0.04
		5.82		
		5.9		
14.7	6.35	14.27	14.36	0.12
		14.49		
		14.32		
23.6	6.35	19.82	19.59	0.22
		19.58		
		19.38		

Table A.4. Bulk Density kg/m^3 of ground loblolly pine at different levels of moisture content and hammer mill screen sizes.

Moisture Level (%w.b.)	Screen Size (mm)	Bulk Density (kg/m^3)	Mean (kg/m^3)	Standard Deviation (kg/m^3)
4.7	1.20	225.96	224.27	1.77
		222.44		
		224.42		
14.7	1.20	274.28	273.36	1.44
		274.10		
		271.70		
23.6	1.20	252.65	256.02	2.95
		258.10		
		257.31		
4.7	3.18	218.70	218.82	1.06
		219.93		
		217.82		
14.7	3.18	251.79	253.01	1.31
		252.84		
		254.40		
23.6	3.18	227.93	228.84	1.35
		230.40		
		228.20		
4.7	6.35	221.25	220.52	1.19
		221.16		
		219.14		
14.7	6.35	231.55	233.26	3.58
		230.86		
		237.38		
23.6	6.35	205.68	206.15	2.32
		204.10		
		208.67		

Table A.5. Particle Density (kg/m^3) of ground loblolly pine at different levels of moisture content and hammer mill screen sizes

Moisture Level (% w.b.)	Screen Size (mm)	Particle Density (kg/m^3)	Mean (kg/m^3)	Standard Deviation (kg/m^3)
		1458.20		
4.7	1.20	1457.30	1457.75	0.64
		1401.50		
14.7	1.20	1413.20	1407.35	42.57
		1469.90		
23.6	1.20	1470.00	1469.95	0.07
		1451.70		
4.7	3.18	1450.19	1450.95	1.07
		1401.30		
14.7	3.18	1412.00	1406.65	7.57
		1467.00		
23.6	3.18	1468.90	1467.95	1.34
		1439.30		
4.7	6.35	1430.20	1434.75	6.43
		1411.80		
14.7	6.35	1397.30	1404.55	10.25
		1453.40		
23.6	6.35	1454.30	1453.85	0.64

Table A.6. Ash Content (% d.b.) of loblolly pine chips at different levels of moisture content and hammer mill screen sizes

Moisture Level (% w.b.)	Screen Size (mm)	Ash Content (% d.b.)	Mean (%d.b.)	Standard Deviation (% d.b.)
		0.58		
4.7	1.20	0.47	0.53	0.08
		0.66		
14.7	1.20	0.56	0.61	0.07
		0.75		
23.6	1.20	0.67	0.71	0.06
		0.50		
4.7	3.18	0.41	0.45	0.06
		0.50		
14.7	3.18	0.72	0.61	0.15
		0.46		
23.6	3.18	0.59	0.52	0.09
		0.59		
4.7	6.35	0.40	0.50	0.13
		0.45		
14.7	6.35	0.43	0.44	0.01
		0.39		
23.6	6.35	0.47	0.43	0.06

Table A.7. Volatile Content (% d.b.) of ground loblolly pine chips at different levels of moisture content and hammer mill screen sizes

Moisture Level (% w.b.)	Screen Size (mm)	Volatile Content (% d.b.)	Mean (% d.b.)	Standard Deviation (% d.b.)
		82.96		
4.7	1.20	83.45	83.21	0.35
		82.21		
14.7	1.20	82.56	82.39	0.25
		82.59		
23.6	1.20	82.91	82.75	0.23
		82.42		
4.7	3.18	82.87	82.65	0.32
		82.70		
14.7	3.18	83.05	82.87	0.25
		82.55		
23.6	3.18	83.04	82.79	0.35
		82.28		
4.7	6.35	81.77	82.02	0.36
		82.17		
14.7	6.35	82.13	82.15	0.02
		83.53		
23.6	6.35	83.01	83.27	0.37

Table A.8. Energy Content (kg/m³) of ground loblolly pine chips at different levels of moisture content and hammer mill screen sizes

Moisture Level (% w.b.)	Screen Size (mm)	Energy Content (MJ/kg)	Mean (MJ/kg)	Standard Deviation (MJ/kg)
		20.57		
4.7	1.20	20.90	20.73	0.23
		20.53		
14.7	1.20	20.40	20.46	0.10
		20.69		
23.6	1.20	20.53	20.61	0.12
		20.67		
4.7	3.18	20.88	20.78	0.15
		20.68		
14.7	3.18	20.54	20.61	0.10
		20.83		
23.6	3.18	20.86	20.85	0.02
		20.80		
4.7	6.35	20.74	20.77	0.04
		20.83		
14.7	6.35	20.64	20.73	0.14
		21.96		
23.6	6.35	22.04	22.00	0.06

Table A.9. Moisture content (% d.b.) of loblolly pine dust at different levels of moisture content and hammer mill screen sizes

Moisture Level (% w.b.)	Screen Size (mm)	Moisture Content (% w.b.)	Mean (% w.b.)	Standard Deviation (% w.b.)
4.7	1.20	6.39	6.51	0.18
		6.72		
		6.43		
14.7	1.20	9.85	9.96	0.10
		10.01		
		10.03		
23.6	1.20	9.38	9.37	0.01
		9.36		
		9.37		
4.7	3.18	6.72	6.53	0.19
		6.52		
		6.34		
14.7	3.18	9.99	10.00	0.01
		10.01		
		10.01		
23.6	3.18	12.67	12.24	0.37
		12.08		
		11.98		
4.7	6.35	6.39	6.49	0.19
		6.70		
		6.37		
14.7	6.35	12.3	12.44	0.14
		12.58		
		12.43		
23.6	6.35	14.22	14.57	0.58
		15.24		
		14.26		

Table A.10. Bulk Density (kg/m³) of loblolly pine dust at different levels of moisture content and hammer mill screen sizes

Moisture Level (% w.b.)	Screen Size (mm)	Bulk Density (kg/m³)	Mean (kg/m³)	Standard Deviation (kg/m³)
4.7	1.20	162.72	163.54	1.15
		163.05		
		164.85		
14.7	1.20	216.59	215.96	1.81
		213.92		
		217.38		
23.6	1.20	211.54	211.76	1.46
		213.32		
		210.42		
4.7	3.18	163.84	164.09	0.79
		163.45		
		164.97		
14.7	3.18	211.56	213.32	1.76
		215.08		
		213.32		
23.6	3.18	214.65	214.42	3.52
		217.82		
		210.78		
4.7	6.35	174.51	175.80	1.21
		176.92		
		175.97		
14.7	6.35	198.65	197.30	1.58
		195.57		
		197.69		
23.6	6.35	178.07	181.07	2.95
		183.96		
		181.20		

Table A.11. Particle Density (kg/m³) of loblolly pine dust at different levels of moisture content and hammer mill screen sizes

Moisture Level (% w.b.)	Screen Size (mm)	Particle Density (kg/m ³)	Mean (kg/m ³)	Standard Deviation (kg/m ³)
4.7	1.2	1468.1 1469.7	1468.90	1.13
14.7	1.2	1425.5 1427.4	1426.45	1.34
23.6	1.2	1491.1 1487.8	1489.45	2.33
4.7	3.18	1466.9 1500.2	1483.55	23.55
14.7	3.18	1426.1 1428.4	1427.25	1.63
23.6	3.18	1493.6 1500.4	1497.00	4.81
4.7	6.35	1449.6 1466	1457.80	11.60
14.7	6.35	1447.5 1457.7	1452.60	7.21
23.6	6.35	1514.4 1514.4	1514.40	0.00

Table A.12. Ash content (% d.b.) of loblolly pine dust at different levels of moisture content and hammer mill screen sizes

Moisture Level (% w.b.)	Screen Size (mm)	Ash Content (% d.b.)	Mean (% d.b.)	Standard Deviation (% d.b.)
4.70	1.20	0.81 0.86	0.84	0.04
14.70	1.20	1.63 1.63	1.63	0.00
23.60	1.20	1.33 1.88	1.61	0.39
4.70	3.18	1.03 0.91	0.97	0.08
14.70	3.18	2.95 2.83	2.89	0.08
23.60	3.18	2.15 2.10	2.13	0.04
4.70	6.35	1.76 1.88	1.82	0.08
14.70	6.35	5.36 5.73	5.55	0.26
23.60	6.35	5.77 5.66	5.72	0.08

Table A.13. Volatile content (% d.b.) of loblolly pine dust at different levels of moisture content and hammer mill screen sizes

Moisture Level (% w.b.)	Screen Size (mm)	Volatile Content (% d.b.)	Mean (d.b.)	Standard Deviation (% d.b.)
4.70	1.20	82.05	83.65	2.26
		85.25		
14.70	1.20	80.54	80.57	0.04
		80.60		
23.60	1.20	80.80	80.70	0.15
		80.59		
4.70	3.18	81.02	81.13	0.16
		81.24		
14.70	3.18	78.87	79.16	0.40
		79.44		
23.60	3.18	80.02	80.31	0.40
		80.59		
4.70	6.35	79.60	79.52	0.11
		79.44		
14.70	6.35	76.14	76.45	0.44
		76.76		
23.60	6.35	76.96	76.87	0.13
		76.78		

Table A.14. Energy content (% d.b.) of loblolly pine dust at different levels of moisture content and hammer mill screen sizes

Moisture Level (% w.b.)	Screen Size (mm)	Energy Content (MJ/kg)	Mean (MJ/kg)	Standard Deviation (MJ/kg)
4.70	1.20	20.84	20.85	0.01
		20.85		
14.70	1.20	20.28	20.36	0.11
		20.43		
23.60	1.20	20.36	20.46	0.14
		20.56		
4.70	3.18	20.69	20.71	0.02
		20.72		
14.70	3.18	20.42	20.37	0.08
		20.31		
23.60	3.18	20.49	20.57	0.11
		20.64		
4.70	6.35	20.85	20.92	0.09
		20.98		
14.70	6.35	20.08	20.08	0.00
		20.08		
23.60	6.35	19.71	19.60	0.16
		19.49		

Appendix B Results of Objective 1 and Objective 2

Table B.1. Amount of dust generated (%) at different moisture content and screen size

Moisture Content (% w.b.)	Screen Size 1.20 mm	Screen Size 3.18 mm	Screen Size 6.35 mm
4.7	21.70 _{a,a}	11.41 _{b,a}	5.431 _{c,a}
14.7	10.10 _{a,b}	8.68 _{a,b}	4.246 _{b,a}
23.6	14.13 _{a,b}	9.63 _{a,b}	5.290 _{a,a}

Subscripts under the values shows the comparison of means according to Tukey test
 First alphabet shows the comparison of means according to moisture content of wood chips
 Second alphabet shows the comparison of means according to screen sizes of hammer mill

Table B.2. Grinding energy at different moisture content and screen size

Moisture Content (%w.b.)	Screen Size 1.20 mm	Screen Size 3.18 mm	Screen Size 6.35 mm
4.7	473.08 _{a,c}	371.77 _{a,b}	168.26 _{a,a}
14.7	760.56 _{b,b}	651.84 _{b,b}	290.13 _{a,a}
23.6	1009.76 _{c,c}	767.55 _{b,b}	333.52 _{b,a}

Subscripts under the values shows the comparison of means according to Tukey test
 First alphabet shows the comparison of means according to moisture content of wood chips
 Second alphabet shows the comparison of means according to screen sizes of hammer mill

Table B.3. Desired MC of loblolly pine chips for experiment, actual MC of loblolly pine chips that was obtained, MC of ground loblolly pine and MC of dust

Desired MC of wood chips (%w.b.)	Actual MC of wood chips (%w.b.)	Screen Size (mm)	MC of Ground Material (% w.b.)	MC of Dust (% w.b.)	MC Designation
5	4.7	1.20	5.83 _{a,a}	6.51 _{a,a}	LMC
15		3.18	5.58 _{a,a}	6.53 _{a,a}	
25		6.35	5.86 _{a,a}	6.49 _{a,a}	
5	14.7	1.20	9.89 _{a,b}	9.96 _{a,b}	MMC
15		3.18	10.80 _{b,b}	10.00 _{a,b}	
25		6.35	14.36 _{c,b}	12.44 _{b,b}	
5	23.6	1.20	9.81 _{a,b}	9.37 _{a,c}	HMC
15		3.18	14.21 _{b,c}	12.24 _{b,c}	
25		6.35	19.59 _{c,c}	14.57 _{c,c}	

Subscripts under the values shows the comparison of means according to Tukey test
 First alphabet shows the comparison of means according to moisture content of wood chips
 Second alphabet shows the comparison of means according to screen sizes of hammer mill

Table B.4. Average particle size (mm) of ground loblolly pine chips and loblolly pine dust.

Material	Moisture Level	Screen Size 1.20 mm	Screen Size 3.18 mm	Screen Size 6.35 mm
Ground Material	LMC	0.42±0.34	0.64±0.62	1.34±1.32
	MMC	0.56±0.53	0.80±0.79	1.73±1.39
	HMC	0.48±0.43	0.86±0.16	1.97±1.72
Dust	LMC	0.34±0.23	0.23±0.15	0.38±0.25
	MMC	0.29±0.18	0.30±0.20	0.31±0.21
	HMC	0.31±0.21	0.29±0.05	0.33±0.07

Table B.5. Bulk density (kg/m³) of loblolly pine chips and loblolly pine dust.

Material	Moisture Content of Wood Chips (w.b. %)	Screen Size 1.20 mm	Screen Size 3.18 mm	Screen Size 6.35 mm
Ground Material	LMC	224.27 _{a,a}	218.82 _{b,a}	220.52 _{b,a}
	MMC	273.36 _{a,b}	253.00 _{b,b}	233.26 _{c,b}
	HMC	256.02 _{a,c}	228.84 _{b,c}	206.15 _{c,c}
Dust	LMC	163.54 _{a,a}	164.09 _{a,a}	175.80 _{b,a}
	MMC	215.96 _{a,b}	213.32 _{a,b}	197.30 _{b,b}
	HMC	211.76 _{a,c}	214.42 _{a,c}	181.07 _{b,c}

Subscripts under the values shows the comparison of means according to Tukey test
 First alphabet shows the comparison of means according to moisture content of wood chips
 Second alphabet shows the comparison of means according to screen sizes of hammer mill

Table B.6. Particle density (kg/m³) of ground loblolly pine chips and loblolly pine dust.

Material	Moisture Content of Wood Chips (% w.b.)	Screen Size 1.20 mm	Screen Size 3.18 mm	Screen Size 6.35 mm
Ground Material	LMC	1457.75 _{a,a}	1450.95 _{a,a}	1434.75 _{b,a}
	MMC	1431.60 _{a,a}	1406.65 _{a,b}	1404.55 _{a,b}
	HMC	1469.95 _{a,a}	1467.95 _{a,a}	1453.85 _{b,a}
Dust	LMC	1468.90 _{a,a}	1483.55 _{a,b}	1457.80 _{a,a}
	MMC	1426.45 _{a,b}	1427.25 _{a,a}	1452.60 _{b,a}
	HMC	1489.45 _{a,c}	1497.00 _{a,b}	1514.40 _{b,b}

Subscripts under the values shows the comparison of means according to Tukey test
 First alphabet shows the comparison of means according to moisture content of wood chips
 Second alphabet shows the comparison of means according to screen sizes of hammer mill

Table B.7. Ash content (% d.b.) of ground loblolly pine chips and loblolly pine dust.

Material	Moisture Content of Wood Chips (% w.b.)	Screen Size 1.20 mm	Screen Size 3.18mm	Screen Size 6.35mm
Ground Material	LMC	0.53 _{a,a}	0.42 _{a,a}	0.50 _{a,a}
	MMC	0.61 _{a,a}	0.61 _{a,a}	0.44 _{a,a}
	HMC	0.71 _{a,a}	0.52 _{a,a}	0.43 _{a,a}
Dust	LMC	0.83 _{a,a}	0.97 _{a,a}	1.82 _{b,a}
	MMC	1.63 _{a,a}	2.89 _{b,b}	5.89 _{c,b}
	HMC	1.60 _{a,a}	2.13 _{b,c}	5.72 _{b,b}

Subscripts under the values shows the comparison of means according to Tukey test
 First alphabet shows the comparison of means according to moisture content of wood chips
 Second alphabet shows the comparison of means according to screen sizes of hammer mill

Table B.8. Volatile content (% d.b.) of ground loblolly pine chips and loblolly pine dust.

Material	Moisture Content of Wood Chips (w.b.%)	Screen Size 1.20 mm	Screen Size 3.18 mm	Screen Size 6.35 mm
Ground Material	LMC	82.86 _{a,a}	83.55 _{a,a}	82.46 _{a,a}
	MMC	82.58 _{a,a}	83.02 _{a,a}	82.63 _{a,a}
	HMC	82.39 _{a,a}	82.55 _{a,a}	83.88 _{a,b}
Dust	LMC	84.71 _{a,a}	81.04 _{a,a}	79.52 _{a,a}
	MMC	80.57 _{a,a}	79.15 _{a,b}	76.46 _{b,b}
	HMC	80.72 _{a,a}	80.17 _{a,a}	76.87 _{b,b}

Subscripts under the values shows the comparison of means according to Tukey test
 First alphabet shows the comparison of means according to moisture content of wood chips
 Second alphabet shows the comparison of means according to screen sizes of hammer mill

Table B.9. Energy content (MJ/kg) of ground loblolly pine chips and loblolly pine dust

Material	Moisture Content of Wood Chips (w.b.%)	Screen Size 1.20mm	Screen Size 3.18mm	Screen Size 6.35mm
Ground Material	LMC	20.76 _{b,a}	20.45 _{b,a}	20.60 _{a,a}
	MMC	20.85 _{a,a}	20.58 _{a,a}	20.88 _{a,a}
	HMC	20.71 _{b,a}	20.73 _{b,a}	22.00 _{a,b}
Dust	LMC	20.81 _{a,b}	20.34 _{a,b}	20.49 _{a,a}
	MMC	20.73 _{a,a}	20.43 _{a,b}	20.56 _{a,b}
	HMC	20.87 _{b,a}	20.07 _{b,a}	19.61 _{a,c}

Subscripts under the values shows the comparison of means according to Tukey test
 First alphabet shows the comparison of means according to moisture content of wood chips
 Second alphabet shows the comparison of means according to screen sizes of hammer mill

Appendix C Physical, Chemical and Ignition Properties Data of Dust Samples

Table C.1. Physical properties of loblolly pine dust fractions (fine dust, medium dust, coarse dust), unfractionated loblolly pine dust and lignite coal

Sample	Moisture Content (% w.b.)	Mean (%w.b.)	Std. Dev. (%w.b.)	Bulk Density (kg/m ³)	Mean (kg/m ³)	Std. Dev. (kg/m ³)	Particle Density (kg/m ³)	Mean (kg/m ³)	Std. Dev. (kg/m ³)
Fine Dust (<90 μm)	9.88			198.63			1454.50		
	9.22	9.20	0.69	213.83	208.33	8.43	1432.60	1443.55	15.49
	8.5			212.52					
Medium Dust (90-180 μm)	9.59			177.33			1446.49		
	9.91	9.46	0.53	179.13	179.14	1.83	1450.08	1448.29	2.54
	8.88			180.98					
Coarse Dust (180-420 μm)	8.08			167.55			1420.70		
	8.68	8.73	0.67	167.36	168.92	2.53	1426.60	1423.65	4.17
	9.42			171.83					
Loblolly Pine Dust (<420 μm)	8.45			192.91			1466.59		
	7.49	8.16	0.58	197.11	196.21	2.95	1449.38	1457.99	12.16
	8.53			198.61					
Lignite Coal Dust (<420 μm)	5.91			530.99			1489.79		
	5.49	5.76	0.23	531.64	521.48	17.04	1536.89	1513.34	33.30
	5.87			501.81					

Table C.2. Chemical properties of loblolly pine dust fractions (fine dust, medium dust, coarse dust), unfractionated loblolly pine dust and lignite coal

Sample	Ash Content (% d.b.)	Mean (% d.b.)	Std. Dev. (% d.b.)	Volatile Matter (% d.b.)	Mean (% d.b.)	Std. Dev. (% d.b.)	Energy Content (MJ/kg)	Mean (MJ/kg)	Std. Dev. (MJ/kg)
Fine Dust (<90 µm)	1.53	1.70	0.23	81.50	82.19	1.74	20.27	20.19	0.07
	1.62			80.90			20.17		
	1.97			84.17			20.13		
Medium Dust (90-180 µm)	1.21	1.27	0.12	81.50	82.07	0.56	20.20	20.25	0.07
	1.18			82.63			20.33		
	1.40			82.07			20.21		
Coarse Dust (180-420 µm)	0.66	0.76	0.11	81.12	83.94	2.99	18.39	19.68	1.12
	0.87			87.08			20.27		
	0.76			83.63			20.39		
Loblolly Pine Dust (<420 µm)	1.08	1.08	0.01	81.50	82.36	0.75	19.98	20.01	0.10
	1.07			82.84			20.13		
	1.09			82.75			19.93		
Lignite Coal Dust (<420 µm)	19.22	19.22	0.10	28.32	31.00	2.32	26.87	26.94	0.10
	19.32			32.30			26.90		
	19.12			32.38			27.06		

Table C.3. TGA properties of loblolly pine dust fractions (fine dust, medium dust, coarse dust), unfractionated loblolly pine dust and lignite coal

Sample	TOD (°C)	Mean (°C)	Std. Dev. (°C)	TMW L (°C)	Mean (°C)	Std. Dev. (°C)	Tch (°C)	Mean (°C)	Std. Dev. (°C)
Fine Dust	275			325			297		
(< 90 µm)	269	272	3.96	325	325	0.53	301	299	3.13
Medium Dust	263			324			307		
(90-180 µm)	266	264	2.33	325	324	0.54	302	304	3.22
Coarse Dust	270			325			305		
(180-420 µm)	267	268	2.54	326	325	0.57	298	301	4.96
Loblolly Pine Dust	273			324			292		
(<420 µm)	273	273	0.15	324	324	0.35	294	293	0.95
Lignite Coal Dust	412			490			412		
(<420 µm)	407	409	3.77	488	489	1.41	421	417	6.36

Table C.4. Exothermic parameters of loblolly pine dust fractions (fine dust, medium dust, coarse dust), unfractionated loblolly pine dust and lignite coal

Sample	TRE (°C)	Mean (°C)	Std. Dev. (°C)	Tmax (°C)	Mean (°C)	Std. Dev. (°C)
Fine Dust	246			395		
(<90 µm)	238	242	5.71	400	397	3.11
Medium Dust	253			409		
(90-180 µm)	253	253	0.28	400	405	6.26
Coarse Dust	262			396		
(180-420 µm)	263	262	1.14	399	398	2.14
Loblolly Pine Dust	234			401		
(<420 µm)	248	241	9.79	400	400	0.85
Lignite Coal Dust	231			455		
(<420 µm)	239	235	5.09	450	453	3.42

Appendix D SAS Code and ANOVA Results

SAS code to determine the effect of moisture content and screen size

```
data guri;
input MC Ssize EC;
datalines;
4.7 1.2 20.84
4.7 1.2 20.85
14.7 1.2 20.28
14.7 1.2 20.43
23.6 1.2 20.36
23.6 1.2 20.56
4.7 3.18 20.69
4.7 3.18 20.72
14.7 3.18 20.42
14.7 3.18 20.31
23.6 3.18 20.49
23.6 3.18 20.64
4.7 6.35 20.85
4.7 6.35 20.98
14.7 6.35 20.08
14.7 6.35 20.08
23.6 6.35 19.71
23.6 6.35 19.49
```

```
;
```

```
Proc anova data=guri;
class MC Ssize;
model EC=MC Ssize;
run;
```

SAS code to determine the effect of particle size on properties

```
data guri;
input fraction$ MC;
datalines;
Fine 9.88
Fine 9.22
Fine 8.5
Medium 9.59
Medium 9.91
Medium 8.88
Coarse 8.08
Coarse 8.68
Coarse 9.42
```

```
;
```

```
Proc anova data=guri;
```

```

class Types;
model MC=fraction;
run;

```

Table D.1. ANOVA results of dust generation (DG) as affected by moisture content and screen size .

The ANOVA Procedure

Dependent Variable: DG

Source	DF	Sum of Squares	Mean Square	F Value	Pr > F
Model	4	401.3826667	100.3456667	15.47	<.0001
Error	13	84.3265333	6.4866564		
Corrected Total	17	485.7092000			

R-Square	Coeff Var	Root MSE	DG Mean
0.826385	25.29187	2.546892	10.07000

Source	DF	Anova SS	Mean Square	F Value	Pr > F
MC	2	319.9537333	159.9768667	24.66	<.0001
ssize	2	81.4289333	40.7144667	6.28	0.0124

Table D.2. ANOVA results of energy required for grinding (ER) as affected by moisture content and screen size.

The ANOVA Procedure					
Dependent Variable: ER					
Source	DF	Sum of Squares	Mean Square	F Value	Pr > F
Model	4	137878.1976	34469.5494	22.55	<.0001
Error	13	19868.5017	1528.3463		
Corrected Total	17	157746.6993			
	R-Square	Coeff Var	Root MSE	ER Mean	
	0.874048	25.32665	39.09407	154.3594	
Source	DF	Anova SS	Mean Square	F Value	Pr > F
MC	2	74823.54841	37411.77421	24.48	<.0001
Ssize	2	63054.64914	31527.32457	20.63	<.0001

Table D.3. ANOVA results of bulk density (BD) of ground material as affected by moisture content and screen size.

The ANOVA Procedure					
Dependent Variable: BD					
Source	DF	Sum of Squares	Mean Square	F Value	Pr > F
Model	4	9310.66497	2327.66624	27.55	<.0001
Error	22	1858.50519	84.47751		
Corrected Total	26	11169.17016			
	R-Square	Coeff Var	Root MSE	BD Mean	
	0.833604	3.912515	9.191165	234.9170	
Source	DF	Anova SS	Mean Square	F Value	Pr > F
MC	2	4893.650163	2446.825081	28.96	<.0001
Ssize	2	4417.014807	2208.507404	26.14	<.0001

Table D.4. ANOVA results of particle density (PD) of ground material as affected by moisture content and screen size.

The ANOVA Procedure					
Dependent Variable: PD					
Source	DF	Sum of Squares	Mean Square	F Value	Pr > F
Model	4	9158.56669	2289.64167	12.76	0.0002
Error	13	2332.88941	179.45303		
Corrected Total	17	11491.45609			
	R-Square	Coeff Var	Root MSE	PD Mean	
	0.796989	0.928988	13.39601	1441.999	
Source	DF	Anova SS	Mean Square	F Value	Pr > F
MC	2	7699.753678	3849.876839	21.45	<.0001
Ssize	2	1458.813011	729.406506	4.06	0.0425

Table D.5. ANOVA results of ash content of ground material as affected by moisture content and screen size.

The ANOVA Procedure					
Dependent Variable: Ash					
Source	DF	Sum of Squares	Mean Square	F Value	Pr > F
Model	4	0.09253333	0.02313333	2.50	0.0934
Error	13	0.12006667	0.00923590		
Corrected Total	17	0.21260000			
	R-Square	Coeff Var	Root MSE	Ash Mean	
	0.435246	18.01942	0.096104	0.533333	
Source	DF	Anova SS	Mean Square	F Value	Pr > F
MC	2	0.01563333	0.00781667	0.85	0.4513
Ssize	2	0.07690000	0.03845000	4.16	0.0401

Table D.6. ANOVA results of volatile content (Vc) of ground material as affected by moisture content and screen size.

The ANOVA Procedure

Dependent Variable: Vc

Source	DF	Sum of Squares	Mean Square	F Value	Pr > F
Model	4	1.02942222	0.25735556	1.24	0.3436
Error	13	2.70768889	0.20828376		
Corrected Total	17	3.73711111			

R-Square	Coeff Var	Root MSE	Vc Mean
0.275459	0.552000	0.456381	82.67778

Source	DF	Anova SS	Mean Square	F Value	Pr > F
MC	2	0.68307778	0.34153889	1.64	0.2317
Ssize	2	0.34634444	0.17317222	0.83	0.4573

Table D.7. ANOVA results of energy content (EC) of ground material as affected by moisture content and screen size.

The ANOVA Procedure

Dependent Variable: EC

Source	DF	Sum of Squares	Mean Square	F Value	Pr > F
Model	4	1.99613333	0.49903333	4.70	0.0145
Error	13	1.38131667	0.10625513		
Corrected Total	17	3.37745000			

R-Square	Coeff Var	Root MSE	EC Mean
0.591018	1.564271	0.325968	20.83833

Source	DF	Anova SS	Mean Square	F Value	Pr > F
MC	2	0.95723333	0.47861667	4.50	0.0326
Ssize	2	1.03890000	0.51945000	4.89	0.0261

Table D.8. ANOVA results of bulk density of loblolly pine dust as affected by moisture content and screen size.

The ANOVA Procedure					
Dependent Variable: BD					
Source	DF	Sum of Squares	Mean Square	F Value	Pr > F
Model	4	9704.88261	2426.22065	25.42	<.0001
Error	22	2099.83848	95.44720		
Corrected Total	26	11804.72110			
	R-Square	Coeff Var	Root MSE	BD Mean	
	0.822119	5.061248	9.769708	193.0296	
Source	DF	Anova SS	Mean Square	F Value	Pr > F
MC	2	8774.046696	4387.023348	45.96	<.0001
Ssize	2	930.835919	465.417959	4.88	0.0177

Table D.9. ANOVA results of particle density of loblolly pine dust as affected by moisture content and screen size.

The ANOVA Procedure					
Dependent Variable: PD					
Source	DF	Sum of Squares	Mean Square	F Value	Pr > F
Model	4	13173.70333	3293.42583	17.51	<.0001
Error	13	2444.73667	188.05667		
Corrected Total	17	15618.44000			
	R-Square	Coeff Var	Root MSE	PD Mean	
	0.843471	0.933772	13.71338	1468.600	
Source	DF	Anova SS	Mean Square	F Value	Pr > F
MC	2	12636.37000	6318.18500	33.60	<.0001
Ssize	2	537.33333	268.66667	1.43	0.2749

Table D.10. ANOVA results of ash content of loblolly pine dust as affected by moisture content and screen size.

The ANOVA Procedure					
Dependent Variable: Ash					
Source	DF	Sum of Squares	Mean Square	F Value	Pr > F
Model	4	46.87038889	11.71759722	20.70	<.0001
Error	13	7.35870556	0.56605427		
Corrected Total	17	54.22909444			
	R-Square	Coeff Var	Root MSE	Ash Mean	
	0.864303	29.26861	0.752366	2.570556	
Source	DF	Anova SS	Mean Square	F Value	Pr > F
MC	2	16.82897778	8.41448889	14.87	0.0004
Ssize	2	30.04141111	15.02070556	26.54	<.0001

Table D.11. ANOVA results of volatile content of loblolly pine dust as affected by moisture content and screen size.

The ANOVA Procedure					
Dependent Variable: VC					
Source	DF	Sum of Squares	Mean Square	F Value	Pr > F
Model	4	112.3601333	28.0900333	27.32	<.0001
Error	13	13.3687167	1.0283628		
Corrected Total	17	125.7288500			
	R-Square	Coeff Var	Root MSE	VC Mean	
	0.893670	1.266310	1.014082	80.08167	
Source	DF	Anova SS	Mean Square	F Value	Pr > F
MC	2	42.49570000	21.24785000	20.66	<.0001
Ssize	2	69.86443333	34.93221667	33.97	<.0001

Table D.12. ANOVA results of volatile content of loblolly pine dust as affected by moisture content and screen size.

The ANOVA Procedure					
Dependent Variable: EC					
Source	DF	Sum of Squares	Mean Square	F Value	Pr > F
Model	4	1.86775556	0.46693889	7.05	0.0030
Error	13	0.86075556	0.06621197		
Corrected Total	17	2.72851111			
	R-Square	Coeff Var	Root MSE	EC Mean	
	0.684533	1.259368	0.257317	20.43222	
Source	DF	Anova SS	Mean Square	F Value	Pr > F
MC	2	1.37521111	0.68760556	10.38	0.0020
Ssize	2	0.49254444	0.24627222	3.72	0.0528

Table D.13. ANOVA results of moisture content (MC) of three dust fractions (fine, medium and coarse).

The ANOVA Procedure					
Dependent Variable: MC					
Source	DF	Sum of Squares	Mean Square	F Value	Pr > F
Model	2	0.82942222	0.41471111	1.03	0.4117
Error	6	2.40966667	0.40161111		
Corrected Total	8	3.23908889			
	R-Square	Coeff Var	Root MSE	MC Mean	
	0.256067	6.942005	0.633728	9.128889	
Source	DF	Anova SS	Mean Square	F Value	Pr > F
Fraction	2	0.82942222	0.41471111	1.03	0.4117

Table D.14. ANOVA results of bulk density of three dust fractions (fine, medium and coarse).

The ANOVA Procedure					
Dependent Variable: BD					
Source	DF	Sum of Squares	Mean Square	F Value	Pr > F
Model	2	2509.604356	1254.802178	46.67	0.0002
Error	6	161.336200	26.889367		
Corrected Total	8	2670.940556			
	R-Square	Coeff Var	Root MSE	BD Mean	
	0.939596	2.795985	5.185496	185.4622	
Source	DF	Anova SS	Mean Square	F Value	Pr > F
Fraction	2	2509.604356	1254.802178	46.67	0.0002

Table D.15. ANOVA results of particle density of three dust fractions (fine, medium and coarse).

The ANOVA Procedure					
Dependent Variable: PD					
Source	DF	Sum of Squares	Mean Square	F Value	Pr > F
Model	2	683.5423000	341.7711500	3.89	0.1469
Error	3	263.6540500	87.8846833		
Corrected Total	5	947.1963500			
	R-Square	Coeff Var	Root MSE	PD Mean	
	0.721648	0.651701	9.374683	1438.495	
Source	DF	Anova SS	Mean Square	F Value	Pr > F
Fraction	2	683.5423000	341.7711500	3.89	0.1469

Table D.16. ANOVA results of ash content of three dust fractions (fine, medium and coarse).

The ANOVA Procedure					
Dependent Variable: Ash					
Source	DF	Sum of Squares	Mean Square	F Value	Pr > F
Model	2	1.33642222	0.66821111	25.28	0.0012
Error	6	0.15860000	0.02643333		
Corrected Total	8	1.49502222			
	R-Square	Coeff Var	Root MSE	Ash Mean	
	0.893915	13.06473	0.162583	1.244444	
Source	DF	Anova SS	Mean Square	F Value	Pr > F
Fraction	2	1.33642222	0.66821111	25.28	0.0012

Table D.17. ANOVA results of volatile matter (vc) content of three dust fractions (fine, medium and coarse).

The ANOVA Procedure					
Dependent Variable: VC					
Source	DF	Sum of Squares	Mean Square	F Value	Pr > F
Model	2	6.61126667	3.30563333	0.81	0.4897
Error	6	24.60713333	4.10118889		
Corrected Total	8	31.21840000			
	R-Square	Coeff Var	Root MSE	VC Mean	
	0.211775	2.447791	2.025139	82.73333	
Source	DF	Anova SS	Mean Square	F Value	Pr > F
Fraction	2	6.61126667	3.30563333	0.81	0.4897

Table D.18. ANOVA results of energy content (EC) of three dust fractions (fine, medium and coarse).

The ANOVA Procedure					
Dependent Variable: EC					
Source	DF	Sum of Squares	Mean Square	F Value	Pr > F
Model	2	0.57726667	0.28863333	0.68	0.5406
Error	6	2.53713333	0.42285556		
Corrected Total	8	3.11440000			
	R-Square	Coeff Var	Root MSE	EC Mean	
	0.185354	3.244877	0.650273	20.04000	
Source	DF	Anova SS	Mean Square	F Value	Pr > F
Fraction	2	0.57726667	0.28863333	0.68	0.5406

Table D.19. ANOVA results of temperature of volatilization (TOD) of three dust fractions (fine, medium and coarse).

The ANOVA Procedure					
Dependent Variable: TOD					
Source	DF	Sum of Squares	Mean Square	F Value	Pr > F
Model	2	56.33333333	28.16666667	3.13	0.1844
Error	3	27.00000000	9.00000000		
Corrected Total	5	83.33333333			
	R-Square	Coeff Var	Root MSE	TOD Mean	
	0.676000	1.118012	3.000000	268.3333	
Source	DF	Anova SS	Mean Square	F Value	Pr > F
Fraction	2	56.33333333	28.16666667	3.13	0.1844

Table D.20. ANOVA results of temperature of maximum mass loss rate (TMWL) of three dust fractions (fine, medium and coarse).

The ANOVA Procedure					
Dependent Variable: TMWL					
Source	DF	Sum of Squares	Mean Square	F Value	Pr > F
Model	2	1.0000000	0.5000000	1.50	0.3536
Error	3	1.0000000	0.3333333		
Corrected Total	5	2.0000000			
	R-Square	Coeff Var	Root MSE	TMWL Mean	
	0.500000	0.177646	0.577350	325.0000	
Source	DF	Anova SS	Mean Square	F Value	Pr > F
Fraction	2	1.0000000	0.5000000	1.50	0.3536

Table D.21. ANOVA results of temperature of oxidation (T_{ch}) of three dust fractions (fine, medium and coarse).

The ANOVA Procedure					
Dependent Variable: Tch					
Source	DF	Sum of Squares	Mean Square	F Value	Pr > F
Model	2	30.3333333	15.1666667	1.01	0.4617
Error	3	45.0000000	15.0000000		
Corrected Total	5	75.3333333			
	R-Square	Coeff Var	Root MSE	Tch Mean	
	0.402655	1.283862	3.872983	301.6667	
Source	DF	Anova SS	Mean Square	F Value	Pr > F
Fraction	2	30.3333333	15.1666667	1.01	0.4617

Table D.22. ANOVA results of temperature of onset rapid exothermic reaction (TRE) of three dust fractions (fine, medium and coarse).

The ANOVA Procedure					
Dependent Variable: TRE					
Source	DF	Sum of Squares	Mean Square	F Value	Pr > F
Model	2	421.0000000	210.5000000	19.43	0.0192
Error	3	32.5000000	10.8333333		
Corrected Total	5	453.5000000			
	R-Square	Coeff Var	Root MSE	TRE Mean	
	0.928335	1.303526	3.291403	252.5000	
Source	DF	Anova SS	Mean Square	F Value	Pr > F
Fraction	2	421.0000000	210.5000000	19.43	0.0192

Table D.23. ANOVA results of maximum temperature during exothermic reaction (T_{max}) of three dust fractions (fine, medium and coarse).

The ANOVA Procedure					
Dependent Variable: Tmax					
Source	DF	Sum of Squares	Mean Square	F Value	Pr > F
Model	2	65.3333333	32.6666667	1.70	0.3203
Error	3	57.5000000	19.1666667		
Corrected Total	5	122.8333333			
	R-Square	Coeff Var	Root MSE	Tmax Mean	
	0.531886	1.094950	4.377975	399.8333	
Source	DF	Anova SS	Mean Square	F Value	Pr > F
Fraction	2	65.3333333	32.6666667	1.70	0.3203

Table D.24. ANOVA results of MC of loblolly pine dust and coal dust.

The ANOVA Procedure					
Dependent Variable: MC					
Source	DF	Sum of Squares	Mean Square	F Value	Pr > F
Model	1	8.64000000	8.64000000	44.46	0.0026
Error	4	0.77733333	0.19433333		
Corrected Total	5	9.41733333			
	R-Square	Coeff Var	Root MSE	MC Mean	
	0.917457	6.336836	0.440833	6.956667	
Source	DF	Anova SS	Mean Square	F Value	Pr > F
Types	1	8.64000000	8.64000000	44.46	0.0026

Table D.25. ANOVA results of bulk density (Bd) of loblolly pine dust and coal dust.

The ANOVA Procedure					
Dependent Variable: BD					
Source	DF	Sum of Squares	Mean Square	F Value	Pr > F
Model	1	158700.8594	158700.8594	1061.48	<.0001
Error	4	598.0346	149.5087		
Corrected Total	5	159298.8940			
	R-Square	Coeff Var	Root MSE	BD Mean	
	0.996246	3.407425	12.22737	358.8450	
Source	DF	Anova SS	Mean Square	F Value	Pr > F
Types	1	158700.8593	158700.8593	1061.48	<.0001

Table D.26. ANOVA results of particle density of loblolly pine dust and coal dust.

The ANOVA Procedure					
Dependent Variable: PD					
Source	DF	Sum of Squares	Mean Square	F Value	Pr > F
Model	1	3064.176025	3064.176025	4.87	0.1579
Error	2	1257.297050	628.648525		
Corrected Total	3	4321.473075			
	R-Square	Coeff Var	Root MSE	PD Mean	
	0.709058	1.687655	25.07286	1485.663	
Source	DF	Anova SS	Mean Square	F Value	Pr > F
Types	1	3064.176025	3064.176025	4.87	0.1579

Table D.27. ANOVA results of ash content of loblolly pine dust and coal dust.

The ANOVA Procedure					
Dependent Variable: Ash					
Source	DF	Sum of Squares	Mean Square	F Value	Pr > F
Model	1	493.5894000	493.5894000	97740.5	<.0001
Error	4	0.0202000	0.0050500		
Corrected Total	5	493.6096000			
	R-Square	Coeff Var	Root MSE	Ash Mean	
	0.999959	0.700132	0.071063	10.15000	
Source	DF	Anova SS	Mean Square	F Value	Pr > F
Types	1	493.5894000	493.5894000	97740.5	<.0001

Table D.28. ANOVA results of volatile matter content (VC) of loblolly pine dust and coal dust.

The ANOVA Procedure

Dependent Variable: VC

Source	DF	Sum of Squares	Mean Square	F Value	Pr > F
Model	1	3957.288017	3957.288017	1330.31	<.0001
Error	4	11.898867	2.974717		
Corrected Total	5	3969.186883			

R-Square	Coeff Var	Root MSE	VC Mean
0.997002	3.042848	1.724737	56.68167

Source	DF	Anova SS	Mean Square	F Value	Pr > F
Types	1	3957.288017	3957.288017	1330.31	<.0001

Table D.29. ANOVA results of energy content (EC) of loblolly pine dust and coal dust.

The ANOVA Procedure

Dependent Variable: EC

Source	DF	Sum of Squares	Mean Square	F Value	Pr > F
Model	1	72.03735000	72.03735000	6774.67	<.0001
Error	4	0.04253333	0.01063333		
Corrected Total	5	72.07988333			

R-Square	Coeff Var	Root MSE	EC Mean
0.999410	0.439205	0.103118	23.47833

Source	DF	Anova SS	Mean Square	F Value	Pr > F
Types	1	72.03735000	72.03735000	6774.67	<.0001

Table D.30. ANOVA results of temperature of volatilization (TOD) of loblolly pine dust and coal dust.

The ANOVA Procedure

Dependent Variable: TOD

Source	DF	Sum of Squares	Mean Square	F Value	Pr > F
Model	1	18632.25000	18632.25000	2981.16	0.0003
Error	2	12.50000	6.25000		
Corrected Total	3	18644.75000			

R-Square	Coeff Var	Root MSE	TOD Mean
0.999330	0.732601	2.500000	341.2500

Source	DF	Anova SS	Mean Square	F Value	Pr > F
Types	1	18632.25000	18632.25000	2981.16	0.0003

Table D.31. ANOVA results of temperature of maximum mass loss rate of loblolly pine dust and coal dust.

The ANOVA Procedure

Dependent Variable: TMWL

Source	DF	Sum of Squares	Mean Square	F Value	Pr > F
Model	1	27225.00000	27225.00000	27225.0	<.0001
Error	2	2.00000	1.00000		
Corrected Total	3	27227.00000			

R-Square	Coeff Var	Root MSE	TMWL Mean
0.999927	0.246002	1.000000	406.5000

Source	DF	Anova SS	Mean Square	F Value	Pr > F
Types	1	27225.00000	27225.00000	27225.0	<.0001

Table D.32. ANOVA results of temperature of oxidation (T_{ch}) of loblolly pine dust and coal dust.

The ANOVA Procedure					
Dependent Variable: Tch					
Source	DF	Sum of Squares	Mean Square	F Value	Pr > F
Model	1	15252.25000	15252.25000	717.75	0.0014
Error	2	42.50000	21.25000		
Corrected Total	3	15294.75000			
	R-Square	Coeff Var	Root MSE	Tch Mean	
	0.997221	1.299442	4.609772	354.7500	
Source	DF	Anova SS	Mean Square	F Value	Pr > F
Types	1	15252.25000	15252.25000	717.75	0.0014

Table D.33. ANOVA results of temperature of rapid exothermic reaction (TRE) of loblolly pine dust and coal dust.

The ANOVA Procedure					
Dependent Variable: TRE					
Source	DF	Sum of Squares	Mean Square	F Value	Pr > F
Model	1	36.0000000	36.0000000	0.55	0.5343
Error	2	130.0000000	65.0000000		
Corrected Total	3	166.0000000			
	R-Square	Coeff Var	Root MSE	TRE Mean	
	0.216867	3.387503	8.062258	238.0000	
Source	DF	Anova SS	Mean Square	F Value	Pr > F
Types	1	36.00000000	36.00000000	0.55	0.5343

Table D.34. ANOVA results of maximum temperature during exothermic reaction (T_{max}) of loblolly pine dust and coal dust.

The ANOVA Procedure					
Dependent Variable: Tmax					
Source	DF	Sum of Squares	Mean Square	F Value	Pr > F
Model	1	2704.000000	2704.000000	416.00	0.0024
Error	2	13.000000	6.500000		
Corrected Total	3	2717.000000			
	R-Square	Coeff Var	Root MSE	Tmax Mean	
	0.995215	0.597775	2.549510	426.5000	
Source	DF	Anova SS	Mean Square	F Value	Pr > F
Types	1	2704.000000	2704.000000	416.00	0.0024

k